METHOD DEVELOPMENT FOR THE QUANTIFICATION OF THE RARE EARTH ELEMENTS EUROPIUM, DYSPROSIUM, TERBIUM AND YTTRIUM

by

Dika Daniel Nhlapo

A thesis submitted in fulfilment of the requirements for the degree of

Master of Science

In the Faculty of Natural & Agricultural Sciences

Department of Chemistry

University of the Free State

Supervisor: Prof. W. Purcell

Co-Supervisor: Dr. J. Venter

December 2015

Declaration by candidate

I hereby declare that the work presented in this thesis, Master of Science, submitted at the University of the Free State is my original work and has never being done or submitted anywhere else by me. Furthermore, extracts of any literature which has been used for this thesis has been properly acknowledged with references.

_____ _____

Dika Daniel Nhlapo Date

Acknowledgements

I thank God (Father, Son and Holy Spirit) for being with me up to thus far. I am also want to thank the following financial institution and people who helped me carry out this challenging study:

I firstly like to thank Inkaba yeAfrica and the University of the Free State for the financial assistance.

Prof. W Purcell (Supervisor), thank you so much for letting me to be part of your group, by also showing the road of how to get started with the research and being always available and prepared to show direction in times of darkness.

Dr. J Venter (Co-supervisor), thanks very much for editing my thesis.

To my colleagues (Dr. M. Nete and S. Xaba) who have being so helpful, I would like to say thank you very much for your kindness, willingness to help and patience. To Dr. T. Chiweshe, H. Mnculwane, Q. Vilakazi, L. Ntoi and G. Malefo, thank you for providing an environment that was conducive to carry out my project.

To my friends (K. Phungula, P. Manana and T. Twala), I just want to tell you that, you have been the best friends ever since from Honours.

Special thanks to my family for the important roles they have played in my life, especially by supporting with prayers from the beginning of my studies. I conclude by saying God is good all the time.

DIKA

TABLE OF CONTENTS

Table of Contents

LIST OF FIQURES

LIST OF TABLES

LIST OF ABBREVIATIONS

Chemicals and ligand:

TPPO	Triphenylphosphine oxide
REEs	Rare earth elements
REMs	Rare earth metals
REOs	Rare earth oxides

Instruments:

ICP-OES	Inductively Coupled Plasma-Optical Emission Spectrometer
ICP-MS	Inductively Coupled Plasma Mass Spectroscopy
IR	Infrared spectroscopy
TGA	Thermogravimetric analysis
UV/Vis	Ultra violet visible spectroscopy

Statistical abbreviations:

LOD	Limit of detection
LOQ	Limit of quantification
SD	Standard deviation
RSD	Relative standard deviation
$\overline{X}$	Mean

1 Aim and motivation of the study

1.1 Background

The rare earth elements (REEs) belong to the lanthanide group of metals with atomic numbers ranging from 57 to 71. In natural minerals such as monazite, bastnasite and xenotime these elements are also commonly associated with scandium and yttrium due to their similar chemistries.[1] They are divided into two subgroups namely light and heavy rare earth elements. The light REEs include lanthanum (La) and cerium (Ce) while the heavy REEs include terbium (Tb), dysprosium (Dy) and europium (Eu).

The REEs generally have high boiling and melting temperatures and are good conductors of heat and electricity. Their natural abundances range from 0.5 to 60 ppm in geological deposits which make them rather abundant in the earth's crust, much higher than their name 'rare' would suggest. For instance, most of the REEs have abundances greater than molybdenum (Mo) and tin (Sn). Cerium (natural abundance = 60 ppm) is also more abundant than copper (Cu) and lead (Pb).[2] The ionic radius decreases from left (lanthanum) to right (lutetium) on the periodic table. The small differences between the ionic radii (as well as the similar +3 oxidation state) of the different REEs make them difficult to separate from one another in mineral ores.

The most abundant REEs containing minerals are monazite, bastnasite and xenotime. Deposits of monazite, bastnasite and xenotime are found in China, Brazil, India, Malaysia and some African countries which include South Africa. China is currently the leading producer and consumer of REEs products.[3]

---

[1] HH Bahti, Y Mulyasih and A Anggraeni. Proceedings of the 2nd international seminar on chemistry, 2011, pp.421-430.

[2] Exploration and mining of rare earth elements (REEs) using tube-based thermo scientific portable XRF analyzers. [Accessed 21-07-2014], Available from: https://www.niton.com/docs/literature/rareearthreeultra.pdf?sfvrsn=2.

[3] China's rare earth elements industry: what can the west learn? [Accessed 03-06-2013], Available from: http://www.iags.org/rareearth0310hurst.pdf.

China alone accounts for approximately 97 % (**Table 1.1**) of global REEs production from different mineral ores. Most of the reserves originate from the Bayan Obo mining district (estimated 81.4 %) which is situated in Inner Mongolia. The remaining percentages come from other districts to account for China's total production.[4] In South Africa the rare earth elements are found in monazite which is mined from the Steenkampskraal mine in the Western Cape Province. Another potential South African mine which is expected to yield significant outputs of monazite is Zandkopsdrift which is situated in the Northern Cape Province.[5] Production in the latter mine is expected to commence between 2015 and 2016. REEs production and industrial consumption are expected to grow exponentially in the next couple of years due to their world-wide demand in electronic applications, as well as green energy technology. Currently the global consumption of the REEs per country depends on the level of technology. The ever improving and need for technology results in a higher REEs demand globally, which is the major driving force behind the rapid increase in REEs prices internationally.

Table 1.1: Global production of REEs from 2008 - 2009.[6]

Country	REEs (tons/year)	Share (%)
China	120 000	97.0
Brazil	650	0.5
India	2 700	2.1
Malaysia	380	0.3
Other countries	270	0.1
Total	**124 000**	**100**

[4] The use and management of NORM residues in processing Bayan Obo ores in China. [Accessed 01-08-2014], Available from: http://qu-wifan.eu-norm.org/index.pdf.

[5] A 21st century scramble: South Africa, China and the rare earth metals industry. [Accessed 31-05-2013], Available from: http://scholar.sun.ac.za/handle/10019.1/21176.

[6] Study on rare earths and their recycling. [Accessed 03-06-2013], Available from: http://www.oeko.de/oekodoc/1112/2011-003-en.pdf.

REEs are used in various products such as permanent magnets, metal alloys, polishing powder and electronic devices. Their outstanding characteristics such as strong magnetic properties but light in weight[7] have made it difficult to find any other materials to replace their use in industries and consumer products. The current importance of REEs in different applications is directing the focus of most countries to increase or maximize their production.[8] Beneficiation of rare earths are time consuming and costly procedures are needed due to problems associated with their separation. Production processes involve mineral mining, crushing, flotation, metallurgical cracking and extraction of the rare earth oxides. These metals are then traded as mischmetals, inorganic compounds or pure metals. The purity requirements of metals or compounds depend on the intended applications. **Table 1.2** shows growth in REEs demands in different industrial applications.

Table 1.2: The expected consumption of REEs in 2015.[9]

Application	Growth rate (% / year)	Expected demand in 2015 ($x10^3$ tons)
Catalysts	0	25.5
Glass additive	0	10
Polishing powder	5-10	23-30
Metal alloys	4-8	36-40
Permanent magnets	10-15	40-45
Phosphors and pigments	4-8	13-15
Ceramics	5-8	9-10
Other	8-12	12-14
Total	**7-10**	**170-190**

[7] Rare earth elements: the basics, economics supply chain and applications. [Accessed 30-05-2013], Available from: http://www.avalonraremetals.com/_resources/REE101-2012efile.pdf.

[8] Rare earth elements. [Accessed 22-07-2014], Available from: Hedrickhttp://www.segemar.gov.ar/bibliotecaintemin/LIBROSDIGITALES/Industrialminerals&rocks7ed/pdffiles/papers/058.pdf.

[9] D Kołodyńska and Z Hubicki. Investigation of sorption and separation of lanthanides on the ion exchangers of various types, *Intech,* 2012, pp.101-112.

Other important mineral ores containing REEs are allanite, apatite and the claysand eudialite.[10] The allanite in uranium mining is produced as a by-product while eudialite as mineral contains mostly heavy REEs. Estimations indicate that the supply of heavy REEs like europium (Eu), terbium (Tb), yttrium (Y) and dysprosium (Dy) will be below demand for the next coming years, resulting in significant market constraints for these metals. These metals are used as phosphors and applied immensely in electronics while dysprosium is used in hybrid engines.[11] Europium is used as a phosphor in computer screens to create red and blue light. Terbium is applied in the production of super magnets in combination with neodymium. Yttrium has medical applications as the radio-isotope yttrium-90 for different diseases such as cancer and arthritis whereas research has proven that dysprosium has the ability to increase the strength of neodymium-iron-boron magnets.[12]

The accurate quantification and separation of REEs from mineral ore to produce high purity metals or chemical compounds is very important for the applications in industries. The success of each separation procedure during the beneficiation process and the isolation of the different elements can only be evaluated and controlled with the use of quantitative analysis products. It is therefore extremely important that an accurate quantitative analysis procedure are first developed before indulging in separation processes. The mineral analysis is therefore significant to produce a reliable, representative and objective composition of the sample.

1.2 Study objectives

The main aim of this study is to develop and validate analytical methods for the accurate quantification of the rare earth elements Eu, Dy, Tb and Y. Further objectives are:

- Perform a detailed literature study on the analytical techniques for the analysis of REEs.

[10] A review of the global supply of rare earths. [Accessed 07-08-2014], Available from: http://www.rsc.org/images/David-Merriman_tcm18-230229.pdf.

[11] Rare earth elements 101 April 2012. [Accessed 07-08-2014], Available from: http://www.iamgold.com/files/ree101_april_2012.pdf.

[12] Zandkopsdrift's rare earths. [Accessed 07-08-2014], Available from: http://www.infomine.com/library/publications/docs/InternationalMining/Chadwick2012l.pdf.

- Determine the ability of different acids with or without the microwave digestion method for dissolving the complexes.
- Quantify REEs (Eu, Tb, Y and Dy) accurately and determine their recoveries in pure REE metal, inorganic compounds and organometallic complexes.
- Compare results by using different techniques such as ICP-OES, IR and CHNS-micro analyser (LECO).
- Statistically validate these methods.

2 Background of rare earth elements

2.1 Introduction

The rare earth elements (REEs) consist of a group of 15 elements with atomic numbers 57 to 71. This group of elements are roughly divided into two main groups, namely the light REEs (LREEs) which include the elements from lanthanum to gadolinium (57 - 64) while the heavy REEs continue from terbium to lutetium (65 - 71). Scandium and yttrium are usually included as REEs due to their occurrence with the REEs in mined deposits as well as the similarity of their chemistry to those of the rare earths. Interestingly is that minerals tend to contain either the LREEs or HREEs as major lanthanides, which are attributed to the easy displacement / exchange of elements with similar ionic radii. This process of ion displacement results in mineral deposits which are normally rich in either LREEs or HREEs. HREEs are less common than the LREEs and therefore more valuable and are extensively used in modern technology applications. Examples of rare earth containing minerals are presented in **Figure 2.1**.

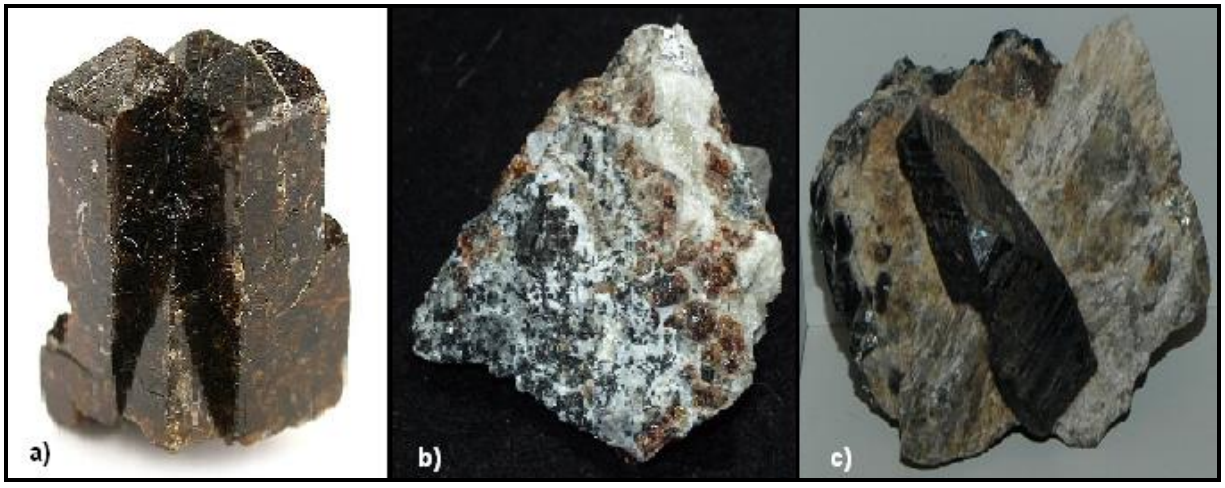

Figure 2.1: Mineral ores (a) xenotime[13], (b) eudialyte[14] and (c) gadolinite[15].

2.2 Discovery of REEs

In 1787 an amateur mineralogist Carl Axel Arrhenius (**Figure 2.2**) discovered a novel black mineral, called gadolinite in Ytterby, Sweden, which later proved to contain numerous HREEs. In 1794, a qualified chemist Johan Gadolin analyzed this black mineral and discovered that the mineral contained iron, silicate and the first rare earth element, called yttria. At a later stage yttria was renamed to yttrium after discovering that this newly identified “element” was indeed a mixture of rare earth oxides which included yttrium (Y), dysprosium (Dy), erbium (Er), ytterbium (Yb), terbium (Tb), holmium (Ho), thulium (Tm), lutetium (Lu) and scandium (Sc) oxides.

During the period 1788 to 1907 considerable attention was given[16] to the separation of the different elements in the yttria mixture. Carl Gustav Mosander studied a gadolinite sample in 1878 and was able to isolate erbium and terbium which were found to be associated with yttrium. In 1879, Lars Frederick Nilson discovered

[13] Xenotime. [Accessed 21-10-2014], Available from: http://commons.wikimedia.org/wiki/File:Xenotime-%28Y%29-Rutile-177576.jpg.

[14] Fine quality mineral specimens for sale [Accessed 09-09-2014], Available: http://www.selectminerals.com/min9.html.

[15] Gadolinite. [Accessed 09-09-2014], Available from: http://hyperphysics.phy-astr.gsu.edu/hbase/minerals/gadolinite.html.

[16] Extractive metallurgy of rare earths. [Accessed 25-08-2014], Available from: http://vector.umd.edu/links_files/Extractive%20Metallurgy%20of%20Rare%20Earths%20%28Gupta%29.pdf.

scandium while trying to isolate ytterbium from gadolinite and euxenite. The process involved the precipitation of $Er(NO_3)_3$ from erbia (Er_2O_3) with the addition of warm HNO_3. To his surprise a small amount of the precipitate remained undissolved and the characterization of this unknown product indicated a new element with low atomic weight. This newly discovered product turned out to be “ekaboron” (Eb) which was predicted by Mendeleev in 1871 and was re-named to scandium (Sc_2O_3 slightly soluble in diluted acids). During the same year, Per Theodor Cleve identified two new rare earth elements namely holmium and thulium. Paul Emile Lecoq de Boisbaudran discovered dysprosium in 1886 (dyprositos in Greek which means hard to get due to the difficulty involved in its detection and isolation). About twenty years later (1907) the French chemist Georges Urban discovered lutetium from what was thought to be an ytterbium sample.

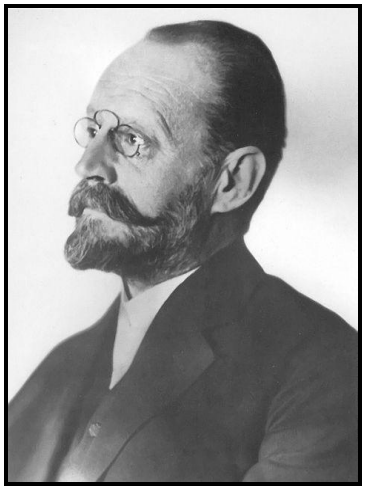

Figure 2.2: Carl Axel Arrhenius.[17]

The next group of rare earths, namely samarium (Sm), gadolinium (Gd), europium (Eu) and terbium (Tb) oxides were discovered in a mineral called samarskite during a period spanning from 1838 to 1904. Paul Emile Lecoq de Boisbaudran discovered samarium in 1879 and a year later, Jean Charles Marignac identified gadolinium while performing chemical separations of other REEs. In 1901 Eugene Demarcay discovered one of the last REEs, namely europium from the same mineral.[16]

[17] Selteneerden. [Accessed 05-09-2014], Available from: http://www.mineralatlas.eu/lexikon/index.php/Mineralienportrait/Seltene%20Erden/Geschichte.

2.3 Occurrence and reserves

REE deposits are widely dispersed throughout the world and with more than 100 minerals that contain REEs, it is only monazite and bastnasite that are commercially important for LREEs mineral beneficiation. REE bearing minerals occurs naturally in heavy mineral placers as residuals[18], in carbonatites (high percentage of REEs), in pegmatites, and finally in weathered and hydrothermal deposits.[13] Significant deposits of REEs are found in China, United States, Australia, India, Malaysia, Brazil and Vietnam in descending order.[19,20] The major global REE deposit locations are indicated in **Figure 2.3** while **Figure 2.4** indicate the % REE deposits per country.

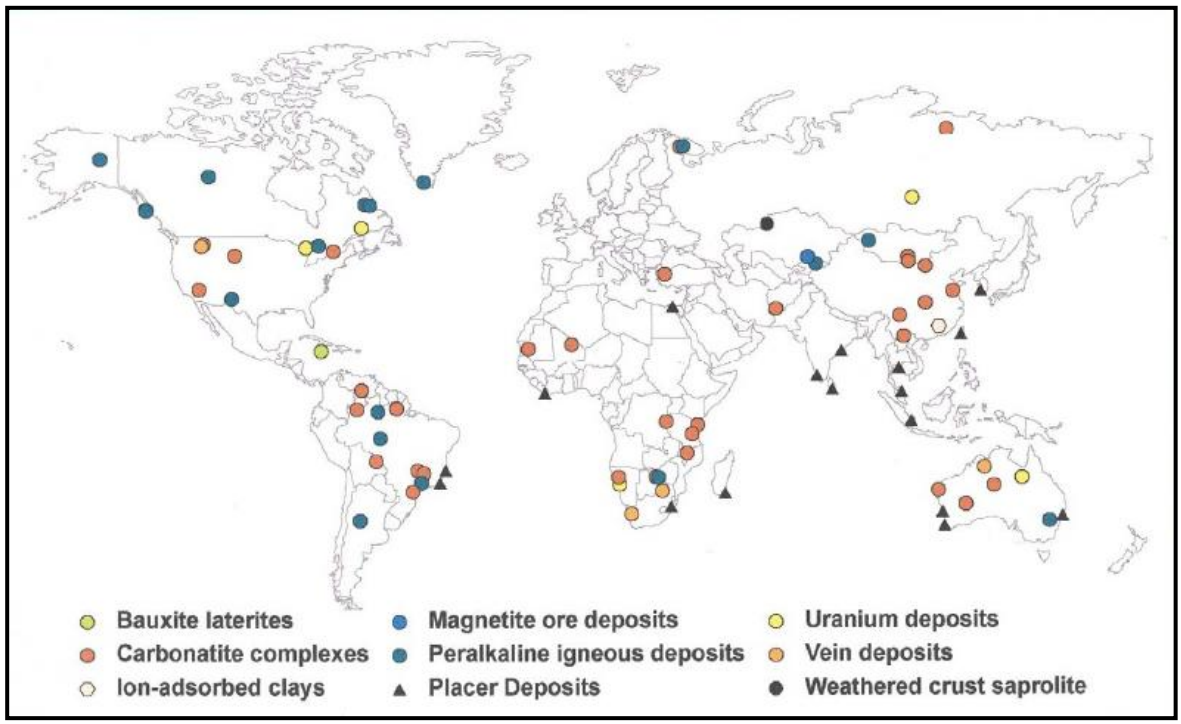

Figure 2.3: The major global REE deposit locations.[21]

[18] Mineral resources supply & information with a focus on rare earth elements. [Accessed 01-092014], Available from: http://ec.europa.eu/enterprise/policies/raw-materials/files/docs/eu-us-meinert2_en.pdf.

[19] Fact sheet: rare earths oxides (REO). [Accessed 09-09-2014], Available from: http://www.polinares.eu/docs/d2-1/polinares_wp2_annex2_factsheet3_v1_10.pdf.

[20] Synopsis. [Accessed 25-08-2014], Available From: http://www.cecd.umd.edu/documents/synopsis-rare-earth.pdf.

[21] Rare-earth elements. [Accessed 20-10-2014], Available from: http://137.229.113.30/webpubs/dggs/ic/text/ic061.pdf.

The Mountain Pass open-pit mine in California used to be the largest global producer of REEs from 1965 to 1985,[22] before China took control of REE production in late 1980s. The rare earth oxides at this mine were deposited as old Precambrian carbonatite minerals and contain 8 - 12 % of rare metal oxides. Current estimation indicates that this mine still contains in excess of 20 million tonnes (Mt) of ore as reserves.[23] China's strategy to flood the markets with low cost REEs forced the closure of Mountain Pass mining operations.

Australia and India also have significant REE deposits. In Australia the REEs are present in the phosphate-monazite fragment of the heavy mineral sands which is mined for other minerals such rutile, zircon, leucocene and ilmenite. The largest REE operations are in South Australia in the so-called Olympic Dam iron-copper-gold deposits. A survey in 2012 projected that the country has 3.19 Mt of economic demonstrated resources, 0.4 Mt paramarginal and 31.1 Mt submarginal resources. In India the state-owned company IREL operates two REE divisions in Kerala state and two in the Tamil Nadu and Orissa states respectively. Estimates indicate that the monazite sands at these locations contain approximately 3.1 Mt of REEs or about 2.2 % of world reserves.

[22] Investigating rare earth element mine development in epa region 8 and potential environmental impacts. [Accessed 27-08-2014], Available from: http://www.miningwatch.ca/files/epa_reportonrareearthelements1.pdf.

[23] Molycorp mountain pass. [Accessed 17-10-2014], Available from: http://www.molycorp.com/about-us/our-facilities/molycorp-mountain-pass/.

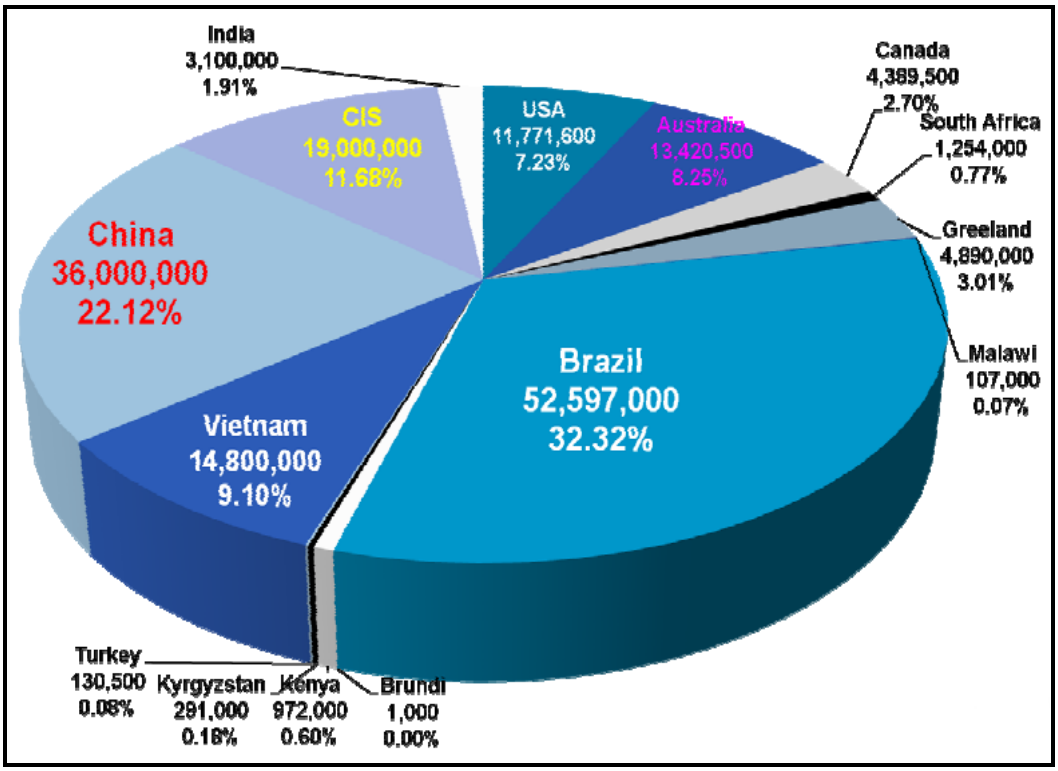

Figure 2.4: Total REEs distribution in 2010.[24]

Recent estimates indicate that Malaysia has about 30 000 t of known REE deposits, but is currently busy with new explorations in Panang where mineral samples indicated the presence of 15 REEs. REE estimates indicate that Brazil have 22 Mt of mineral deposits which account for about 20 % of world reserves with the largest neodymium deposits of 28 Mt in the Bahia state. Significant rare-earth deposits have recently also been discovered at the Salobo copper mine at Carajas in the Para state. Vietnam is presently one of the smallest of REE producers, but it is expected that this will increase significantly in future with new joint-ventures recently signed with Japan. In South Africa the REE deposits are situated in the Western Cape at Steenkampskraal and Zandkopsdrift. The rich monazite deposits at these locations account for 0.8 % of world reserves and the mine at Steenskampskraal started production in 2013.

Two new players in the REE sector are Russia and Japan. Resent exploration results in the east of Russia reported REE deposits containing approximately 154 Mt of

[24] How to make the separation of rare earth more green and efficient. [Accessed 27-08-2014], Available from: http://asmic.akademisains.gov.my/download/RareEarth/symposium/Yan.pdf.

REEs.[25] In 2013 Japan discovered large rare earth deposits in the sea around the island of Minami-Torishiba and estimates indicate that it contains about 50 % of heavy rare earths, which rival the China's dominance in this sector of the market. An added advantage of these deposits is that they would be easy to mine and beneficiate due to the absence of any radioactive thorium.[26]

China currently has one of the largest documented and economically viable REE deposits with estimates of between 22 and 40 % of world reserves. In 2010 the major deposits of REEs in China were located in Bayan Obo and Baotou mines in the Sichuan and Gantsu Provinces where they were mined as by-products of iron processing and occur as carbonatite-syenite minerals. Other important source of REE deposits are the lateritic ion adsorption clays found in southern China which comprise mainly of HREEs and xenotime (yttrium source) mineral. The iron-LREE-niobium deposits in the Bayan Obo mining district (discovered in 1927 by Daoheng) is presently known to have the largest REE reserves in the world.[27]

2.4 Production and supply

China is by far the largest REE producer and account for more than 90 % (100 000 Mt) of the world production (see **Figure 2.5**). This dominance is not only due to the large REE deposits located in the country, but also their ability to develop processes and technology to separate and purify these highly similar chemical elements from the minerals. The major LREE production (70 %) in China takes place at Bayan Obo in Inner Mongolia while both LREEs and HREEs are mined in the southern districts which include Jiangxi, Guangdong, Fujian, Hunan, Guangxi and Yunnan, which

[25] Russia wakes sleeping rare earth giant. [Accessed 17-10-2014], Available from: http://www.mining.com/russia-wakes-sleeping-rare-earth-giant-17116/.

[26] Japan breaks China's stranglehold on rare metals with sea-mud bonanza. [Accessed 17-10-2014], Available from: http://www.telegraph.co.uk/finance/comment/ambroseevans_pritchard/9951299/Japan-breaks-Chinas-stranglehold-on-rare-metals-with-sea-mud-bonanza.html.

[27] China's rare earth elements industry: what can the west learn? [Accessed 03-06-2013], Available from: http://www.iags.org/rareearth0310hurst.pdf.

account for 27 % of the production. Production in the western Sichuan province district accounts for approximately 10 % of Chinese production.[28]

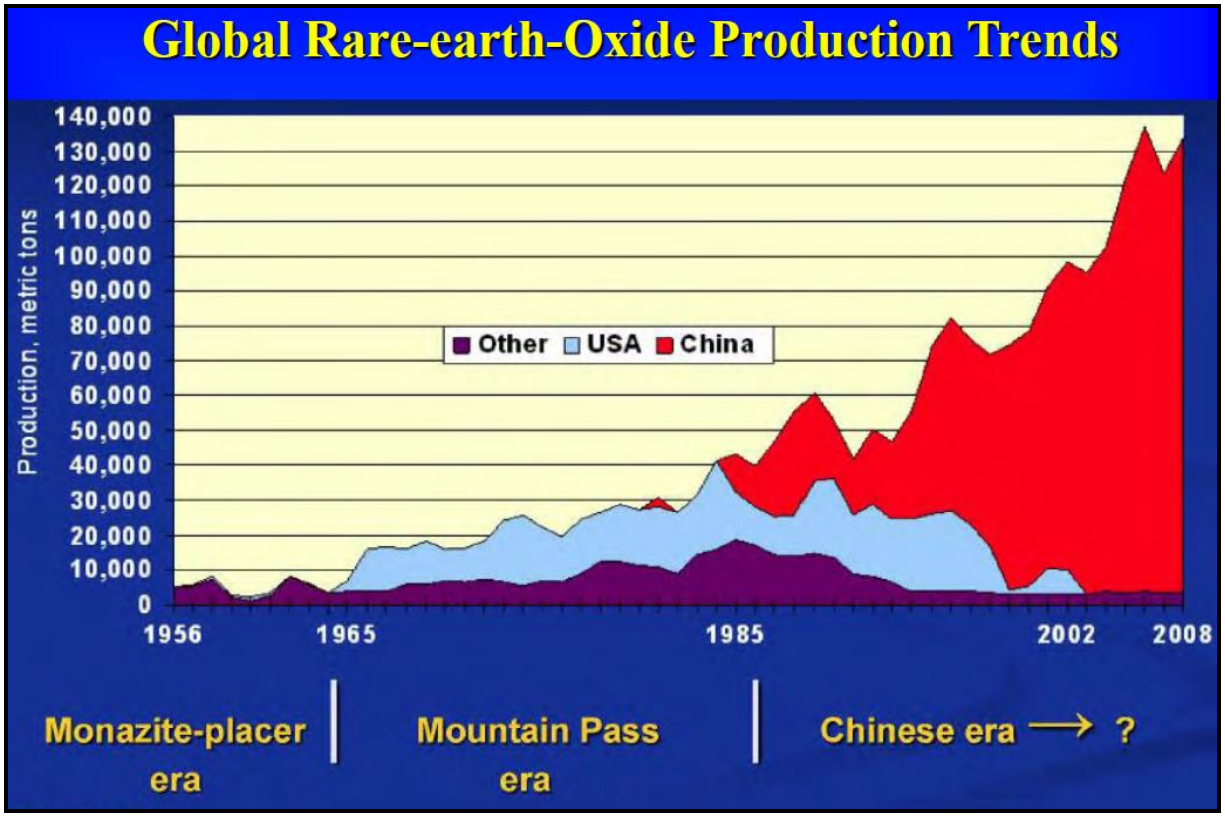

Figure 2.5: The Chinese dominance in the production of RE oxides.[29]

The USA accounts for 4,000 Mt of world production, India for 2,900 Mt, Russia for 2,400 Mt, Australia for 2,000 Mt and Vietnam for 220 Mt. Brazil accounts for 140 Mt rare earth oxide production while Malaysia produces about 100 Mt of these metals.

In 2010 China restricted the export of REEs which resulted in the rapid escalation of REE prices (see **Figure 2.6**).[30] The prices of metallic europium and terbium rose from $485 and $600 to $6 620 and $3 200 per kilogram respectively. This rapid increase in REE prices continued until the middle of 2011 after which the REE market

[28] A review of the global supply of rare earth. [Accessed 27-08-2014], Available from: http://www.rsc.org/images/David-Merriman_tcm18-230229.pdf.

[29] Overview of the rare earth industry. [Accessed 20-10-2014], Available from: http://www.ausimm.com.au/content/docs/branch/2014/melbourne_2014_05_presentation.pdf.

[30] Postnote rare earth metals. [Accessed 27-08-2014], Available from: http://www.parliament.uk/documents/post/postpn368rare_earth_metals.pdf.

stabilized due to increased, as well as new production outputs and supply by the other global suppliers.[31,32]

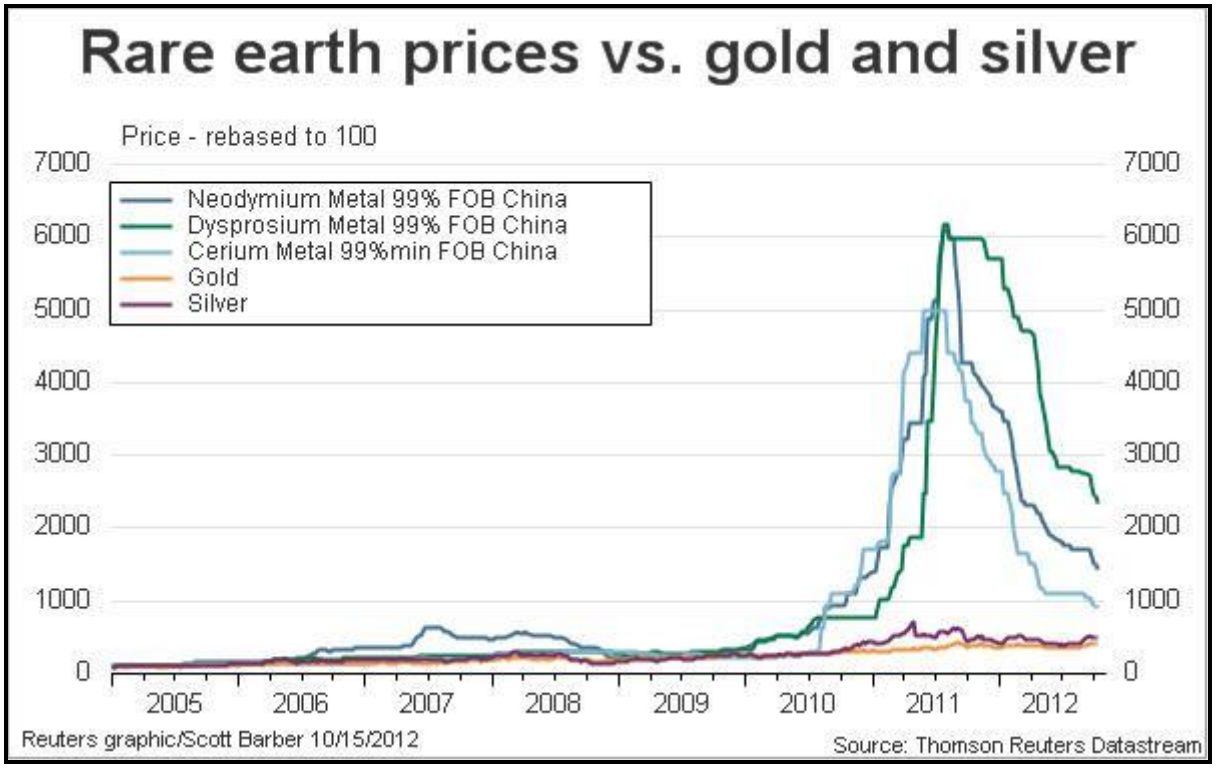

Figure 2.6: The REE prices compared to gold and silver.[33]

2.5 Mining and beneficiation

The processing of REEs involves a number of primary steps which was mentioned in **Chapter 1, Section 1.1**. The mineral ores are commonly acquired from underground mining, although open pit mines such as the Bayan Obo mine in the Inner Mongolia district near Baotou City are also used for REE mineral extractions. The ores are then crushed into gravel size (**Figure 2.7**) and washed with water (usually to remove soil impurities). After separation from associated minerals, either by gravity, magnetic and/or electrostatic methods, the REE containing mineral is subjected to chemical treatment and hydrometallurgical processes. However, it is worth noting at this stage

[31] Investigation of sorption and separation of lanthanides on the ion exchangers of various type. [Accessed 09-09-2014], Available from: http://cdn.intechopen.com/pdfs-wm/40696.pdf.

[32] Fact sheet: rare earths oxides (REO). [Accessed 25-08-2014], Available from: http://www.polinares.eu/docs/d2-1/polinares_wp2_annex2_factsheet3_v1_10.pdf.

[33] Situation and policies of china's rare earth industry. [Accessed 18-08-2014], Available from: http://ycls.miit.gov.cn/n11293472/n11295125/n11299425/n14676844.files/n14675980.pdf.

that the mineral treatment processes depend on the ore composition, the concentrations of the target elements as well as the level of purity required in the final products. For example, the extraction of REEs from xenotime mineral ore commences with the dissolution of the ore with concentrated NaOH (65 %) at 140 °C. The REEs are then extracted from the resultant slurry with water and the individual elements are ultimately separated from each other in the water solution using solvent extraction. The presence of high concentrations of radioactive thorium and uranium sometimes complicates this beneficiation route by rendering sample handling difficult and environmentally unfriendly.

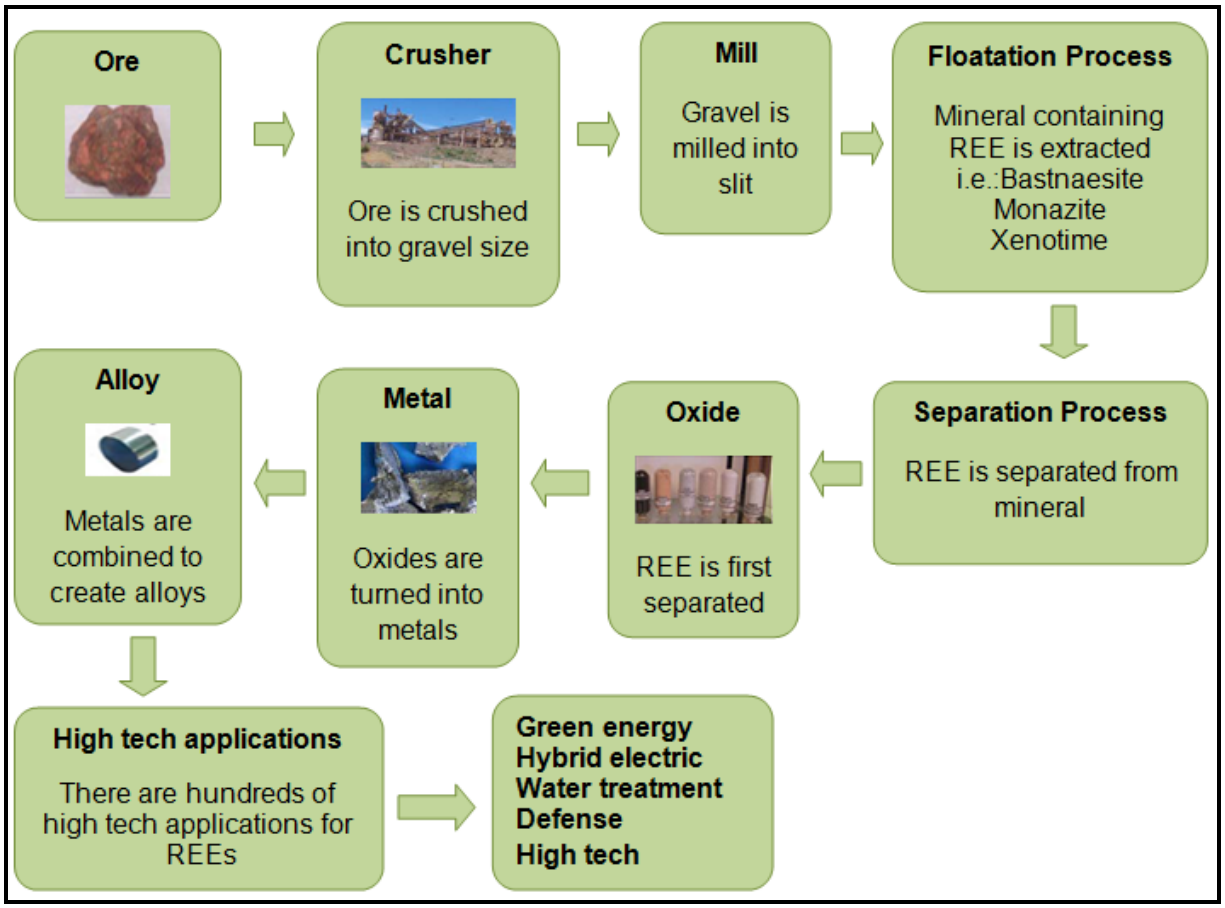

Figure 2.7: The processing of REEs.[34]

The separation and purification of the rare earths is not only a difficult and complicated process, but also a long and costly exercise. The similarity between the chemical and physical properties of all 17 elements for instance results in that there

[34] Mining and exploitation of rare earth elements in Africa as an engagement strategy in US Africa command. [Accessed 25-08-2014], Available from:www.dtic.mil/cgi-bin/GetTRDoc?AD=ADA545604.

are no known chemical reagents that can be used across the board for efficient REE flotation. The most stable oxidation state for all these are +3 and lanthanide contraction also has the effect that the ionic radii for all the elements are very similar. The British chemist Charles James used fractional crystallization to separate the REEs in the early 1900s. This process required daily recrystallization for four years to isolate relatively pure holmium, totalling 15,000 crystallization steps.

Hydrometallurgical processing, involving the total dissolution and then REE separation using fractional crystallization, ion-exchange and solvent extraction processes, are currently used to produce pure rare earth metals and chemical compounds. The final steps in this process involve the isolation of the different elements into usable oxides and purified metals or chemical compounds using chemical or electrolytic processes.[35]

The mineral xenotime(Y,HREE)PO is one of the most important REEs containing minerals which contain large concentrations of yttrium as yttrium orthophosphate (YPO_4) as well the heavier REEs, namely erbium, dysprosium, terbium, gadolinium and ytterbium. The mineral is commonly found in small amounts of metapelitic and placer deposit rocks, and less abundant in calcic and mafic bulk compositions. Large resources of this mineral are located in Western Australia and China. The presence of uranium and thorium render the mineral weakly to strongly radioactive. Representative analysis of a number of xenotime samples are given in **Table 2.1**, indicating the relative abundance of the heavier REEs.

[35] Rare earth elements: what and where they are. [Accessed 20-10-2014], Available from: www.springer.com/cda/content/.../cda.../9783642354571-c2.pdf?

Table 2.1: Analysis of numerous xenotime mineral samples showing the percentage composition of the different REE's.[36]

Sample:	BF-55	BF-15	93-19	BF-17	BF-38	TM-445	TM-637	SP-9B1	89-9	89-22	BF-78	BF-92	BF-14	V6B	V7D
Analysis:	525/2	204/2	187	178	179	455	415	18	464	261/3	65/1	577/2	129/1	7	6
P_2O_5	34·09	34·97	35·96	36·82	35·56	36·37	35·71	36·38	35·87	36·53	36·67	35·34	35·62	37·78	36·72
SiO_2	2·13	0·27	0·15	0·53	0·54	0·26	0·56	0·13	0·62	0·10	0·20	0·94	0·14	0·15	0·08
CaO	0·14	0·05	0·04	0·14	0·09	0·13	0·12	0·11	0·07	0·07	0·04	0·09	n.d.	0·07	0·03
PbO	0·11	n.d.	0·10	n.d.	n.d.	n.d.	0·17	0·03	0·17	n.d.	n.d.	0·10	n.d.	0·05	0·06
ThO_2	0·78	0·42	0·35	n.d.	0·05	n.d.	n.d.	0·15	0·07	n.d.	n.d.	0·16	0·23	0·11	0·11
UO_2	n.d.	0·08	n.d.	n.d.	0·25	0·69	1·72	n.d.	0·25	n.d.	n.d.	0·22	n.d.	n.d.	n.d.
Y_2O_3	**40·43**	**42·47**	**42·85**	**44·88**	**43·28**	**46·03**	**42·79**	**44·25**	**43·83**	**44·31**	**43·87**	**47·12**	**43·11**	**47·23**	**44·24**
La_2O_3	n.d.	n.d.	n.d.	n.d.	n.d.	n.d.	n.d.	n.d.	n.d.	0·05	n.d.	n.d.	n.d.	0·10	n.d.
Ce_2O_3	n.d.	n.d.	n.d.	n.d.	n.d.	n.d.	0·32	n.d.	n.d.	0·05	n.d.	0·07	0·05	0·06	0·12
Pr_2O_3	n.d.	0·18	n.d.	n.d.	n.d.	n.d.	n.d.	n.d.	0·07	n.d.	n.d.	n.d.	n.d.	n.d.	0·08
Nd_2O_3	0·06	0·19	0·13	0·06	0·15	0·28	0·36	0·21	0·15	0·41	0·28	0·32	0·44	0·20	0·39
Sm_2O_3	n.d.	n.d.	0·25	n.d.	n.d.	0·23	0·18	0·31	n.d.	n.d.	n.d.	n.d.	n.d.	n.d.	0·06
Gd_2O_3	**5·36**	**2·37**	**3·28**	**2·93**	**2·33**	**2·53**	**2·33**	**1·58**	**1·24**	**2·09**	**1·83**	**2·45**	**1·36**	**2·07**	**2·84**
Dy_2O_3	**8·79**	**5·37**	**7·20**	**8·56**	**5·98**	**7·20**	**6·05**	**3·52**	**3·28**	**6·00**	**5·60**	**6·93**	**4·98**	**6·77**	**7·11**
Ho_2O_3	1·02	1·18	1·29	1·22	1·17	1·64	1·42	1·19	1·13	1·50	1·47	1·29	1·42	1·25	1·55
Er_2O_3	**3·46**	**4·80**	**4·60**	**2·54**	**4·25**	**3·10**	**4·15**	**4·75**	**5·52**	**4·54**	**4·88**	**3·23**	**5·72**	**2·63**	**3·96**
Yb_2O_3	2·46	4·66	3·65	1·28	4·04	0·93	3·15	6·75	6·81	3·83	4·91	1·41	6·07	2·02	2·43
Total	98·83	97·01	99·85	98·96	97·69	99·39	99·03	99·36	99·08	99·48	100·11	99·67	99·14	100·49	99·84
X_{YPO4}	0·7504	0·7868	0·7740	0·8134	0·7964	0·8187	0·7831	0·7988	0·7980	0·7986	0·7938	0·8260	0·7812	0·8355	0·7965

Bold = major elements in mineral

2.6 Applications of REEs

The current popularity of the REEs is directly connected to global warming concerns. These elements are widely used in vital green energy technologies and their role to limit green-house gas emissions. These metals are used in the production of hybrid and electric vehicles (~ 28 kg REE/vehicle) and wind power generators, resulting in a

[36] Monazite-xenotime-garnet equilibrium in metapelites and a new monazite–garnet thermometer. [Accessed 20-10-2014], Available from: http://ees2.geo.rpi.edu/metapetaren/publications/pdfpapers/jpet_grt-mnz.pdf.

reduction of hydrocarbon energy consumption and CO_2 emissions. REEs are also used as catalysts for large scale chemical compound production, in the electronic sector as display phosphors and in glass and ceramic production. They are also used for hydrogen storage in metal alloys, as powerful magnets in wind turbines, for water treatment and as nuclear control rods.

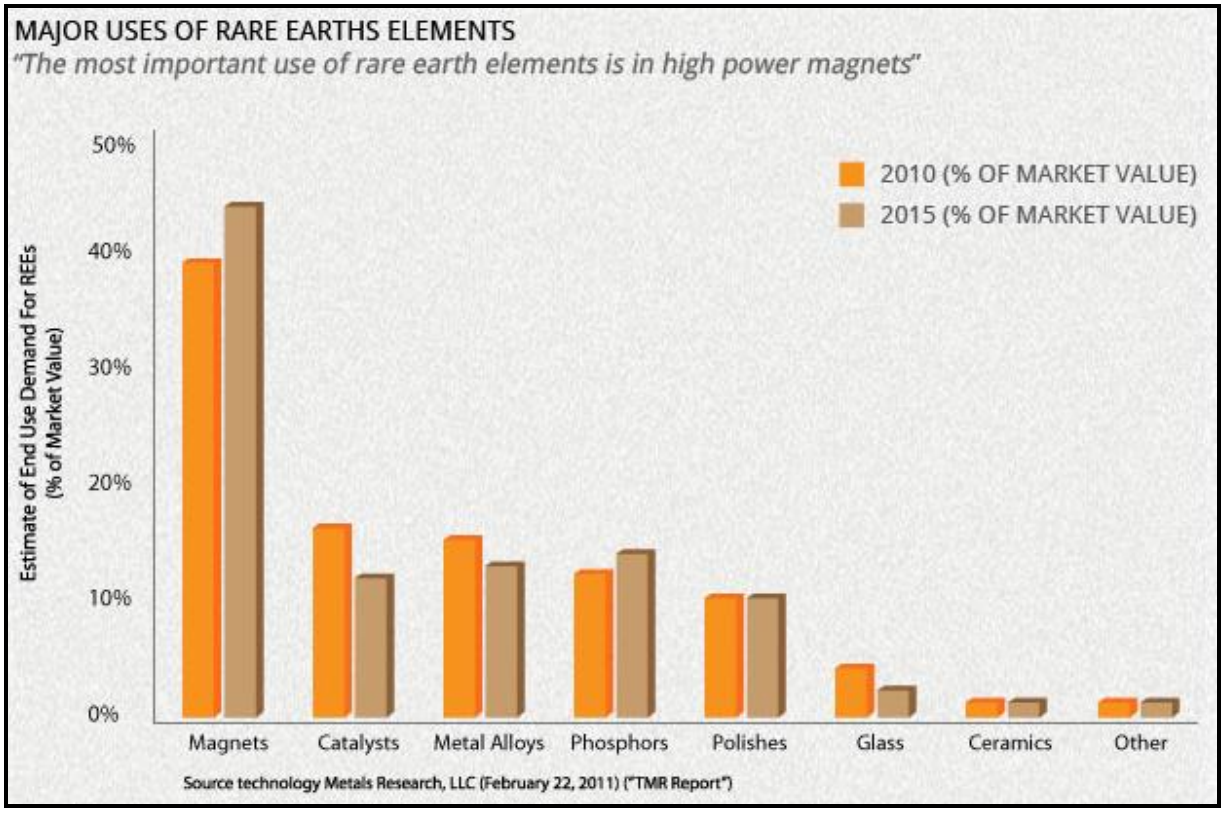

Figure 2.8: The uses of REEs in 2010 and 2015.[37]

The major uses of all the REEs are summarized in **Table 2.2**. It is clear that the production of permanent magnets is still the major consumer of REEs, with catalysts, metal and alloys and phosphors following in decreasing order of consumption.

[37] High demand for rare earths. [Accessed 20-10-2014], Available from: http://www.namibiarareearths.com/market-demand.asp.

Table 2.2: The applications of REEs.[38]

Element	Applications
Lanthanum	Ceramic glazes, high optical glass, camera lenses, microwave crystals, ceramic capacitors, glass polishing powders, petroleum cracking.
Cerium	Glass polishing, petroleum cracking catalysts, alloys - with iron for sparking flints for lighters, with aluminium, magnesium and steel for improving heat and strength properties, radiation shielding, many others.
Praseodymium	Yellow ceramic pigments, tiles, ceramic capacitors. With neodymium in combination for goggles to shield glass makers against sodium glare, permanent magnets. Cryogenic refrigement.
Neodymium	Ceramic capacitors, glazes and coloured glass, lasers, high strength permanent magnets as neodymium-iron-boron alloy, petroleum cracking catalysts.
Promethium	Radioactive promethium in batteries to power watches, guided missile instruments, etc, in harsh environments.
Samarium	In highly magnetic alloys for permanent magnet as Samarium-Cobalt alloy; probably will be supersed by neodymium. Glass lasers. Reactor control and neutron shielding.
Europium	Control rods in nuclear reactors. Coloured lamps, cathode ray tubes. Red phosphor in colour television tubes.
Gadolinium	Sold state lasers, constituent of computer memory chips, high temperature refractories, cryogenic refrigerants.
Terbium	Cathode ray tubes, magnets, optical computer memories, future hard disk components; magnetostrictive alloys.
Dysprosium	Controls nuclear reactors. Alloyed with neodymium for permanent magnets. Catalysts.
Holmium	Controls nuclear reactors; catalysts; refractors.
Erbium	In ceramics to produce a pink glaze; infra-red absorbing glasses.
Thulium	X-ray source in portable X-ray machines.
Ytterbium	Practical values presently unknown. Research.
Lutetium	Deoxidiser in stainless steel production, rechargeable batteries, medical uses, red phosphors for colour television, superconductors.
Yttrium	Deoxidiser in stainless steel production, rechargeable batteries, medical uses, red phosphors for colour television, superconductors.
Scandium	X-ray tubes, catalysts for polymerisation, hardened Ni-Cr superalloys, dental porcelain.

Some applications of the individual REEs are listed in **Table 2.2**. Neodymium and samarium-cobalt are predominantly used in the manufacturing of strong permanent magnets used in wind turbines due to their great strength, heat resistance and ability to maintain their magnetism for long period. The small sized neodymium permanent

[38] Lanthanide rare-earth metal element set. [Accessed 09-09-2014], Available from: http://www.elementsales.com/set-re-1.htm.

magnets are mainly use in computers (**Figure 2.9**),[39] and other consumer applications such as headphones and speakers. The application of the different REEs in consumer products such as a hybrid motorcars is highlighted in **Fig. 2.10**.

Figure 2.9: Application of neodymium permanent magnets in (a) Computer[40] and (b) wind turbines[41].

REEs are also extensively used in phosphor applications such as fluorescent lamps and TV plasma displays which consume more than 90 % of europium and terbium, as well as other elements such as yttrium, gadolinium, cerium and lanthanum due to their excellent colour displays in the visible region.[42] Europium oxide (Eu_2O_3) in combination with yttrium oxide (Y_2O_3) are replacing zinc-cadmium sulfide in the television industry due to their ability to produced brighter coloured pictures on television screens.[43]

[39] Rare earth elements 101. [Accessed 27-08-2014], Available from: http://www.iamgold.com/files/ree101_april_2012.pdf.

[40] Bluesmansbillypcfix. [Accessed 22-09-2014], Available from: http://bluesmanbillypcfix.blogspot.com/.

[41] The value of rare earths April 2012. [Accessed 25-08-2014], Available from: http://www.iamgold.com/files/HongKong2012REEPresentationFINAL.pdf.

[42] Orbite: a strategic rare earth elements producer. [Accessed 09-09-2014], Available from: http://www.orbitealuminae.com/media/upload/filings/Rare_earth_elements_Version_1_1.pdf.

[43] Chemistry of lanthanides and actinides. [Accessed 09-09-2014], Available from:http://unaab.edu.ng/opencourseware/Chemistry%20of%20Lanthanides%20and%20Actinides.pdf.

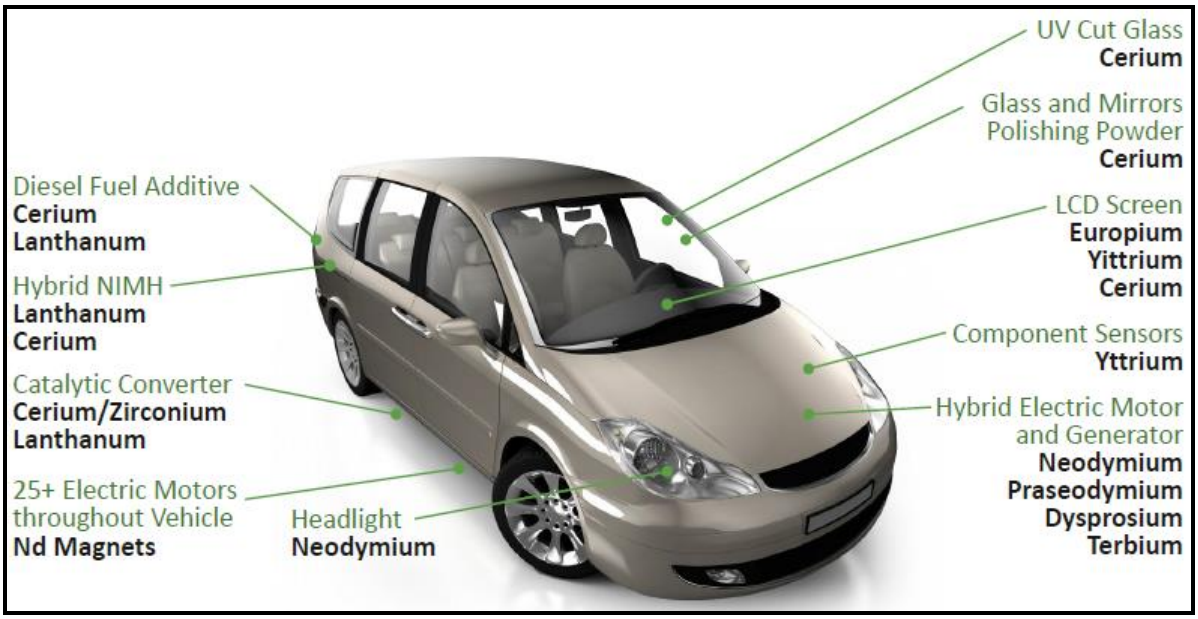

Figure 2.10: The application of REEs in a hybrid car.[11]

2.7 Properties and chemistry of REEs

2.7.1 General physical properties of the REEs

Rare earth metals are shiny with a silver-gray to white colour as shown in **Figure 2.11**. All the metals are classified as soft while their hardness increases slightly with an increase in atomic number and they also have high melting and boiling points. The metals are also very reactive and react with water to slowly liberate hydrogen (H_2) in cold water but much quicker upon heating. All the REEs have a stable +3 oxidation state and the radii of this group of cations decrease steadily from left to right (increasing atomic number) due to 'lanthanide contraction' (**Figure 2.12**). Lanthanide cations also easily form hydrated species in aqueous solutions. At room temperature the elements react exothermically with dilute acids to produce H_2. They are strong reducing agents, their compounds are generally ionic of nature and at elevated temperatures metals also ignite and burn vigorously. Most of the REEs are also strongly paramagnetic and have strong fluorescence properties under ultraviolet light. Lanthanide ions in aqueous solutions have pale colours resulting from weak, narrow, forbidden *f* to *f* orbital optical transitions. Interestingly, the magnetic moments of the lanthanides and iron ions oppose each other. The REEs also react with most non-metals and produce binaries upon heating. Finally, the coordination numbers of inorganic and organometallic lanthanide compounds are high, generally greater than 6, usually 8 or 9, but also as high as 12.

These metals react (oxidize) at different rates when exposed to air to form the metal oxides. Some corrode very rapidly, especially some of HREMs[13] while others remain un-oxidized for longer times (see **Figure 2.13**).

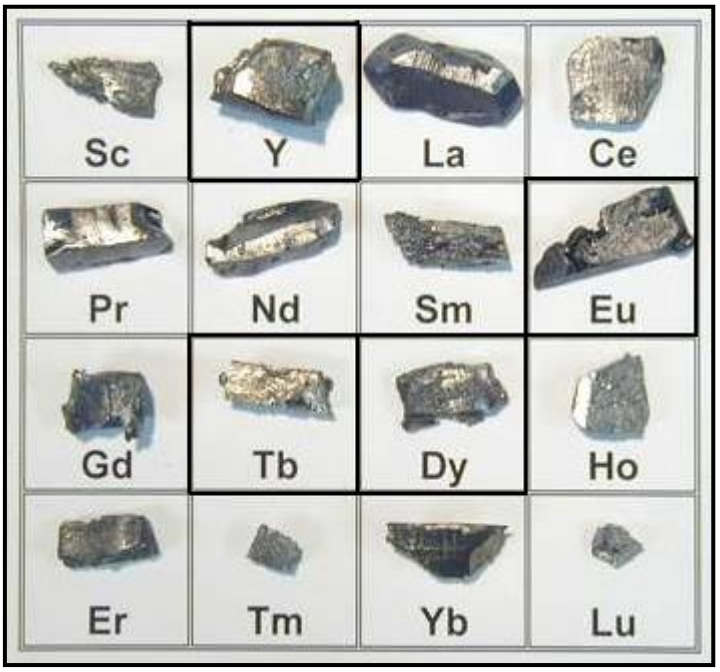

Figure 2.11: Photographs of pieces of rare earth metals.[44]

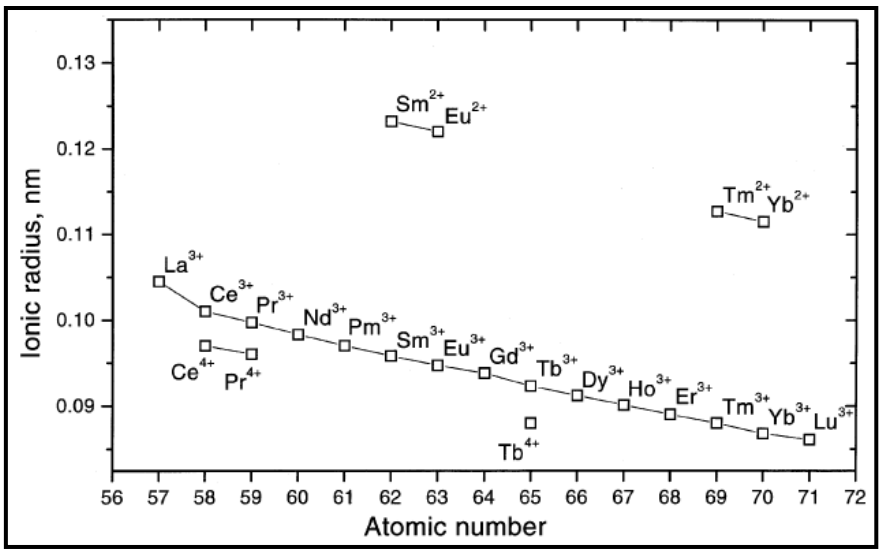

Figure 2.12: Lanthanide contraction of the REEs.[13]

[44] Lanthanide rare-earth metal element set. [Accessed 09-09-2014], Available from: http://www.elementsales.com/set-re-1.htm.

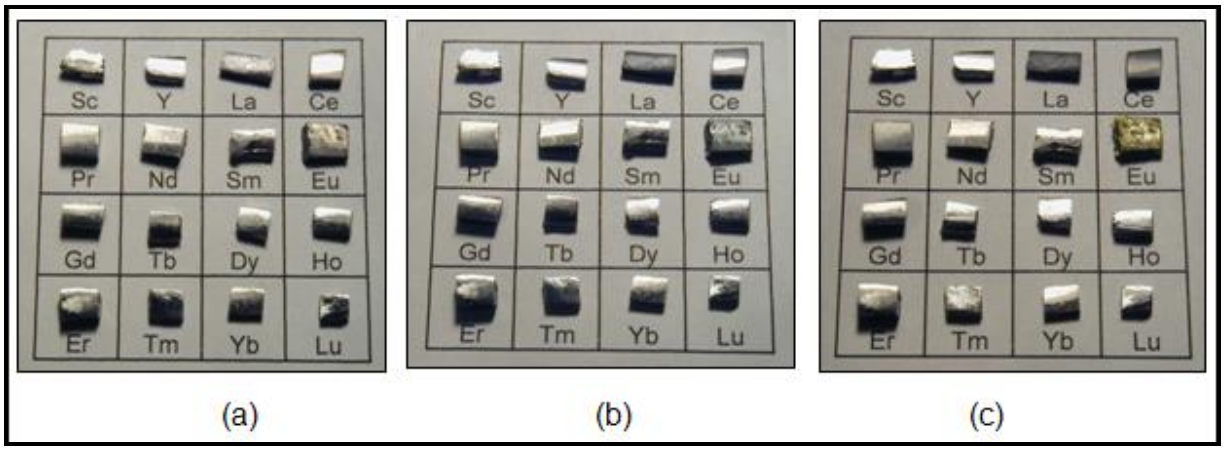

Figure 2.13: REEs oxidation as a function of time (a) After 2 hours Eu begins to tarnish, (b) after 2 days La turns black and (c) Ce turns black after day 5.[45]

Although the most common and stable oxidation state of the REEs is +3, elements such europium, samarium, thulium and ytterbium also exhibit a stable +2 oxidation state while others such as cerium, praseodymium and terbium exhibit a stable +4 oxidation state. The physical properties of the different REEs are listed in **Table 2.3**.

Table 2.3: General physical properties of the REEs.[46]

Chemical element	La	Ce	Pr	Nd	Pm	Sm	Eu	Gd	Tb	Dy	Ho	Er	Tm	Yb	Lu
Atomic number	57	58	59	60	61	62	63	64	65	66	67	68	69	70	71
Image															
Density (g/cm^3)	6.162	6.770	6.77	7.01	7.26	7.52	5.244	7.90	8.23	8.540	8.79	9.066	9.32	6.90	9.841
Melting point (°C)	920	795	935	1024	1042	1072	826	1312	1356	1407	1461	1529	1545	824	1652
Boiling point (°C)	3464	3443	3520	3074	3000	1794	1529	3273	3230	2567	2720	2868	1950	1196	3402
Atomic electron configuration*	$5d^1$	$4f^1 5d^1$	$4f^3$	$4f^4$	$4f^5$	$4f^6$	$4f^7$	$4f^7 5d^1$	$4f^9$	$4f^{10}$	$4f^{11}$	$4f^{12}$	$4f^{13}$	$4f^{14}$	$4f^{14} 5d^1$
Metal lattice (RT)	dhcp	fcc	dhcp	dhcp	dhcp	**	bcc	hcp	hcp	hcp	hcp	hcp	hcp	hcp	hcp
Metallic radius pm	162	181.8	182.4	181.4	183.4	180.4	208.4	180.4	177.3	178.1	176.2	176.1	175.9	193.3	173.8
Resistivity (25 °C) /μ Ohm cm	57–80 20 °C	73	68	64		88	90	134	114	57	87	87	79	29	79
mag susceptibility χ_{mol} /10^{-6}($cm^3 \cdot mol^{-1}$)	+95.9	+2500 (β)	+5530 (α)	+5930 (α)		+1278 (α)	+30900	+185000 (350 K)	+170000 (α)	+98000	+72900	+48000	+24700	+67 (β)	+183

The lanthanides have the general electron configuration of $[Xe]4f^x5d^y6s^2$ and the exact configurations are listed in **Table 2.4**.[47]

[45] Rare-earth metal long term air exposure test. [Accessed 20-10-2014], Available from: http://www.elementsales.com/re_exp/.

[46] Lanthanide. [Accessed 20-10-2014], Available from: http://en.wikipedia.org/wiki/Lanthanide.

[47] FA Cotton, G Wilkinson and PL Gaus. *Basic Inorganic Chemistry*, 3rd edition. John Wiley and Sons, INC, New York, 1995, p.50.

Table 2.4: The electron configuration of the different lanthanides.[47,48]

Elements	Electron configuration
Lanthanum	$[Xe]4f^{0}5d^{1}6s^{2}$
Cerium	$[Xe]4f^{2}5d^{0}6s^{2}$
Praseodymium	$[Xe]4f^{3}5d^{0}6s^{2}$
Neodymium	$[Xe]4f^{4}5d^{0}6s^{2}$
Promethium	$[Xe]4f^{5}5d^{0}6s^{2}$
Samarium	$[Xe]4f^{6}5d^{0}6s^{2}$
Europium	$[Xe]4f^{7}5d^{0}6s^{2}$
Gadolinium	$[Xe]4f^{7}5d^{1}6s^{2}$
Terbium	$[Xe]4f^{9}5d^{0}6s^{2}$
Dysprosium	$[Xe]4f^{10}5d^{0}6s^{2}$
Holmium	$[Xe]4f^{11}5d^{0}6s^{2}$
Erbium	$[Xe]4f^{12}5d^{0}6s^{2}$
Thulium	$[Xe]4f^{13}5d^{0}6s^{2}$
Ytterbium	$[Xe]4f^{14}5d^{0}6s^{2}$
Lutetium	$[Xe]4f^{14}5d^{1}6s^{2}$

2.7.2 General chemistry of the REEs

Trivalent compounds of REEs (Eu, Sa, Tu and Yb) containing anions such as OH^{-}, NO_3^{-}, SO_4^{2-}, CO_3^{2-} and $C_2O_4^{2-}$ decompose to their respective oxides when heated. Trivalent REE complex formation is determined by charge, size and chelating properties of both the metal cation and the counter anion.

Most of the REEs react rapidly with hot water (than in cold water) to form basic hydroxides (**Equation 2.1**). The basicity of the different compounds decreases with

[48] RD Harrison, H Ellis and HDB Jenkis. *Book of Data*, 1st edition. Longman Group Limited, 1988, p.47.

an increase in atomic number (**Figure 2.12**) with $La(OH)_3$ the most basic and $Lu(OH)_3$ is the least basic hydroxide.

$$2REE_{(s)} + 6H_2O_{(l)} \rightarrow 2REE\,(OH)_{3(aq)} + 3H_{2(g)} \quad \textbf{2.1}$$

REEs also form hydrides when heated in presences of hydrogen at temperature between 300 - 400°C. These hydrides are capable of conducting heat and are relatively stable at high temperature of about 900 °C. They also release hydrogen from water and form oxides (**Equation 2.2**).[49]

$$CeH_2 + 2H_2O \rightarrow CeO_2 + 3H_2 \quad \textbf{2.2}$$

Anhydrous halides are formed when heating the metal in the presence of halogens or by heating the oxide with excess ammonium halide at approximately 300°C (**Equation 2.3**).[47]

$$REE_2O_3 + 6NH_4Cl \rightarrow 2REECl_3 + 6NH_3 + 3H_2O \quad \textbf{2.3}$$

Transition-metal and main-group elements usually have coordination numbers of 2 to 6. The REEs however have CN larger than 6 with resulting coordination polyhedra that includes trigonal prisms with CN = 6 to numerous variations with a stepwise capping of the prism face to form complexes with CN = 9. Other coordination polyhedra include the formation of square antiprisms (CN = 8) and dodecahedra with CN = 12. Complexes with coordination numbers as high as 16 have also been documented. The coordination geometries are believed to be directed by ligand steric factors rather than crystal field effects. The correlation between coordination number and ionic radii is given in **Table 2.5**.

[49] The chemistry of lanthanides. [Accessed 25-08-2014], Available from: http://unaab.edu.ng/opencourseware/Chemistry%20of%20Lanthanides%20and%20Actinides.pdf.

Table 2.5: Effect of coordination number on ionic radii of the REEs.[50]

Ion	CN[a]	Radii	Ion	CN[a]	Radii	Ion	CN[a]	Radii
La^{3+}	6	103.2	Tb^{3+}	7	98.0	Br^{-}	6	196
	7	110.0		8	104.0	Br^{3+}	4	59
	8	116.0		9	109.5	Br^{5+}	3	31
	9	121.6	Tb^{4+}	6	76.0	Br^{7+}	4	25
	10	127.0		8	88.0		6	39
	12	136.0	Dy^{2+}	6	107.0	I^{-}	6	220
Ce^{3+}	6	101.0		7	113.0	O^{2-}	2	135.0
	7	107.0		8	119.0		3	136.0
	8	114.3	Dy^{3+}	6	91.2		4	138.0
	9	119.6		7	97.0		6	140.0
	10	125.0		8	102.7		8	142.0
	12	134.0		9	108.3	S^{2-}	6	182.0
Ce^{4+}	6	87.0	Ho^{3+}	6	90.1	S^{4+}	6	34.0
	8	97.0		8	101.5	S^{6+}	4	12.0
	10	107.0		9	107.2		6	29.0
	12	114.0		10	112.0	Se^{2-}	6	198.0
Pr^{3+}	6	99.0	Er^{3+}	6	89.0	Se^{4+}	6	50.0
	8	112.6		7	94.5	Se^{6+}	4	28.0
	9	117.9		8	100.4		6	42.0
Pr^{4+}	6	85.0		9	106.2	Te^{2-}	6	221.0
	8	96.0	Tm^{2+}	6	103.0	Te^{4+}	3	52.0
Nd^{2+}	8	129.0		7	109.0		4	66.0
	9	135.0	Tm^{3+}	6	88.0		6	97.0
Nd^{3+}	6	98.3		8	99.4	Te^{6+}	4	43.0
	8	110.9		9	105.2		6	56.0
	9	116.3	Yb^{2+}	6	102.0	N^{3-}	4	146.0
	12	127.0		7	108.0	N^{3+}	6	16.0
Sm^{2+}	7	122.0		8	114.0	N^{5+}	3	-10.4
	8	127.0	Yb^{3+}	6	86.8		6	13.0
	9	132.0		7	92.5	P^{3+}	6	44
Sm^{3+}	6	95.8		8	98.5	P^{3+}	4	17
	7	102.0		9	104.2		5	29
	8	107.9	Lu^{3+}	6	86.1		6	38
	9	113.2		8	97.7	As^{3+}	6	58
	12	124.0		9	103.2	As^{3+}	4	33.5
Eu^{2+}	6	117.0	Sc^{3+}	6	74.5		6	46
	7	120.0		8	87.0	C^{4+}	3	-8
	8	125.0	Y^{3+}	6	90.0		4	15
	9	130.0		7	96.0		6	16
	10	135.0		8	101.9	Si^{4+}	4	26.0
Eu^{3+}	6	94.7		9	107.5		6	40.0
	7	101.0	F^{-}	2	128.5	Ge^{2+}	6	73
	8	106.6		3	130.0	Ge^{4+}	4	39
	9	112.0		4	131.0		6	53
Gd^{3+}	6	93.8		6	133.0	Sn^{4+}	4	55
	7	100.0	Cl^{-}	6	181.0		5	62
	8	105.3	Cl^{5+}	3	12.0		6	69.0
	9	110.7	Cl^{7+}	4	8.0	H^{+}	1	-38
Tb^{3+}	6	92.3		6	27		2	-18

[50] Rare earth coordination chemistry. [Accessed 20-10-2014], Available from: http://fs1.uclg.ru/books/pdf/1356799053_Huang_Ch._ _Rare_Earth_Coordination_Chemistry_%5B2010,_ENG%5D.pdf.

The REEs with their relatively high oxidation state (+3) are inclined to form numerous complexes with electron donor ligands with high electronegativity which is situated on the left hand side of the spectrochemical series ($I^- < Br^- < S^{2-} < SCN^- < Cl^- < NO_3^- < N_3^- < F^- < OH^- < C_2O_4^{2-} \approx H_2O < NCS^- < CH_3CN < py < NH_3 < en < bipy < phen < NO_2^- < PPh_3 < CN^- \approx CO$).Typical complexes include $[Er(NCS)_6]^{3-}$and YbI_2(CN = 6), $[Y(PhCOC_6H_4COMe)_3].H_2O$ (CN = 7), Gd_2S_3 (CN = 8), $[Sc(\eta^1\text{-}NO_3)(\eta\text{--}NO_3)(Ph_3PO)_2]$ (CN = 9), $[La_2(CO)_3].8H_2O$ (CN = 10) and $[Ce(NO_3)_6]^{3-}$ (CN = 12).

2.8 Conclusion

The above discussion has shown that the REEs with their unique chemical and physical properties are currently amongst the most valuable elements (like gold, copper etc.) in the world. It is anticipated that their demand will continue to increase in the near future to keep in step with an increase in global demand and the development as well as improvement of new technologies. The ever increasing REE demands, especially in the electronic and energy replacement industry, are expected to put pressure on the production of these elements and in the process put upward pressure on the metal prices. Economic and political decisions made by large market participants such as China will inevitability lead to REE production and supply fluctuations and thereby influence the future of this group of elements.

3 Chemical analysis of different samples containing REEs: Literature survey

3.1 Introduction

The early history of the REEs is predominantly based on the separation and purification of the individual elements from mineral ores a tough challenge due to their chemical similarity. REEs were originally isolated as oxides from bearing minerals in the 18th and 19th centuries. Development in new separation techniques, especially extraction methods during the 20th century, allowed for the isolation of these elements as pure metals by extraction methods (**Chapter 2, Section 2.5**).[51]

The driving force for the development in the separation and isolation of these elements are mainly due to their important applications in the electronic and technology fields as magnets, phosphors, metal alloys, etc. (see **Chapter 2**, **Table 2.2**). The difficulty in separation and isolation of the individual REEs from natural minerals stems from the resistance of this group of elements to chemical attack by many mineral acids and alkalis. This resistance to chemical attack not only complicates the separation techniques, but also the accurate analysis of the REEs in different host materials. Complete or effective sample dissolution remains a cornerstone in the proper and accurate characterization and quantification of any mineral or ore sample. Analytical methods such as X-ray fluorescence and neutron activation analysis, which do not require sample dissolution have become very handy for the accurate analysis of REEs in higher concentrations, especially in mineral ores, but have however has limited application in trace and ultratrace analysis.

[51] Rare earth elements. [Accessed 09-09-2014], Available from: http://www.sgtk.ch/rkuendig/dokumente/HS11_Rare_Earth_Elements.pdf.

This chapter discusses the progress made in the dissolution and accurate quantification of REEs in different compounds. Furthermore, the use of various analytical techniques such as spectrometry and digestion techniques will be discussed with the aim of identifying suitable techniques for the quantifying of REE complexes as well as the determination of their purity.

3.2 Digestion techniques

Complete sample dissolution remains one of the most important steps for the complete or total quantification of chemical compounds, minerals or mineral ores. Lanthanide phosphate minerals obtained from apatite weathering is notoriously insoluble or chemically inert. The three basic techniques available to effect the complete dissolution of these highly inert materials include open beaker acid / base reactions at elevated temperatures (wet ashing), the use of fluxes (anionic liquids) and finally microwave digestion at high pressure and temperature.

Ivanova *et al.*[52] used microwave digestion and four different combinations of H_3BO_3, HNO_3, H_2O_2 and HF dissolution procedures (A, A', B and B') to investigate the dissolution of REEs quantitatively in NIST-SRM-2709 (San J. Soil) and other samples. All the resultant solutions obtained from the different digestion procedures were analyzed using inductively coupled plasma mass spectrometry (ICP-MS) and the results for the NIST-SRM-2709 (San J. Soil) analysis is presented in **Table 3.1**. These results indicate that procedure B' gave the best REE recoveries compared to their expected or certified values. Each reported value is the mean of five parallel determinations and is characterized by the respective standard deviation (SD).

[52] J Ivanova, R Djingova, S Korhammer and B Markert. *Talanta,* 2001, **54**, pp.567-574.

Table 3.1: Results from the analysis of NIST-SRM-2709 (San J. Soil), (mg/kg).[52]

Element	Five replicates (Mean (SD))				Certified values (SD)
	Procedure A	Procedure A'	Procedure B	Procedure B'	
Ce	18.6(6)	26(1)	30(7)	43.1(1)	42
Dy	1.7(1)	2.1(2)	2.1(2)	3.07(7)	3.5
Eu	0.54(2)	0.67(2)	0.70(7)	1.06(5)	0.9
Gd	1.3(1)	2.96(5)	3.02(6)	4.6(2)	-
Ho	0.35(2)	0.39(1)	0.43(3)	0.65(2)	0.54
La	4.6(3)	11.6(2)	5.1(8)	21.1(9)	23
Lu	0.150(7)	0.18(1)	0.19(2)	0.23(1)	0.272(7)
Nd	7.0(6)	11(1)	8.4(8)	17.5(1)	19
Pr	1.0(1)	2.73(5)	1.9(2)	4.4(3)	-
Sm	1.7(1)	2.5(2)	2.0(2)	3.48(5)	3.8
Tb	0.29(1)	0.34(1)	0.33(3)	0.56(2)	0.52(5)
Y	9.0(5)	11.3(1)	10(2)	17.6(6)	18
Yb	1.03(5)	1.6(1)	1.3(1)	1.80(3)	1.6

Procedure A: The NIST-SRM-2709 + HNO_3 + H_2O_2 + HF in Teflon pressure vessels introduced to microwave digestion

Procedure A': The overnight stay of the NIST-SRM-2709 + HNO_3 + H_2O_2 + HF in Teflon pressure vessels at room temperature before introduced to microwave digestion.

Procedure B: The NIST-SRM-2709 + HNO_3 + HF in Teflon pressure vessels introduced to microwave digestion and addition of H_3BO_3.

Procedure B': The overnight stay of the NIST-SRM-2709 + HNO_3 + HF in Teflon pressure vessels at room temperature before introduced to microwave digestion and addition of H_3BO_3.

Kashiwakura *et al.*[53] determined the concentration of REEs present in coal fly ash particles. In their method, the coal ash particles were transferred to a teflon beaker and digested using mineral acids such as HNO_3, HCI and HF on a hot plate (open beaker). The solutions were analyzed using ICP-MS (**Table 3.2**).

Table 3.2: Comparison of the determined REE contents in coal fly ash particles (Ash A and Ash B).[53]

Sample (mg/kg)	%Element															
	Sc	**Y**	**La**	**Ce**	**Pr**	**Nd**	**Sm**	**Eu**	**Gd**	**Tb**	**Dy**	**Ho**	**Er**	**Tm**	**Yb**	**Lu**
Ash A	12.7	71	49.8	123	14.5	62	16.8	3.2	15.6	2.5	14.4	2.7	8.7	1.0	7.7	1.0
Ash B	13.5	51	54.2	117	13.4	54	10.8	2.4	9.3	1.5	8.8	1.7	5.7	0.7	5.4	0.7

Krachler *et al.*[54] used three methods, namely closed vessel acid digestion on a hot plate, microwave digestion and high pressure ashing for the dissolutions of the REEs in peat samples. They used different volumes of acids (HNO_3, HBF_4 and HF) for digestion. The use of the fluorinated acid resulted in the precipitation of the fluoride compounds which they dissolved using boric acid (H_3BO_3). Samples were characterized with ICP-MS (**Table 3.3**). Microwave digestion turned out to be the best method for digestion of peat samples compared to hot plate and high pressure ashing as indicated by the REE recoveries reported in **Table 3.3**.

[53] S Kashiwakura, Y Kumagai, H Kubo and K Wagatsuma. *Open Journal of Physical Chemistry*, 2013, **3**, pp.69-75.

[54] M Krachler, C Mohl, H Emons and W Shotyk. *J. Anal. At. Spectrom*, 2002, **17**, pp.844-851.

Table 3.3: Recovery (µg/g) of REEs as determined in the reference material GBW 07602 Bush Branches and Leaves.[54]

Element	Closed pressurised digestion (Mean (SD))			Certified value
	Hot plate	High pressure asher	Microwave	
La	1.16(3)	1.01(5)	1.37(8)	1.23(7)
Ce	2.41(5)	2.01(1)	2.50(9)	2.4(2)
Pr	282(7)	237(1)	283(11)	210
Nd	1.020(3)	0.87(1)	1.05(4)	1.1
Sm	189(5)	167(1)	193(7)	190(10)
Eu	37.1(6)	32.3(6)	37(1)	37(2)
Gd	153(3)	143(1)	170(6)	180
Tb	21.2(9)	20.7(4)	24.4(8)	26
Dy	119(3)	110(1)	138(4)	120
Ho	21.3(8)	20.9(6)	26.4(8)	27
Er	56.9(8)	52.8(4)	73(3)	60
Tm	7.7(4)	8.0(7)	10.4(3)	8
Yb	47(2)	44.3(9)	66(3)	63(8)
Lu	6.4(3)	6.8(5)	10.6(3)	12

Vozzella and Condit[55] studied the quantification of yttrium in complex nickel-base super alloys. The initial step was to dissolve the yttrium containing alloy in different HF concentrations using microwave digestion. Their results showed that the stability of the yttrium solution increased in 5 % HF, compared to the other acid concentrations investigated. The solutions were analyzed using ICP-OES and yttrium was quantitatively recovered with RSD smaller than 5 % obtained for these analysis.

Chung *et al.*[56] investigated the solubility of lanthanum, cerium, neodymium, samarium, europium, gadolinium, dysprosium, erbium, ytterbium and yttrium oxalates in different acids (nitric and oxalic). In their method, the REEs were mixed with

[55] PA Vozzella and DA Condit. *Anal. Chem.,*1988, **60**, pp.2497-2500.

[56] DY Chung, EH Kim, EH Lee and JH Yoo. *Journal of Industrial and Engineering Chemistry*, 1998, **4**, pp.277-284.

oxalate and centrifuged to separate/concentrate the newly formed precipitate from the mother solution. They analyzed the filtrate using ICP-OES to investigate the effect of oxalic acid concentration on the solubility of rare earth oxalate in HNO_3 and *vice versa* to study the effect of HNO_3 on the solubility of rare earth oxalates. Microwave digestion[52,54,55] was often used in this study to digest REE samples prior to analysis due to its ability to accelerate sample dissolution time.

3.3 Inductively Coupled Plasma Optical emission spectrometry (ICP-OES)

ICP has become the method of choice to do simultaneous multi-element analysis in complex matrices, which are also able to detect in the micro and ultra micro ranges with calibration curves which are linear over orders of magnitude. Not surprisingly, this method has also extensively been used to quantify REEs.

Bangia *et al*.[57] dissolved REEs into a nuclear grade graphite (containing thulium) to synthesize a REE-graphite compound. They dry-ashed the synthetic compound of REEs at 900 °C and dissolved the ashed samples in diluted HCl, and then analyzed it with ICP-OES. Their results indicated dysprosium, europium, gadolinium and samarium recoveries between 88 - 125 % with the RSD of 3 - 4 % as shown in **Table 3.4**.

Table 3.4: The recoveries of REEs after being introduced to ICP-OES.[57]

Element	Wavelength (nm)	Added amount (ppm)	Amount recovered (ppm)	%recovery	%RSD
Dy	346.5	1	0.96	96	3
Eu	420.5	1	1.18	118	3
Gd	379.6	1	0.88	88	3
Sm	442.4	2	2.5	125	4

[57] TR Bangia, BA Dhawale, VC Adya and MD Sastry. *Fresenius Z. Anal. Chem*, 1988, **332**, pp.802-804.

In another study Gasquez *et al*.[58] extracted REEs from a granite pegmatite, using a cation exchange resin with different HNO_3 concentrations as eluent. They collected the REE samples and analyzed six replicates using ICP-OES (**Table 3.5**). REEs were recovered at HNO_3 < 0.14 mol/L and only recoveries with eluent concentrations above 0.14 mol/L are reported in **Table 3.5**.

Table 3.5: REEs (µg/g) in apatite extracted from granite pegmatite using different HNO_3 concentrations.[58]

Element	HNO_3			
	14 mol/L	7 mol/L	1.4 mol/L	0.14 mol/L
La	171(11)	176(16)	172(12)	174(16)
Ce	436(26)	419(24)	410(26)	425(27)
Nd	414(20)	397(16)	405(18)	390(22)
Sm	175(17)	172(16)	179(19)	169(17)
Eu	31.2(4)	29(3)	30(4)	30(4)
Gd	168(12)	172(14)	171(12)	174(15)
Dy	240(15)	238(15)	241(12)	249(14)
Yb	115(10)	116(8)	115(9)	118(9)
Lu	18.5(3)	19(2)	189(3)	18(3)

Bentlin *et al*.[59] digested coal fly ash (SRM 1633b), river sediment (BCR 320), Tibet sediment (NCS DC70319) and river water to accurately determine the REEs. Decontaminated polyethylene flasks were used to collect water samples, which were then transported to the laboratory where the samples were filtered and acidified with 5 % HNO_3. Two different dissolution techniques were used for the sediments and coal fly ash samples to produce homogeneous solutions. In the first method the samples were digested in a mixture of HNO_3, HF and H_2O_2 and allowed to stand for 60 minutes. Each mixture was then heated in a metallic block for 6 hours at 200 °C. After completion, the samples were cooled to room temperature, and 20 % H_3BO_3 was added to the mixtures and heated a second time, for 90 minutes at 160 °C. The samples were allowed to cool to room temperature and the solutions were transferred

[58] J A Gasquez, E Delima, RA Olsina, LD Martinez and M Guardia. *Talanta*, 2005, **67**, pp.824-828.

[59] FRS Bentlin and D Pozebon. *J. Braz. Chem. Soc.*, 2010, **21** (4), pp.627-634.

to a 50 mL polypropylene flask. In the second method, the samples were weighed and transferred to Pt crucibles containing concentrated HNO_3. The crucibles were then heated on a hot plate in order to evaporate the acid. Concentrated HF was added and allowed to evaporate. $Na_2B_4O_7{\cdot}7H_2O$ was then added to the crucibles and placed in a muffle furnace (1 100 °C) for 1 hour. After cooling to room temperature, the clear melt was dissolved in 10 % HCl at 90 °C. Once the melts were dissolved, the solutions were transferred to 50 mL polyethylene flasks containing concentrated HNO_3 and H_2O. These solutions were then diluted ten-fold with water before analyzed with ICP-OES. The ICP-OES method produced REE recoveries which were compatible with those specified for the CRM as shown in **Table 3.6**.

Table 3.6: ICP-OES analysis of REE content in Tibetan sediment samples after alkali decomposition.[59]

Element	Coal fly ash (µg/g)		River sediment (µg/g)		Tibet sediment (µg/g)		River water (µg/L)
	Certified	Found	Certified	Found	Certified	Found	Found
La	94	95(2)	45.7	45(2)	43(2)	42.1(9)	<0.010
Ce	190	195(3)	94.4	99(2)	78(5)	79(2)	0.72(2)
Pr	3.3	3.2(3)	0.50	0.48(4)	8.57(3)	9.0(3)	<0.036
Nd	85	86.3(8)	-	43.9(5)	30.6(8)	29(1)	0.36(1)
Sm	20	20.3(3)	-	11.3(7)	5.4(3)	5.4(7)	<0.062
Eu	4.1	4.42(1)	2.02(7)	2.12(1)	0.97(5)	1.03(2)	<0.003
Gd	13	12.1(9)	-	65(2)	4.6(2)	4.7(1)	<0.036
Tb	2.6	2.64(9)	1.0	1.1(1)	0.70(4)	0.9(1)	<0.023
Dy	17	18.1(3)	-	3.4(1)	3.91(1)	3.6 (2)	<0.007
Ho	3.5	3.3(1)	2.50	2.53(3)	0.79(6)	0.71(4)	<0.008
Er	10.4	11(1)	-	4.32(8)	2.4(1)	2.45(9)	<0.013
Tm	2.1	2.26(6)	-	0.63(2)	0.38(2)	0.43(3)	<0.009
Yb	7.6	7.62(2)	-	2.39(2)	2.55(8)	2.2(2)	<0.003
Lu	1.2	1.38(5)	-	0.37(2)	0.39(2)	0.41(2)	<0.003

3.4 Limit of detection and quantification (LOD and LOQ)

Limit of detection and quantification are very important parameters which normally indicate the sensitivity and accuracy which can be obtained with a certain method or

equipment. As such, they are useful to show or indicate the lowest levels of observation and lowest levels at accurate quantification which are possible for an analysis.

Oliveira *et al.*[60] used two different laboratories to investigate the presence of samarium, europium, dysprosium, terbium and ytterbium in gadolinium oxide (Gd_2O_3) as impurities. They used ICP-OES at different conditions (wavelengths, parameter conditions) in both laboratories to determine the LODs (**Figure 3.1**). Lab A reported lower LODs compared to Lab B, except for samarium (330.637 nm) and terbium (356.174 nm).

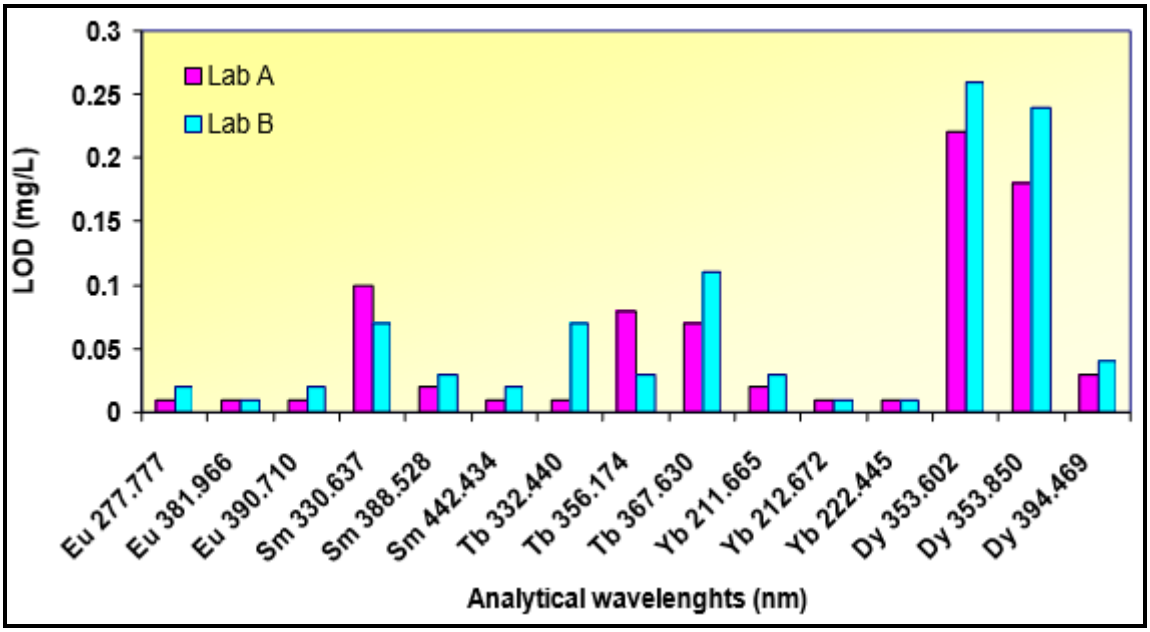

Figure 3.1: The LODs of the REEs at different wavelengths.[60]

Bentlin *et al*.[59] determined the LODs of REEs with 10 measurements of the blank solution before analyzing coal fly ash (SRM 1633b), river sediment (BCR 320), Tibet sediment (NCS DC70319) and river water. They used ICP-OES and found that the ultrasonic nebulization and axially viewed plasma provided the lowest LODs (**Table 3.7**) for the same samples analyzed.

[60] LC Oliveira, IS Silva and MI Rucandio. *International Nuclear Atlantic Conference (INA), Rio de Janeiro (RJ), Brazil, September 27 to October 2, 2009.*

Table 3.7: The LODs (mg/L) as a function of the nebulizer and plasma view.[59]

Element	Nebulizer and Plasma View			
	Pneumatic		Ultrasonic	
	Axial	Radial	Axial	Radial
La	0.164	0.818	0.010	0.073
Ce	1.436	4.799	0.069	0.272
Pr	1.114	2.767	0.036	0.237
Pr	0.834	3.401	0.041	0.205
Nd	1.252	2.696	0.060	0.194
Sm	0.804	2.023	0.062	0.417
Sm	2.077	3.398	0.039	0.221
Eu	0.034	0.140	0.003	0.019
Gd	0.504	2.684	0.036	0.309
Gd	0.196	0.659	0.012	0.106
Tb	0.349	1.942	0.023	0.211
Tb	1.354	4.610	0.039	0.239
Dy	0.165	0.579	0.007	0.045
Ho	0.167	0.512	0.008	0.065
Er	0.160	0.922	0.013	0.137
Tm	0.433	1.050	0.009	0.080
Yb	0.018	0.061	0.003	0.090
Lu	0.017	0.124	0.003	0.014

In another study Bangia *et al*.[57] determined LODs using blank solutions before analyzing the digested REE samples. They used two techniques namely ICP-OES and DC arc-OES. Their findings are illustrated in **Table 3.8** and the LODs ranged between 0.01 - 0.2 µg/mL and 0.004 - 0.1 µg/mL when using ICP-OES and DC arc-OES respectively, suggesting that DC arc-OES produces better results (lower detection) compared to ICP-OES for REE analysis.

Table 3.8: The LODs (µg/mL) of REEs investigated with ICP-OES and DC arc-OES.[57]

Element	ICP-OES	DC arc-OES
Ce	-	0.1
Dy	0.2	0.05
Er	-	0.025
Eu	0.01	0.05
Gd	0.02	0.01
Ho	-	0.025
La	-	0.025
Lu	-	0.025
Sm	0.1	0.1
Sc	-	0.01
Tb	-	0.1
Yb	-	0.004
Y	-	0.01

Santoyo *et al*.[61] used high performance liquid chromatography (HPLC) to separate REEs from a synthetic standard (81 B), where the LODs were determined in a 100 µL injection loop volume. Interestingly, they found that the LODs of the elements with even atomic numbers to be higher than elements with odd atomic numbers (**Table 3.9**). The LODs and LOQs ranged between 0.3 - 5.8 ng and 1.0 - 19.3 ng respectively.

[61] E Santoyo, M Guevara and SP Verma. *Journal of Chromatography A*, 2006, 1118, pp.73-81.

Table 3.9: The LODs of the REEs obtained from a synthetic standard (81-B).[61]

Element	Amount injected (ng)	%RSD		LOD (ng)	LOQ (ng)
		Retention time	Peak area		
La	18.89	0.4	4.9	3.7	12.3
Ce	**45.63**	**0.3**	**3.2**	**5.8**	**19.3**
Pr	6.98	0.3	4.0	1.0	3.3
Nd	**34.06**	**0.3**	**2.5**	**3.0**	**10.0**
Pm	-	-	-	-	-
Sm	**10.67**	**0.4**	**2.1**	**0.8**	**2.7**
Eu	4.34	0.3	1.8	0.3	1.0
Gd	**14.68**	**0.4**	**4.5**	**2.3**	**7.7**
Tb	2.70	1.1	5.3	0.6	2.0
Dy	**18.07**	**1.0**	**3.9**	**2.7**	**9.0**
Ho	3.77	0.8	4.1	0.6	2.0
Er	**11.78**	**1.02**	**3.3**	**1.5**	**5.0**
Tm	1.93	1.3	4.8	0.4	1.3
Yb	**12.26**	**1.5**	**2.5**	**1.2**	**4.0**
Lu	1.79	1.9	5.1	0.3	1.0

Bolded: REEs with even number atomic numbers.

Johns *et al*.[62] used the two complexing agents, 2-hydroxyisobutyric acid (HIBA) and lactic acid, in conjuction with chrysoidine (dye) to separate REEs and other metals (K, Ba, Sr, Ca, Na, Mg, Mn, Cr, Fe, Co and Li) with anion exchange chromatography. They found that both complexing agents showed good separation, while HIBA reduced the mobility of the analytes compared to that of lactic acid. The LODs of HIBA and lactic acid ranged between 0.22 - 0.61 µM and 0.12 - 1.43 µM respectively (**Table 3.10**).

[62] C Johns, M Macka and PR Haddad. *Journal of Chromatography A*, 2003, 997, pp.87-94.

Table 3.10: The LODs (µM) of REEs using HIBA and lactate.[62]

Element	HIBA	Lactate
	LOD (µM)	LOD (µM)
La	0.23	0.24
Ce	0.27	0.27
Pr	0.27	0.24
Nd	0.29	0.23
Sm	0.30	0.23
Eu	0.28	0.12
Gd	0.25	-

3.5 Ultraviolet and visible absorption spectroscopy (UV/Vis)

UV/Vis spectroscopy is one of the older analytical techniques that are used to quantify elements. A pre-requirement for this technique is the formation of coloured compounds while its main limitations remain interfering absorbances from other elements and concentration restrictions due to limitations of Beer's law (curvature of calibration curve at high concentration). A few examples of the use of UV/Vis to quantify REEs are discussed in the following paragraphs.

Iljas *et al*.[63] used microwave digestion to dissolve monazite sand samples of approximately 0.1 g using different acids (HNO_3, HF, $HClO_4$). After complete sample digestion, the acids were evaporated before adding water to the samples. The solutions were then filtered and the REE filtrates were separated with solvent extraction. Di-n-buthyldithiocarbamate (DBDTC) was used as complexing agent for gadolinium and cerium. In the next step these elements were separated using petroleum ether as organic phase and water as aqueous phase. Concentrations of gadolinium and cerium were determined in both the organic and aqueous phases using UV/Vis at the wavelengths of 268 and 274 nm respectively. They reported

[63] N Iljas, D Hendrati and V Srigati. *Proceeding of The International Seminar on Chemistry*, 2002, pp.93-99, Jatinangor, 30-31 October 2008.

percentage recoveries of 96.42 and 92.12 % (compared to XRF values) for gadolinium and cerium respectively.

In another study, Tan and Le[64] dissolved cerium nitrate in water and mixed it with benzoic acid azo phenylcalix[4]arene (BAPC), a complexing agent, which were dissolved in double distilled water. The solution was analyzed using UV/Vis at 515 nm. This method was successfully applied to analyse cerium in soil samples collected from Kontum. The resultant amounts of cerium are presented in **Table 3.11**.

Table 3.11: UV/Vis analysis of cerium in Kontum samples.[64]

Sample	Cerium (mg/kg)
1	58.2
2	159.1
3	70.5
4	163.6
5	217.4

Borai and Mady[65] separated the REEs, thorium and uranium in a monazite sample. The sample was dissolved in hot concentrated H_2SO_4. Thorium, uranium and REEs were separated using gradient elution. The UV/Vis analysis showed concentrations of 4.77 ± 0.1 and 0.427 ± 0.04 % for ThO_2 (λ = 660 nm) and U_3O_8 (λ = 660 nm) respectively.

Tarafder *et al*.[66] complexed REEs with 2,3-dihydroxynaphthalene and water and extracted the REEs from the aqueous solution at pH > 8 using ethyl acetate. The organic phase containing the REEs were selectively stripped at the pH of 6.3. The separated REEs (solution) were reacted with arsenazo(III) and their concentrations

[64] LV Tan and NTN Le. *International Journal of Chemical Engineering and Applications*, 2011, **2**, pp.381-385.

[65] EH Borai and AS Mady. *Applied Radiation and Isotopes*, 2002, 57, pp.463-469.

[66] PK Tarafdar, SK Pradhan, RK Mondal and JK Sircar. *J. Indian Chem. Soc.*,2013, 90, pp.1975-1982.

were determined using a spectrophotometric analysis showing all REE recoveries to be above 98 %.

3.6 Complexes of REEs

Coordination chemistry of REEs has developed rapidly since the 1940's and the chemistry of rare earths has been studied intensively due to their unique property to form complexes with large coordination numbers. This unusual coordination behavior (coordination numbers from 3 to 12) of lanthanides complicate the characterization of these complexes and a suite of different techniques which include IR, UV/Vis and elemental composition (C N O H) are usually employed for proper characterization. [DyNTA]·$4H_2O$ and [PrNTA]·$3H_2O$ were for example wrongly characterized and later corrected to be eight and nine coordinated complexes for dysprosium and praseodymium.[67]

Huang *et al.*[68] synthesized four lanthanide nitrilotriacetate complexes [Ln(NTA)]·nH_2O (Ln = lanthanum, praseodymium, neodymium and europium; n = number of water molecules) to determine the coordination number of each complex. Their method of synthesis entailed the mixing of equal molar quantities of lanthanides and H_3NTA at pH ~5.5 (adjusted using NaOH solution). The mixtures were then heated at 140 - 150 ˚C in sealed teflon-lined stainless steel vessels. The resultant solutions were separated from the undissolved solids by filtration and cooled to room temperature, which resulted in the crystallization of the desired compounds. The crystals were then separated from the mother solution by filtration and washed with ethanol. The chemical composition (given in **Table 3.12,** column 1) of their complexes were confirmed by X-ray diffraction (XRD) and elemental analysis as well as infrared spectroscopy (IR).

[67] KA Gschneidnerjr and L Eyring. *Handbook on the Physics and Chemistry of Rare Earths: Non-Metallic Compounds I*. North-Holland Publishing Company, Amsterdam, New York, Oxford, 1979, **3**, pp.81-297.

[68] L Huang, L Zhang and LL Jin. *Journal of Molecular Structure*, 2004,**692**, pp.121-126.

In another study, Wang *et al.*[69] synthesized $Na_z[Dy(L)]\cdot nH_2O$ (L = DTPA, EDTA, NTA; z = number of sodium atoms; n = number of water molecules) by dissolving Dy_2O_3 and the different potential ligands in a 1:1 molar ratio (Dy:L) to obtain the different compounds reported in **Table 3.12** (column 2) at a pH 6.5 (adjusted using $NaHCO_3$) and leaving the solutions to stand for two weeks at room temperature to crystallize. All the isolated complexes (**Table 3.12**) were characterized by single-crystal X-ray diffraction, elemental analysis, FT-IR and TG-DTA.

Zhongcheng *et al.*[70] synthesized different terbium complexes by mixing $TbCl_3$ with phthalic acid, iso-phthalic acid, o-aminobenzoic acid, salicylic acid and sulfosalicylic acid as potential ligands in 1:3 or 2:3 molar ratios. The Tb compounds presented in **Table 3.12** (column 3) were obtained at pH of 6.0 - 6.5 (using NaOH to adjust the pH). These complexes were characterized by elemental analysis, IR and UV spectra.

Table 3.12: The characterization of different REEs complexes.

Complex[68]	**Complex[69]**	**Complex[70]**
$LaC_6H_8NO_7$	$Na_4[Dy(DTPA)_2]\cdot 2H_2O$	$[Tb(BA)_3]$
$PrC_6H_8NO_7$	$Na[Dy(EDTA)]\cdot 6.25H_2O$	$[Tb(o\text{-}amino)_3]$
$NdC_6H_8NO_7$	$Na_3[Dy(NTA)_2]\cdot H_2O$	$[Tb(Sal)_3]$
$EuC_6H_8NO_7$		$[Tb_2(Ssal)_3]$
		$[Tb_2(Phth)_3]\cdot 4H_2O$
		$[Tb_2(iso\text{-}Phth)_3]\cdot 4H_2O$

Yang *et al.*[71] synthesized europium and terbium complexes with 2,6-bis[(indol-2-ylmethylene)amino]pyridine as ligand (L) by dissolving 2,6-diaminopyridine and indole-2-carbaldehyde with 1:2 molar ratios in ethanol. The final products were obtained after the solutions have been stirred at room temperature for 3 hours, filtered and washed with ethanol and dried in a vacuum. They found these complexes

[69] J Wang, G Gao, Z Zhang, X Zhang and Y Wang. *Journal of Coordination Chemistry,* 2007, **60** (20), pp.2221-2241.

[70] Z Zhongcheng, S Wangen, R Jianming, H Baiyun and L Younian. *Trans. Nonferrous Met. Soc. China,* 2005.

[71] TL Yang, WW Qin, ZF Xiao and WS Liu. *Chem. Pap*., 2005,**59** (1), pp.17-20.

to be soluble in methanol, dimethylformamide and DMSO, partially soluble in chloroform and ethanol, and insoluble in benzene, diethyl ether, and tetrahydrofuran. The composition of the synthesized complexes and ligand in **Table 3.13** (column 1) were characterized by elemental analysis, conductivity, ^{1}H NMR and IR.

Table 3.13: The characterization of different REE complexes.

Complex[71]	Complex[73]	Complex[74]	Complex[75]
$[EuL(NO_3]\cdot 2H_2O$	H_5DTPA	$[Eu(PicNO)_3Cl_3]$	$[Dy(DBM)_3]$
$[TbL(NO_3]\cdot 2H_2O$	$(NH_4)_2[(Dy(DPTA)]\cdot 4H_2O$	$[Eu(TPPO)_3Cl_3]$	$[Dy(DBM)_3phen]$
	$(NH_4)_2[(Ho(DPTA)]\cdot 4H_2O$	$[Eu(PicNO)_8I_3]$	$[Dy(DBM)_3dmphen]$
	$(NH_4)_2[(Er(DPTA)]\cdot 4H_2O$	$[Eu(PicNO)_8(ClO_4)_3]$	$[Dy(DBM)_3tmphen]$
	$(NH_4)_2[(Yb(DPTA)]\cdot 4H_2O$	$[Eu(PicNO)_8(PF_6)_3]$	$[Dy(DBM)_3dpphen]$
		$[Eu(Phen)(OAc)_3]$	
		$[Eu(Phen)Cl_3]\cdot 3H_2O$	
		$[Eu(Phen)(NO_3)_3]$	
		$[Eu(Tripy)Cl_3]\cdot H_2O$	
		$[Tb(Tripy)(NO_3)_3]\cdot H_2O$	

L=2,6-bis[(indol-2-ylmethylene)amino]pyridine

In another REE study Yamakawa[72] synthesized samarium tris-trifluoroacetylacetonate by dissolving the samarium chloride in methanol and mixing it with methanolic solutions of trifluoroacetylacetone. The same procedure was applied for the preparation of terbium tris-trifluoroacetylacetonate, but in this case ammonium hydroxide was used to deprotonate the bidentate ligand instead of potassium carbonate.

In the same study Yamakawa[72] also synthesized four new complexes with praseodymium, erbium, samarium and terbium. The different REE salts were dissolved in ethanol and added to solutions containing thienyl and piperidine. The resulting complexes were identified as praseodymium-thienyl ($[Pr(C_{24}H_{12}O_6F_9S_3)]$), erbium-thienyl ($[Er(C_{24}H_{12}O_6F_9S_3)]$), samarium-thienyl ($[Sm(C_{24}H_{12}O_6F_9S_3)]$) and

[72] KA Yamakawa. Interim Engineering Report for 1 November - 31 January 1963. [Accessed 25-11-2014], Available from: www.dtic.mil/cgi-bin/GetTRDoc?AD=AD0296419.

terbium-thienyl ([Tb($C_{24}H_{12}O_6F_9S_3$)]). These complexes were characterized by elemental analysis, melting point determination and fluorescence spectra.

Inomata *et al.*[73] synthesized REE (erbium, holmium, dysprosium and ytterbium) complexes with diethylenetriamine-N,N,N^{I},N^{II},N^{II}-pentaacetic acid (H_5DTPA). They dissolved $Ln_2(CO_3)_3 \cdot nH_2O$ in aqueous solutions of H_5DTPA in 1:1 molar ratios. The complexes in **Table 3.13** (column 2) were characterized by elemental analysis, thermal analysis, infrared (IR) absorption spectra and X-ray diffraction.

A REE study was conducted by Melby *et al.*[74] who synthesized numerous europium complexes using 4-picoline N-oxide (PicNO), triphenylphosphine oxide (TPPO), 1.10-phenanthroline (Phen) and tripyridyl (Tripy) as ligands. Europium-tris(4-picoline N-oxide)chloride was synthesized by dissolving europium oxide in HCl and adding 4-picoline N-oxide. The mixture was evaporated to dryness and hot ethanol was added. The mixture was filtered and the solution was treated with ethyl acetate. Other complexes which include $[Eu(TPPO)_3]Cl_3$ and $[Eu(PicNO)_3]I_3$ were synthesized using the same procedure, which was also successfully used as the starting material for the synthesized $[Eu(PicNO)_3Cl_3]$. One of their other synthetic efforts entailed the dissolution of ammonium hexafluorophosphate, 4-picoline N-oxide and europium chloride in water, followed by the gradual addition of ethanol, boiling acetone or ether to obtain the europium octakis(4-picoline N-oxide)hexafluorophosphate complex. The different complexes obtained from various synthetic procedures are listed in **Table 3.13** (column 3) and were characterized by elemental analysis and melting point determinations.

Rashid *et al.*[75] synthesized $[Dy(DBM)_3]$ by dissolving dysprosium and dibenzoylmethane (DBM) in ethanol in a 1:3 molar ratio. The addition of a second ligand (phen / dmphen / tmphen / dpphen) (L_2), dissolved in ethanol, to $[Dy(DBM)_3]$ in molar ratios of 1:3:1 yielded the $[Dy(DBM)_3L_2]$ type complexes. The different

[73] Y Inomata, T Sunakawa and FS Howell. *Journal of Molecular Structure,* 2003, **648**, pp.81-88.

[74] LR Melby. J Rose, E Abramson and JC Caris. *Synthesis and Fluorescence of Trivalent Lanthanide Complexes*, 1964, **86,** pp 5117-5124.

complexes (**Table 3.13,** column 4) were characterized by elemental analysis, infrared (IR) spectra, thermogravimetric analysis (TGA), differential scanning calorimetry (DSC) and fluorescence spectrometry.

A final example of the interesting REE complexes that were reported are those synthesized by Guo *et al.*[76]*.* They succeeded in isolating new complexes by using 4-hydroxybenzaldehyde and 2-amino-6-nitrobenzothiazole dissolved in benzene in a 1:1 molar ratio. They dissolved the newly formed product in THF and added triethylamine, followed by the dropwise addition of methacryloyl chloride to form the shiff-base monomer. Methyl methacrylate and ethyl acrylate were then added to a solution containing the newly synthesized shiff-base monomer in dry N,N-dimethylformamide (DMF). The shiff-base macromolecular ligand and the terbium-complex polymer were found to be soluble in absolute ethanol with heating and also demonstrated good solubility in toluene and THF. The complex was characterized using FT-IR, NMR, UV/Vis, fluorescence spetrophotometry and Waters Gel Permeation Chromatography.

3.7 Separation methods (ion exchange and solvent extraction)

The biggest challenge in REE chemistry is the separation and purification of the different elements. The dominance of the +3 oxidation state of all 17 elements in this group, as well as the similarity of their chemistry not only complicate their separation but also involve numerous separation steps which utilizes some small differences in their chemistry. The synthesis of different REE complexes was initially developed with the intention of separating REEs using ion (anion or cation) exchange chromatography and solvent extraction (**Chapter 2, Section 2.5**). Developments in this field as well as extensive research resulted in the availability of the different REEs in high purity due to the efficiency of the ion exchange and solvent extraction methods employed in the separation and purification of the different metals.

[75] MAA Rashid, B Saad, EM Negim and MI Saleh. *World Applied Sciences Journal*, 2012, **17**(8), pp.958-963.

[76] L Guo, S Wu, F Zeng and J Zhao. *European Polymer Journal,* 2006, **42**, pp.1670-1675.

Fractional crystallization, fractional precipitation and liquid-liquid extraction have also been used successfully to separate the REEs from each other.

3.7.1 Ion (anion or cation) exchange chromatography

Initially the complexing agents EDTA and NTA were found to be effective for the separation of some of the REEs. In 1952, Vikery used EDTA and NTA to separate REEs using cation exchange chromatography. He reported the precipitation of EDTA and NTA in the resin bed at high hydrogen concentration presenting the coordination of the REEs with these complexing agents. The precipitate problem was solved by Powell, Spedding and Wheelwright. EDTA has been used by Mayer and Freiling for the separation of terbium, europium and samarium in a synthetic mixture by cation exchange chromatography. They eluted the REEs at concentrations of 0.026 M and 0.017 M eluents of EDTA.[77] The quantitative separation of a mixture of samarium, neodymium, praseodymium and lanthanum with NTA was performed by Holleck and Hartinger.[77] They reported the elution of samarium as the first REE from the column, followed by neodymium, praseodymium and lanthanum respectively, in the pH range of 3.5 to 4.2.

Campbell (1973) used α-hydroxyisobutyrate (α-HIB) on a cation exchange resin for the separation of REEs. A similar study was carried out by Chopin and Silva using α-HIB for the separation of REEs. In another study Karol used 2-hydroxy-2-methylbutyrate as complexing agent and it was found to be a more effective complexing agent compared to α-HIB for the separation of REEs.[67]

Ishikawa *et al.*[78] separated REEs from different rock samples using α-hydroxyisobutyric acid (α-HIBA) as the eluent. They digested samples on a hot plate in teflon-vials. Before analysis of these solutions, cation exchange chromatography was used to eliminate matrix elements or impurities which could potentially interfere with REE analysis using HPIC analysis. The analysis of basalt (JB-1a and JB-2) (**Table 3.14**) and other samples were investigated.

[77] FH Spedding and AH Daane. *The Rare Earths.* John Wiley and Sons, Inc., New York and London, 1961, pp.55-73.

[78] T Ishikawa, K Sugimoto and K Nagaishi. *Geochemical Journal*, 2003, **37**, pp.671-680.

Table 3.14: HPIC analysis of basalt (JB-1a and JB-2) samples.[78]

Element	JB-1a (µg/g)	Certified values (µg/g)	JB-2 (µg/g)	Certified values (µg/g)
La	38.0	37.6	2.35	2.35
Ce	65.2	65.9	7.07	6.76
Pr	7.10	7.30	1.19	1.01
Nd	26.8	26.0	6.84	6.63
Sm	5.09	5.07	2.38	2.31
Eu	1.55	1.46	0.920	0.86
Gd	4.57	4.67	3.33	3.28
Tb	0.733	0.69	0.636	0.60
Dy	4.08	3.99	4.13	3.73
Ho	0.829	0.71	0.944	0.75
Er	2.19	2.18	2.55	2.60
Tm	0.342	0.33	0.402	0.41
Yb	2.12	2.10	2.78	2.62
Lu	0.331	0.33	0.395	0.40

Bahti *et al.*[79] used dibutylthiocarbamic (DBDTC) and dibutylthiophosphoric (DBDTP) to separate the elements lanthanum, cerium, neodymium, praseodymium, yttrium and gadolinium present in xenotime and monazite. They recovered the REEs between 58 - 79 % and 80 - 100 % at the pH range of 2.0 - 7.0 using DBDTC and DBDTP respectively, and the products were characterized by IR, UV and mass spectrometry.

In another study, Strelow and Jackson[80] separated a number of REEs with cation exchange chromatography, and characterized the products with spark source mass spectrometry. They managed to recover lanthanum, cerium and lutetium up to 99.7 % (**Table 3.15**).

[79] HH Bahti, Y Mulyasih and A Anggraeni. *Proceedings of the 2nd International Seminar on Chemistry,* Jatinangor, 24-25 November 2011, pp.421-430.

[80] FWE Strelow and PFS Jackson. *Analytical Chemistry*, 1974, **46**(11), pp.1481-1486.

Table 3.15: The analysis of REEs with spark source mass spectrometry.[80]

Element	Concentration (ppm)	%CV
La	27(2)	6.37
Ce	52(3)	5.69
Pr	8.2(4)	5.26
Nd	33.8(1)	3.17
Sm	6.76(9)	7.2
Eu	1.70(5)	3.11
Gd	5.48(9)	7.07
Tb	0.813(7)	5.75
Dy	4.43(3)	5.08
Ho	0.917(9)	8.58
Er	2.70(7)	6.20
Tm	0.422(8)	4.35
Yb	3.10(2)	7.06
Lu	0.506(1)	6.14

In another study by Pierce and Peck[81] all the REEs (except scandium) were separated from an aqueous perchlorate phase at different acidities using di-(2-ethylhexyl)hydrogenphosphate.

3.7.2 Solvent extraction

Currently, solvent extraction is widely used in the commercial processing of rare earth compounds. Separation of REEs by this technique depends upon a preferential distribution of individual REEs between two immiscible solvents with the K_d value (**Equation 3.1**) a semi-quantitative indication of separation.

$$K_d = \frac{C_{org}}{C_{aq}}, \ (C_{org} = \text{organic phase}, \ C_{aq} = \text{aqueous phase}) \qquad \textbf{3.1}$$

[81] TB Pierce and PF Peck. *Analyst*, 1963, **88**, pp.603-607.

This technique was first used in the 1950s for REE separation, but it required the complexation of the REEs with appropriate ligands prior to separation. Complexing agents included di(2-ethyl-hexyl)phosphoric acid (D_2EHPA)[82] and tributyl phosphate (TBP) and have been reported as the most successful extractants for the REEs.

The TBP / HNO_3 system was found to be highly successful for separation of mixtures of lanthanum, neodymium and praseodymium (**Equation 3.2**)[67] but was found to be less successful for the separation of elements beyond terbium in the REE group.

$$Ln(NO_3)_{3(aq)} + 3TBP(H_2O)_{(org)} \rightarrow [Ln(TBP)_3(NO_3)_3]_{(org)} + 3H_2O \qquad \textbf{3.2}$$

The extraction of REEs using TBP was also studied[67] using thiocyanate as ligand but the separation was not very successful. Other solvent systems which have been investigated include di-2-ethylhexyl orthophosphoric acid (HDEHP). Tomioka *et al.*[83] investigated supercritical CO_2 as an extracting solvent of REE oxides (Nd_2O_3 and Gd_2O_3) using the TBP / HNO_3 solvent system. Tomioka *et al.* reported higher extraction of neodymium compared to gadolinium as the supercritical CO_2 pressure increased as reported in **Table 3.16**.

Table 3.16: Fraction of extracted lanthanide ions from their oxides.[83]

	The extracted fraction			
	Nd		**Gd**	
Supercritical CO_2 pressure	12 MPa	15 MPa	12 MPa	15 MPa
%Extraction	51 %	45 %	46 %	28 %

Swain and Otu[84] separated a number of REE nitrates using bis(2,4,4-trimethylpentyl)phosphinic acid. The REE nitrate compounds were dissolved in $HClO_4$ and the NO_x were subsequently removed by evaporation. The remaining solution was diluted with water and extracted with (2,4,4-trimethylpentyl)phosphinic

[82] JM Sanchez, M Hidalgo and V Salvad. *Solvent Extraction and Ion Exchange*, 1999, **17**(3), pp.455-474.

[83] O Tomioka, Y Enokida and I Yamamoto. *Journal of Nuclear Science and Technology*, 1998, **35**(7), pp.515-516.

acid. Zamani *et al.*[85] improved the separation of lanthanum and europium with bis(2-ethylhexyl)phosphoric acid (DEHPA) by adding the 12-crown-4 ether ($12C_4$) as a masking agent to the aqueous phase. This crown ether was found to have a positive impact in stabilizing the lanthanum in the aqueous phase as compared to the addition of 18-crown-6 ($18C_6$).[86]

Li *et al.*[87] investigated the separation of REEs with 2-ethylhexyl hydrogen-2-ethylhexylphosphonate (EHEHP) by solvent extraction. They used equal volumes of the EHEHP and water (pH = 4, adjusted using NaOH) in a separating funnel in the presence of $KMnO_4$. The organic phase was analyzed by ICP-MS (**Table 3.17**) and the results indicated recoveries of 95 - 102 % of REEs with the limit of detection (LOD) and limit of quantification (LOQ) values between 0.007 - 0.024 and 0.02 - 0.08 respectively with RSD of 0.7 - 2.8 %.

[84] B Swain and EO Otu. *Elsevier*. *Separation and Purification Technology*, 2011, **83**, pp.82-90.

[85] AA Zamani, MR Yaftian and N Dallali. *Iran. J. Chem. Chem. Eng..* 2006, **25**(3), pp.15-19.

[86] ZA Ali, YM Reza and D Naser. *Iran. J. Chem. Chem. Eng.*, 2006, **25**(3).

[87] B Li, Y Zhang and M Yin. *Analyst*, 1997, **122**, pp.543-547.

Table 3.17: The analysis of REEs separated by solvent extraction using EHEHP.[87]

Element	Five replicates		LOD	LOQ	%RSD
	Determined	%Recovery			
La	95.6	95.2	0.007	0.02	0.98
Pr	101.5	101	0.019	0.05	1.0
Nd	98.7	98.3	0.003	0.06	1.0
Sm	99.9	99.9	0.013	0.04	1.8
Eu	98.1	98.0	0.01	0.03	1.2
Gd	97.1	96.7	0.02	0.07	2.8
Tb	99.7	99.6	0.013	0.04	1.6
Dy	101	101	0.024	0.08	0.73
Ho	102	102	0.007	0.02	1.1
Er	98.5	98.5	0.026	0.09	1.2
Tm	97.3	97.2	0.01	0.03	1.7
Yb	94.3	94.2	0.025	0.08	2.3
Lu	97.6	97.5	0.01	0.03	2.3
Y	99.1	97.9	0.009	0.03	2.3

3.8 Conclusion

In the above discussions it was demonstrated that different digestion techniques, complex formation and separation methods were intensively applied in the processing and analysis of REEs. The digestion techniques are significant for wet analysis of REEs using techniques such as ICP-OES. Microwave digestion was applied more than other digestion methods due to its efficiency in digesting most of the REE compounds with an added advantage of clean digestion products. A micro analyzer was used (for C, H, N and O analysis) by most of the researchers for the identification of the synthesized compounds. Finally, analysis of REEs in different materials can be performed with a combination of analytical techniques.

4 Selection of analytical techniques used in this study

4.1 Introduction

Different types of analytical techniques have been used for the accurate determination of REEs to date. It is noteworthy that there is no one-size fits all technique which can provide all the information about the different REE complexes. The different techniques are designed to provide a certain aspect or provide information on the compound to solve the concrete problems of analysis either qualitatively or quantitatively. This chapter focuses on the theoretical principles of selected instrumental methods and main components to give an overview of well-established methods which are commonly used for REE analysis. The discussion will include the use as well as the pros and cons of analytical techniques such as inductively coupled plasma-optical emission spectrometry (ICP-OES), CHNS-micro analyser, infrared spectroscopy (IR), melting point determination, digestion (microwave and open) methods and thermogravimetric analysis (TGA) which were used in this study.

4.2 Thermogravimetric Analysis (TGA)

Thermogravimetric analysis (TGA) is the technique used to determine the change in mass of the sample as a function of temperature or time. The TGA technique has an advantage of simple sample preparation procedure which does not require a prior dissolution of the sample. Analysis can be performed under increased temperature or under constant temperature but increasing exposure of the sample.[88]

The change of a sample's mass (due to change in properties such as melting, volatization, sublimation, etc.) is measured and recorded as demonstrated in

[88] Thermogravimetric analysis (TGA). [Accessed 04-03-2015], Available from: http://www.perkinelmer.com/cmsresources/images/44-74556gde_tgabeginnersguide.pdf.

Figure 4.1. The decomposition pattern (change of mass as function of temperature) of a sample provides useful information such as the amount of water, or the organic or ash content of the sample.[89] A main advantage of TGA is that is not restricted to samples or compounds with low melting points.

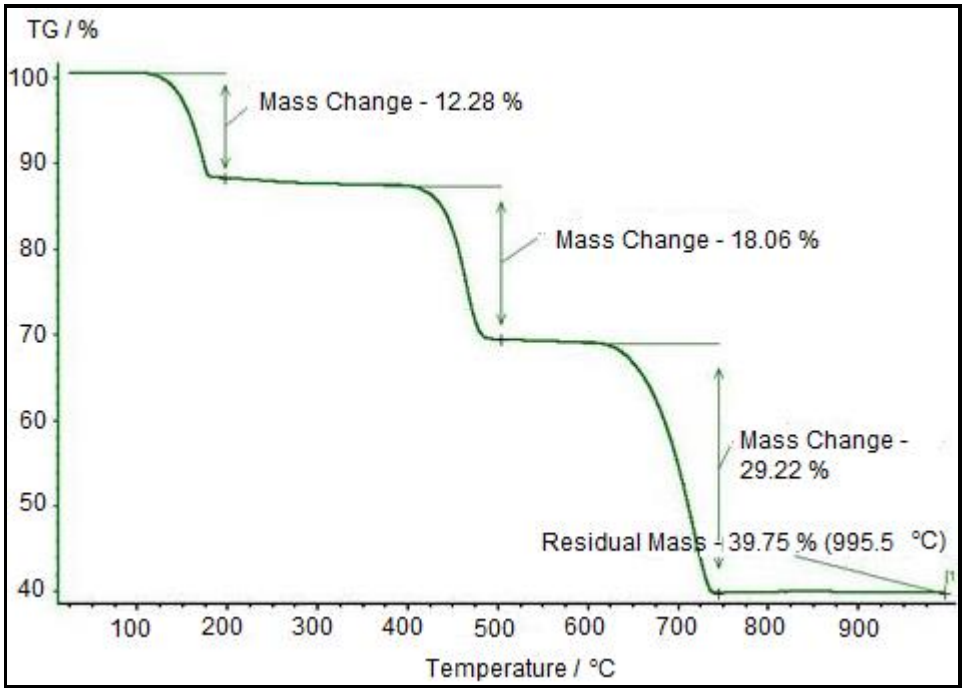

Figure 4.1: Typical profile of the mass loss as a function of temperature.[90]

4.3 Digestion (dissolution) methods

Sample dissolution can be a highly challenging step especially for unknown compounds. In wet acid digestion, sample dissolution is an important step to convert the solid sample to a homogeneous aqueous solution for qualitative and/or quantitative determinations. Some samples require extreme conditions such as high temperature and pressure to convert them into water soluble species in solution. Some of the commonly used techniques (such as microwave digestion) are discussed in the following sections.

[89] Interpreting TGA curves. [Accessed 04-03-2015], Available from: Interpreting TGA curves http://www.masontechnology.ie/x/Usercom_13.pdf

[90] Whewellite heat decomposition mass curve. [Accessed 04-03-2015], Available from: http://ookaboo.com/o/pictures/picture/13003656/Whewellite_calcium_oxalate_monohydrate_h.

4.3.1 Microwave digestion

Microwave ovens were introduced to chemical laboratories in the late 1980's due to the development of this industrial technique for commercial usage which clearly demonstrated their ability to completely heat/digest chemical samples within a short period of time. Microwaves are known as radiation with a frequency range between 300 MHz - 300GHz and a wavelength of 0.1 - 100 cm (**Figure 4.2**).[91] A microwave oven's main component is the magnetron which is a high power microwave oscillator that produces the required microwaves for its particular purpose.

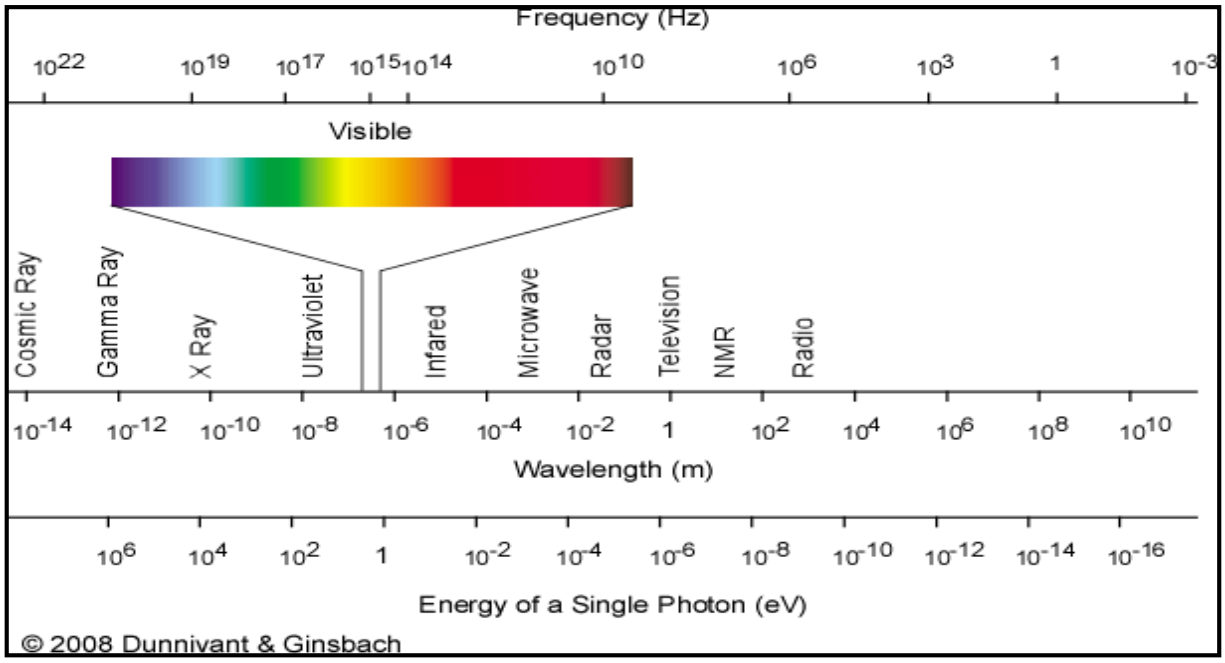

Figure 4.2: The electromagnetic spectrum.[92]

Microwaves heat the sample (see **Figure 4.3**) directly with a rapid increase in temperature and pressure and is independent of the thermal conductivity of the vessel materials. This property enables the microwave digestion technique to dissolve many materials using different acids. The choice of an acid or acid mixture for digestion normally depend on the analyte of interest and no single acid or acid mixture is universally applicable to all analyte groups. The digestion of metals, alloy or rock samples require higher temperatures and pressures to dissolve. The

[91] BL Hayes. *Microwave Synthesis: Chemistry at the Speed of Light*. CEM Publishing, USA, 2002, pp.7-28.

[92] The interaction of electromagnetic radiation with sample molecules. [Accessed 04-03-2015], Available from: http://people.whitman.edu/~dunnivfm/FAASICPMS_Ebook/CH1/1_2.html.

equipment is expensive and thereby makes this method of dissolution a relatively costly procedure. In addition, sample holders have a limited volume capacity. During the microwave process, the heat is directed to the sample and not the vessel containing it. The boiling of the solvent at this stage is not taken in consideration while any knowledge of the sample and solvent is important prior to digestion to avoid explosion.

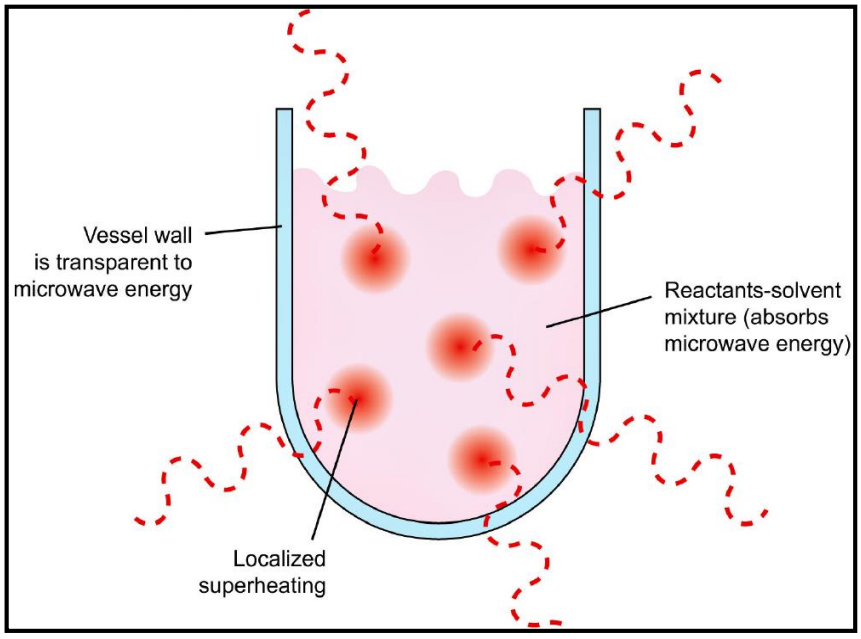

Figure 4.3: Heating of a sample by microwave digestion.[91]

4.3.2 Open vessel digestion (wet ashing)

Open vessel digestion (wet ashing) is easier, cheaper and the most commonly used method for samples dissolution. This method entails dissolution of the sample with the heating and stirring of the sample in an acidic environment at atmospheric pressure in an open beaker and allows the use of higher sample masses and acid volumes. However, the boiling point of the solvent is normally the limiting factor to determine the maximum temperature for digestion of a sample. Disadvantages of this digestion technique is its potential for contamination (from the surrounding environment), the loss of some volatile elements during the heating and the usually long digestion times. For samples that are difficult to digest completely, a combination of acids are normally used in wet ashing (**Table 4.1**) in an effort to dissolve different samples.

Table 4.1: Acids used for dissolution of different compounds.[93]

Acid	Typical Uses
HF	Removal of silicon and destruction of silicates; dissolves oxides of Nb, Ta, Ti, and Zr, and Nb, and Ta ores.
HCl	Dissolves many carbonates, oxides, hydroxides, phosphates, borates, and sulfides; dissolves cement.
HBr	Distillation of bromides (e.g., As, Sb, Sn, Se).
HI	Effective reducing agent; dissolves Sn^{+4} oxide and Hg^{+2}sulfide
H_2SO_4	Dissolves oxides, hydroxides, carbonates, and various sulfide ores; hot concentrated acid will oxidize most organic compounds.
H_3PO_4	Dissolves Al_2O_3, chrome ores, iron oxide ores, and slag.
HNO_3	Oxidizes many metals and alloys to soluble nitrates; organic material oxidized slowly.
$HClO_4$	Extremely strong oxidizer; reacts violently or explosively to oxidize organic compounds; attacks nearly all metals.

4.3.3 Flux or ionic liquids

Some samples such as soils, silicates, other oxides and sludges may also not be soluble in acids even under microwave conditions and in these cases the fusion method is used for dissolution. This technique requires a homogeneous mixture of a salt (the flux) and the sample in a specific sample-flux ratio to be heated to a temperature that exceeds the melting point of the salt. The sample is allowed to react (acid/base or redox) with the flux at high temperature. The resultant melt of the sample/flux mixture is allowed to cool to room temperature and is subsequently dissolved in diluted or concentrated acid solution or water and the solution is analyzed using wet analytical techniques such as ICP-OES / -MS. Some of the commonly used fluxes and the samples which they are used for are listed in **Table 4.2.**

[93] Multi-Agency Radiological Laboratory Analytical Protocols Manual: MARLAP, July 2004. [Accessed 16-08-2012], Available from: http://www.epa.gov/rpdweb00/docs/marlap/402-b-04-001b-13-final.pdf.

Table 4.2: Different conditions for the use of fluxes to decompose samples.[93]

Flux (mp, ˚C)	Fusion temperature, ˚C	Type of crucible	Types of sample decomposed
$Na_2S_2O_7$ (403)	Up to red heat	Pt, quartz, porcelain	For insoluble oxides and oxide-containing samples, particularly those of Al, Be, Ta, Ti, Zr, Pu, and the rare earths.
KOH (404)	450-600	Ni, Ag, glassy carbon	For silicates, oxides, phosphates, and fluorides.
Na_2CO_3 (853)	900-1 000	Ni, Pt for short periods (use lid)	For silicates and silica-containing samples (clays, minerals, rocks, glasses), refractory oxides, quartz, and insoluble phosphates and sulfates.
Na_2O_2 (460)	600	Ni, Ag, Au, Zr, Pt (< 500 ˚C)	For sulfides; acid-insoluble alloys of Fe, Ni, Cr, Mo, W, and Li; Pt alloys; Cr, Sn, and Zn minerals.
H_3BO_3 (160)	250	Pt	For analysis of sand, aluminum silicates, titanite, natural aluminum oxide (corundum), and enamels.
$Na_2B_4O_7$ (878)	1000-1 200	Pt	For Al_2O_3; ZrO_2 and zirconium ores, minerals of the rare earths, Ti, Nb, and Ta, aluminum-containing materials; iron ores and slags.
$LiBO_2$ (845)	1000-1 100	Pt, graphite	For almost anything except metals and sulfides. The tetraborate salt is especially good for basic oxides and some resistant silicates. The metaborate is better suited for dissolving acidic oxides such as silica and TiO_2 and nearly all minerals.
KF (857)	900	Pt	For the removal of silicon, the destruction of silicates and rare earth minerals, and the analysis of oxides of Nb, Ta, Ti, and Zr.

Literature indicates that minerals present as oxides, silicates and carbonates can be successfully dissolved using fusion digestion.[93] Samples present in other chemical forms such as metals, sulfides or organics should preferably be oxidized prior to the execution of a fusion procedure.

4.4 Inductively Coupled Plasma-Optical Emission Spectrometry (ICP-OES)

ICP-OES is an analytical technique used for the determination of most of the elements on the periodic table in a variety of aqueous matrices. This spectrometric technique has been proven successful for rapid multi-elemental analysis. A major requirement for this technique is the complete convertion of the sample into a homogenous solution (preferably aqueous) for accurate analysis.

The ICP consists of a peristaltic pump which transfers the sample to a nebulizer and then into a spray chamber and ultimately into the plasma (6000 - 10 000 K)[94] using argon as carrier and plasma gas (**Figure 4.4**). Atoms are excited in the plasma and emit their characteristic emission lines. Quantitative analysis are based on the fact that the emission intensities correspond to the concentrations of the analytes in the solution.

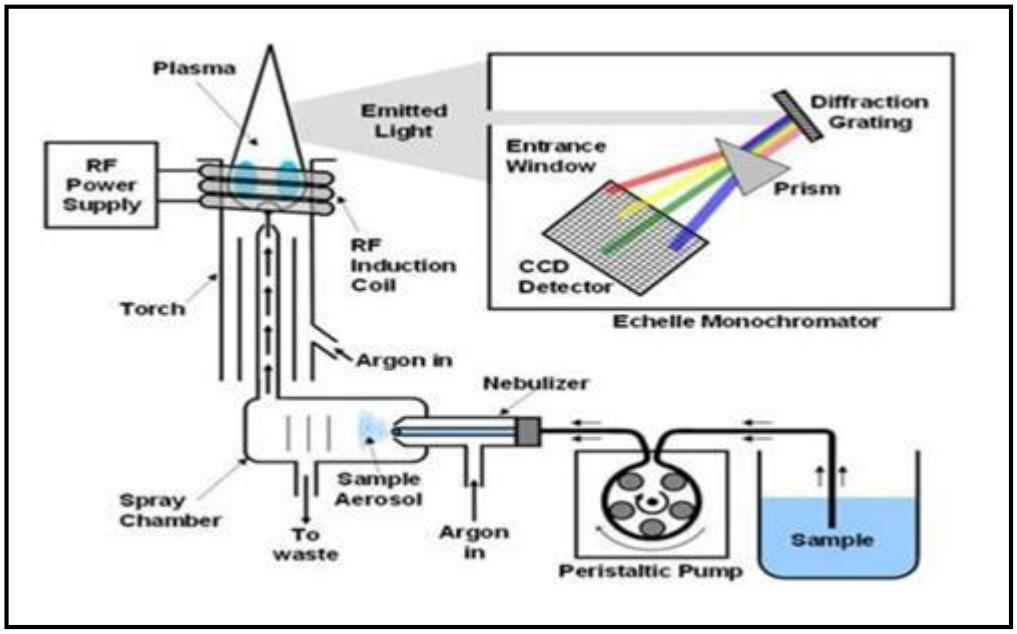

Figure 4.4: Schematic diagram of sample introduction to ICP-OES.[95]

4.4.1 Nebulizer and plasma torch

The most commonly used nebulizer (**Figure 4.5**) is a concentric quartz tube. In the nebulizer a sample is sucked into the capillary tube by a high pressure stream of argon gas flowing around the tip of the tube, and is converted into an aerosol. These fine droplets then occupy the spray chamber and are transferred subsequently to the plasma. The presence of high concentrations of totally dissolved solids is a major drawback of this type of a nebulizer as the solids may salt out and accumulate at the tip of the nebulizer and clog it.

[94] The inductively coupled plasma-atomic emission spectrometry. [Accessed 16-02-2015], Available from: http://people.whitman.edu/~dunnivfm/FAASICPMS_Ebook/Downloads/CH3_FINAL.pdf.

[95] Inductively coupled plasma. [Accessed 16-02-2015], Available from: http://www.rohs-cmet.in/content/icp-oes.

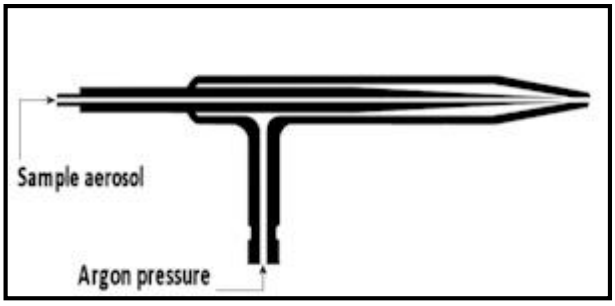

Figure 4.5: Concentric tube nebulizer.[96]

The inductively coupled plasma source is the energy source which reduce and activate the species in the aerosol (presented in **Figure 4.6**). It consists of three concentric quartz tubes through which a stream of argon gas flows. The tube is surrounded by a water-cooled induction coil that is powered by radio-frequency. Ar is converted to $Ar^+ + e^-$ and these cations and electrons flow in closed annular paths resulting in ohmic heat when an electrical current is passed through a conductor. Water is circulated in the coil to control the temperature experienced by the coil and to avoid the melting of the quartz torch due to continuous heating of the plasma.[97]

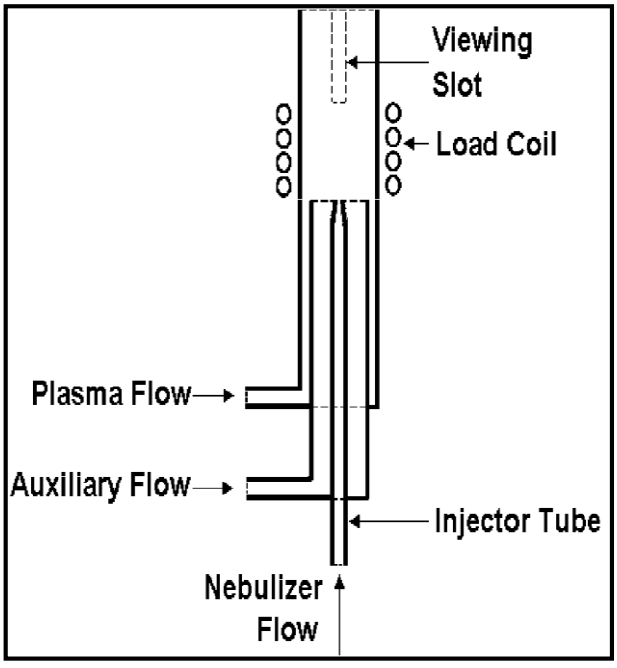

Figure 4.6: Plasma torch.[97]

[96] Inductively coupled plasma-optical emission spectrometry (ICP-OES). [Accessed 16-02-2015], Available from: http://www.chemiasoft.com/chemd/node/52.

[97] CB Boss and KJ Fredeen. *Concepts Instrumentation and Techniques in Inductively Coupled Plasma Optical Emission Spectrometry, 2nd edition*. The Perkin-Elmer Corporation, USA, 1997.

A monochromator (**Figure 4.7**) collects the light from the atomic emission of the sample and produces single spectra from a multi-wavelength source by allowing only specific lines to exit and strike the photo multi-playa. The entrance and exit slit control the size of the passing light passing through the monochromator.[98]

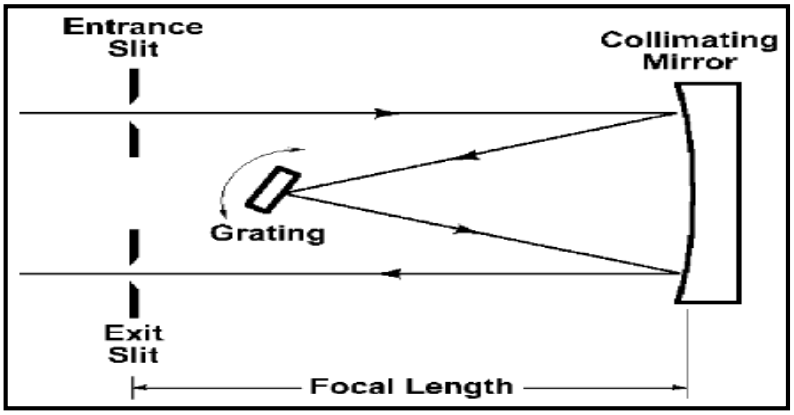

Figure 4.7: Monochromator.[97]

4.4.2 Wavelength selection

The primary goal of inductively coupled plasma is to activate a large amount of the elements present in the sample to emit their characteristic wavelengths which can be used to measure quantitatively and/or qualitatively each element present in the sample. Each element[97] has several specific wavelengths of varied sensitivity in the spectrum range which could be used for analysis. However, the wavelength to be used for a particular analysis is normally carefully selected to prevent any spectral overlap while still keeping in mind the need for the optimum sensitivity of the selected emission line for accurate analysis. The advantages and disadvantages of ICP-OES are presented in **Table 4.3**.

Table 4.3: Advantages of ICP-OES as analytical technique.[97]

Advantages	Disadvantages
Wide linear dynamic ranges, good sensitivity, low detection limits, good quantitative multi-element capability, limited spectral and chemical interferences.	Unable to determine halogens, Cl, Br and I. Analyse aqueous sample only.

[98] Turnablemonochromator. [Accessed 07-03-2015], Available from: http://www.shsu.edu/chm_tgc/primers/pdf/mono.pdf.

4.5 CHNS-micro analyser

The CHNS-micro analyser is a sealed gas analyser which convert the C, N, H and S to gaseous species at high temperatures which can be used to determine the molecular formula of an organic or organometallic compound (**Figure 4.8)**.[99]

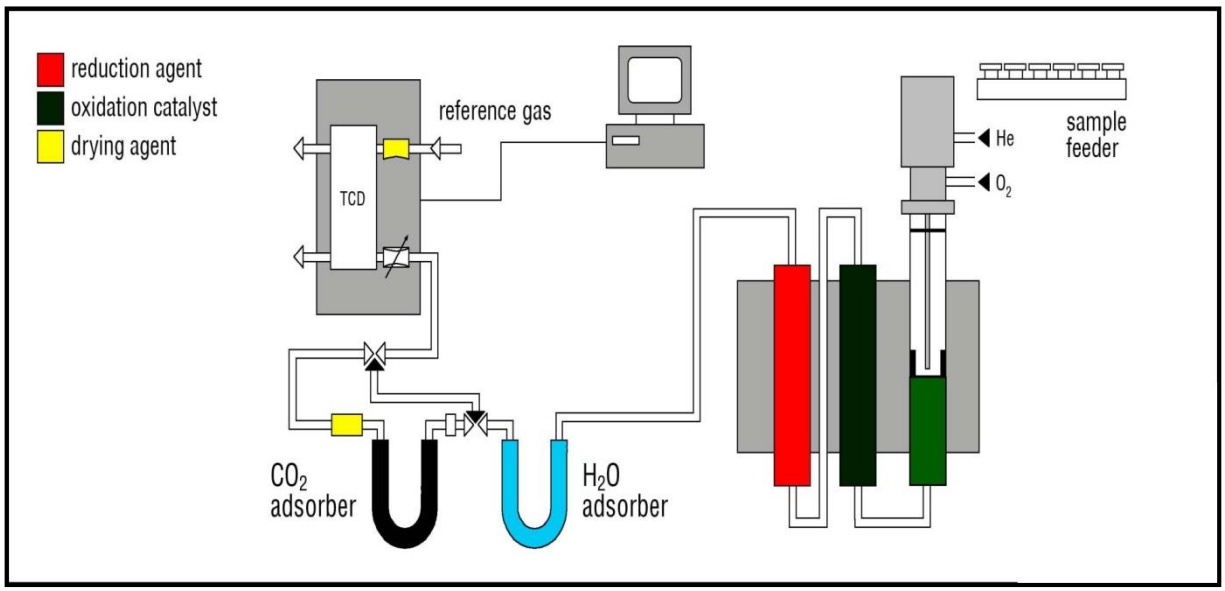

Figure 4.8: The operation of the CHNS micro analyser.[100]

The CHNS micro analyser is easy to operate and involves the weighing of a sample and its introduction into the analyzer, which automatically calculate the % C, N, H and S in the sample. High purity helium carrier gas is used to carry the sample contained in the tin capsules into the combustion chamber, then to the chromatographic separator and finally to the thermal conductivity detector (TCD) for CHNS analysis as N_2, CO_2, H_2O and SO_2. The gases are separated and transferred to the TCD which determine the quantity of each element in the sample. The elemental peaks of a sample is as illustrated in **Figure 4.9**.[101]

[99] M Thompson. Analytical Methods Committee: CHNS Elemental Analysers. The Royal Society of Chemistry, April 2008. [Accessed 10-03-2015], Available from:http://www.rsc.org/images/CHNS-elemental-analysers-technical-brief-29_tcm18-214833.pdf.

[100] Vario macro cube. [Accessed 10-03-2015], Available from: http://jdelement.com/ProductShow.asp?ID=121.

[101] Elemental combustion system chns-o. [Accessed 10-03-2015], Available from: http://www.costechanalytical.com/documentation/ECS%204010%20Brochure.pdf.

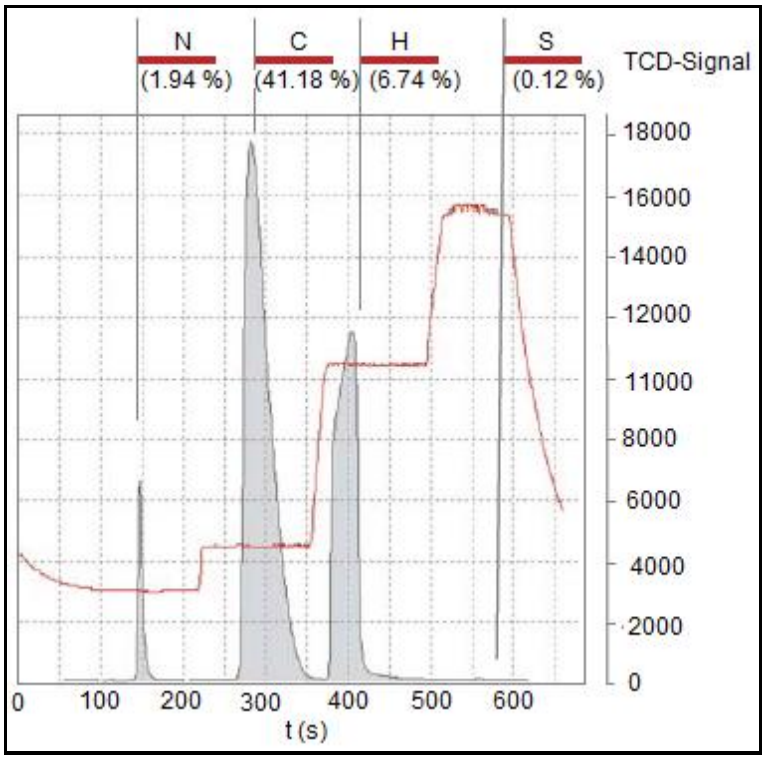

Figure 4.9: Typical micro analyser output indicate C, H, N and S content.[102]

4.6 Infrared spectroscopy (IR)

Infrared spectroscopy (IR) is a technique that is based on the absorption of electromagnetic radiation between 2.5 - 25 µm with the wavenumber ranging from 4000 - 400 cm^{-1} (mid-infrared)[103] and normally provides information about the functional groups present in a sample. However, it does not give detailed information about the structure of a compound and are seldomly used for quantitative purposes. The information contained in an IR spectrum comes from molecular vibrations (stretching, wagging and bending), **Figure 4.10**. The mid-infrared region can be divided into four sub-regions, namely stretching (4000 - 2500 cm^{-1}), triple-bond (2500 - 2000 cm^{-1}), double-bond (2000 - 1500 cm^{-1}) and the fingerprint region (1500 - 600 cm^{-1}). The other types of infrared such as near-infrared (< 400 cm^{-1}) and far-infrared (13 000 - 4000 cm^{-1}) are also used to obtain useful information of the compounds.[104]

[102] Elementar. [Accessed 10-03-2015], Available from: http://www.vertex.es/portal/docs/elementar/C_Elementar_vario_MICRO_cube.pdf.

[103] F Rouessac and A Rouessac. *Chemical Analysis: Modern Instrumentation Methods and Techniques,* 2nd edition. John Wiley and Sons, Ltd, San Francisco, 2007, pp.207-240.

[104] B Stuart. *Infrared Spectroscopy: Fundamentals and Applications, Analytical Techniques in the Sciences*. John Wiley. [Accessed 01-03-2015], Available from: http://www.researchgate.net/.

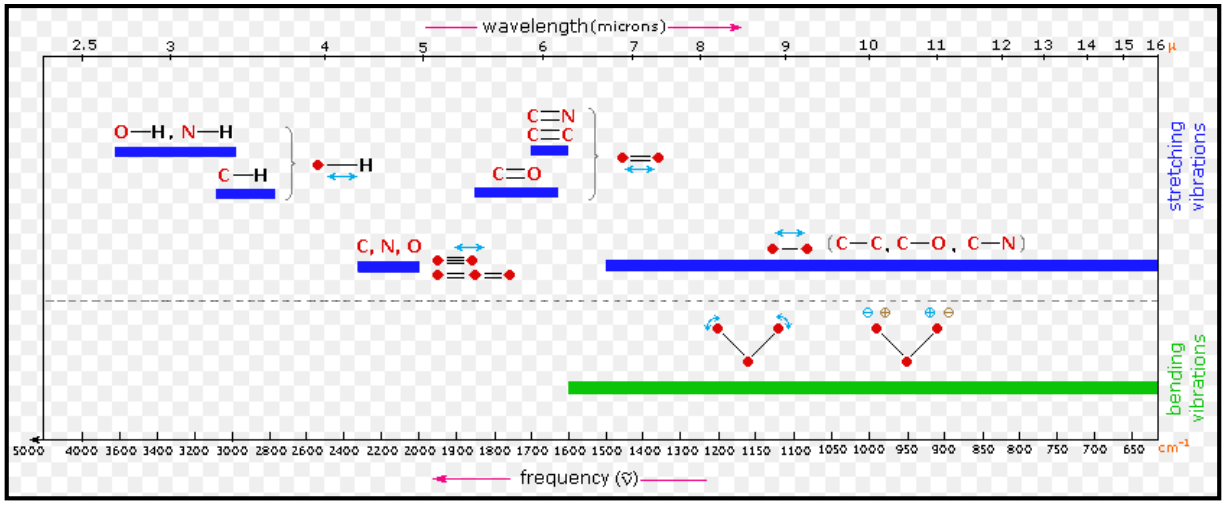

Figure 4.10: IR spectroscopy chart showing different regions of various kinds of vibrational bands.[105]

The fundamental purpose of infrared spectroscopy is based on the identification of functional groups that are present in the organometallic compound. Light from the source passes through the mirror, where it is divided into two ways, one passes through the sample and the other one simultaneously towards the reference detector (**Figure 4.11**).

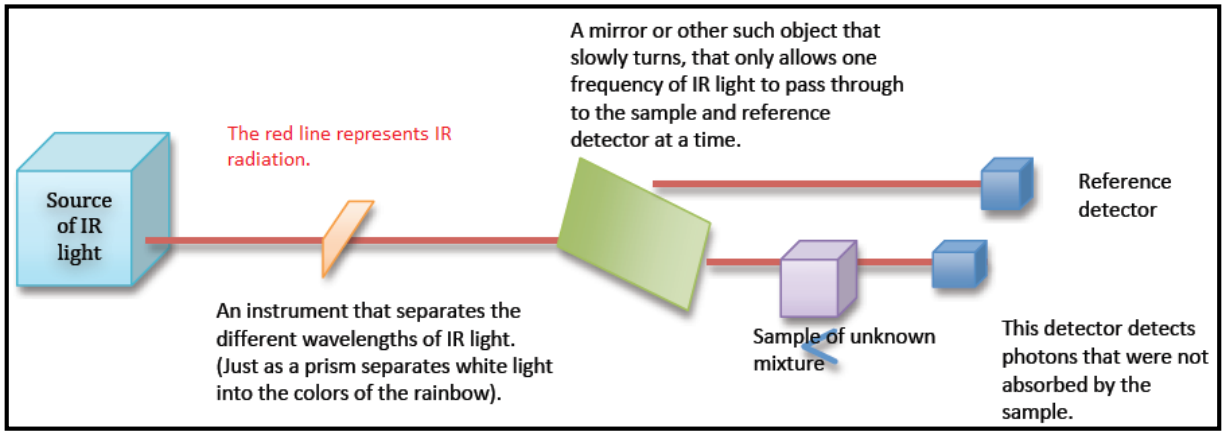

Figure 4.11: A simplified IR spectrometer.[106]

The light from its source gets absorbed upon the interaction with the chemical bonds in the sample. Two different atoms in a compound form an electric dipole moment

[105] Infrared spectroscopy. [Accessed 10-03-2015], Available from: http://chemistry.tutorvista.com/organic-chemistry/ir-spectroscopy.html.

[106] Molecular vibrations and infrared spectroscopy. [Accessed 10-03-2015], Available from:http://www.chem.ucla.edu/harding/ec_tutorials/tutorial31.pdf.

which oscillates with a unique frequency upon absorption of light. The irradiation of compounds containing non-polar bonds such as such as N_2, O_2 and Cl_2 results in no absorption of light due to the non-coupling with the infrared wave.[103] The process involved during the irradiation of the sample by the infrared light source is illustrated in **Figure 4.12**.

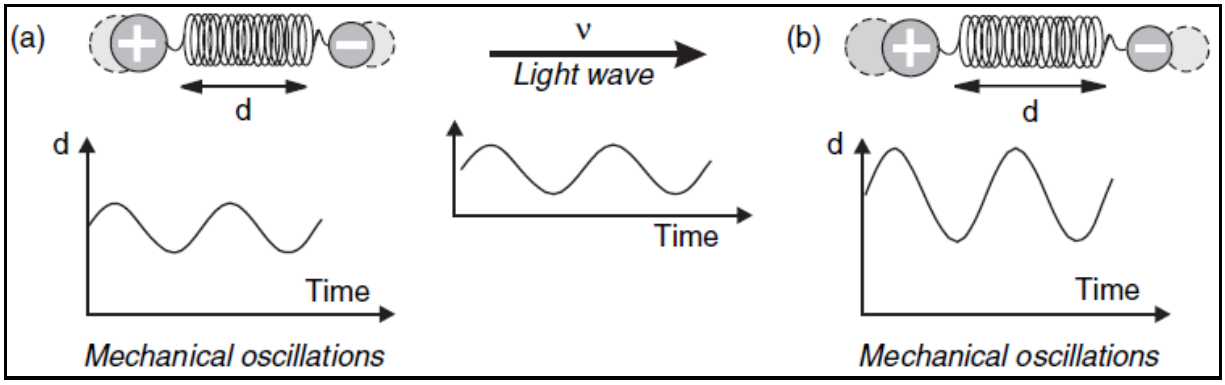

Figure 4.12: The mechanical interpretation of the interaction between a light wave and a polar bond.[103]

Upon irradiation with infrared light, certain bonds respond by increased vibration, stretching or wagging (faster vibrations). This response can be detected and translated into a visual representation (a spectrum) indicated in **Figure 4.13**. The energy at which any peak in an absorption spectrum appears, corresponds to the frequency of a vibration of a part of a sample molecule. Infrared spectroscopy requires a relatively small sample (solid or liquid) for analysis compared to other techniques such as UV/Vis. Factors such as baseline correction, smoothing, derivatives, deconvolution and curve-fitting are taken in consideration for quantitative analysis.

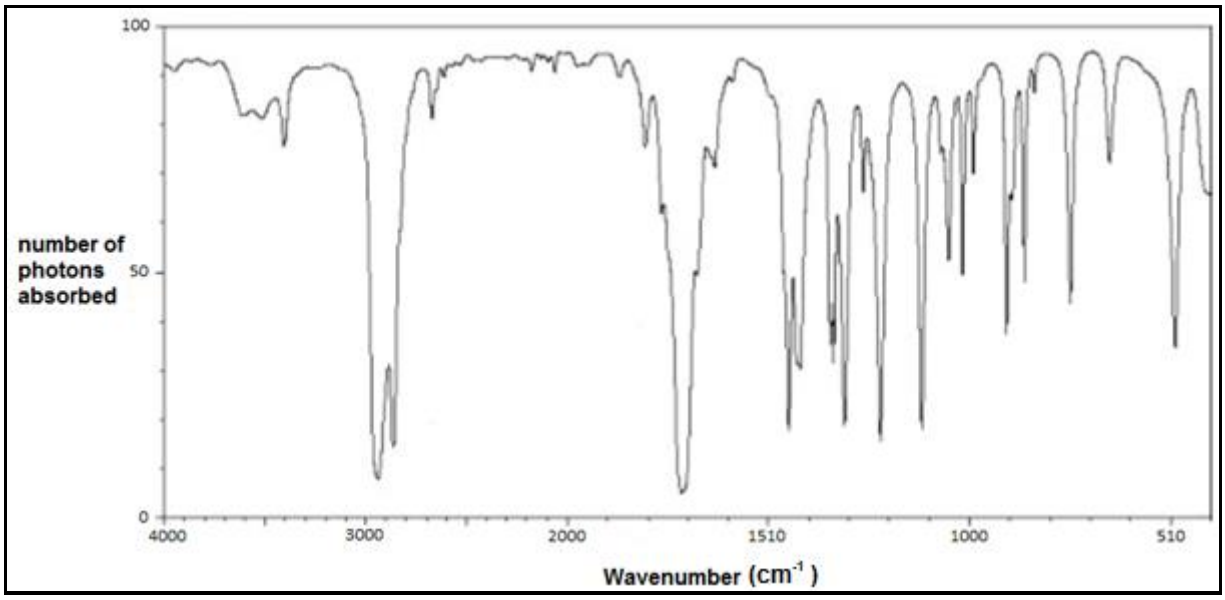

Figure 4.13: Infrared profile for cyclohexanone.[106]

4.7 Melting point determination

The melting point of solid samples can easily be determined to a high degree of accuracy and only a small amount of the sample is usually required. The melting point is an important physical property of a solids as each solid has a unique temperature at which it can be converted into a liquid.

The melting point apparatus shown in **Figure 4.14** is used to determine the melting point of samples using a thermometer. The melting point determination procedure entails the packing of the solid sample tightly to a certain depth in a melting point tube and placing it into the heating chamber to ensure that the temperature of the hot plate, thermometer and sample is in thermal equilibrium.[107]

A melting point apparatus is fast and easy to use, but is limited to analyse only solid homogeneous samples that have to be dry. Sample particle sizes also need to be small to ensure good heat distribution and homogeneous packing to obtain accurate results. The other disadvantage includes that the size of the sample should be enough to fill the capillary tube within the 2 - 3 mm range for quick melting point

[107] Melting point determination. [Accessed 10-03-2015], Available from: http://www.chem.wisc.edu/courses/342/Fall2004/Melting_Point.pdf.

determination. During heating the melting point is measured by a thermometer alongside the sample tube, exposed to the same heat source.[108]

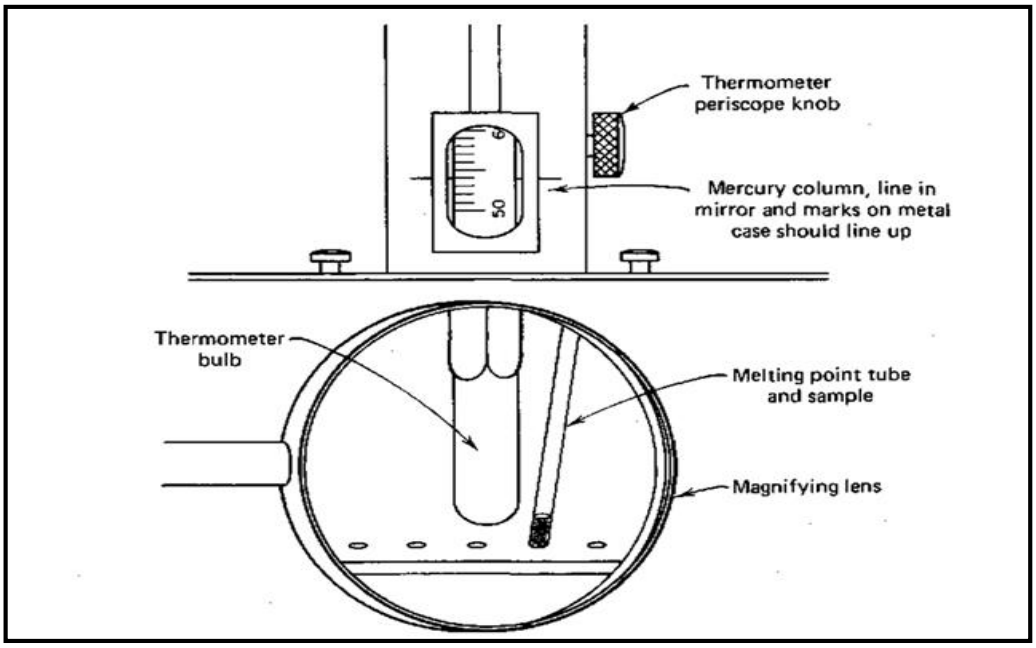

Figure 4.14: Melting temperature apparatus.[109]

4.8 Summary

The equipment discussed in this chapter was extensively used in this study. Microwave digestion was found to effectively dissolve the samples quicker and allowed the study to proceed under cleaner conditions, which means samples are less prone to cross contamination, and was therefore chosen for the preferred digestion method of the REE samples. ICP-OES was chosen for the quantification of the REEs in the different compounds due to its wide linear dynamic range, excellent sensitivity, low detection limits, good quantitative multi-element capability, as well as limited spectral and chemical interferences. In addition, the use of the CHNS-micro analyser was used to determine the non-metal component in the different REE compounds which were reacted with the ligands of choice. Infrared was also used in combination with the previous mentioned methods to identify the functional groups

[108] Melting point determination. [Accessed 22-04-2015], Available from: http://www.thinksrs.com/downloads/PDFs/ApplicationNotes/MPProcedure.pdf.

[109] Operation of the Thomas-hoover apparatus. [Accessed 10-03-2015], Available from: http://what-when-how.com/organic-chemistry-laboratory-survival-manual/the-melting-point-experiment-part-2-laboratory-manual/.

present in a complexes. TGA was effectively used to quantify the amount of water molecules to confirm the chemical composition.

5 Quantitative analysis of REEs and method validation

5.1 Introduction

One of the main challenges for analytical chemists is to accurately quantify specific elements such as REEs in different compounds and matrices. These may include water soluble organometallic complexes as well as mineral ores which may be relatively insoluble and which may contain numerous other elements. The first step in a analysis process involves the successful or complete dissolution of the samples followed by the separation and isolation of the target elements. At each step in this process the accurate quantification of the target elements are important. This accurate and reproducible quantification of the different elements then require harmony between the analytical method, the equipment that is used as well as the skills of the analytical chemist.

The separation of REEs is extremely difficult but can be achieved using different inorganic and organic ligands which produce new complexes with significantly different chemical properties which will allow separation. Once they are complexed, separation is carried out using selective precipitation, solvent extraction and ion exchange techniques. Quantification and characterization of the different REE complexes are sometimes challenging due to the wide range of coordination numbers these complexes may have as well as the difficulty in the complete dissolution of the products formed. Literature studies (**Chapter 3**, **Section 3.2**) has indicated that there are already several reliable dissolution techniques which are extensively used for the dissolution of REE compounds in different matrices. However, less attention has been given to the digestion of synthesized REE complexes using microwave and open beaker methods in many of these studies. Microwave digestion has been identified as one of the techniques that is fast and safe for the dissolution of different REE samples (see **Chapter 3**, **Section 3.2**). Fusion dissolution was also used for the digestion of samples that are resistant to microwave digestion and open acid dissolution methods.

This chapter focuses on the development and validation of analytical methods for the accurate quantification of a number of RE metals. The whole development and validation process include the analysis of the pure metals and the metal nitrate compounds as well as the synthesis, the dissolution and characterization of europium, terbium, dysprosium and yttrium triphenylphosphine oxide complexes (TPPO). Techniques that have been discussed in **Chapter 4** will be used to digest and quantify the different compounds used in this study. Validation parameters will be used to verify the efficiency of analytical methods applied in this research.

5.2 Equipment

5.2.1 Balances

All the samples were accurately weighed to 0.1 mg using a Shimadzu AW 320 at room temperature. For micro analysis the REEs complexes were weighed in tin capsules using a Sartorius CPA2P electronic scale.

5.2.2 Microwave digestion

An Anton Paar Multiwave 300 microwave digestion system (**Figure 5.1**) equipped with an 8 SXF100 rotor and PTFE vessels was used in this study for the digestion of synthesized TPPO complexes and pure yttrium metal. The selected operating conditions for this technique are presented in **Table 5.1**.

Figure 5.1: The Anton Paar Multiwave 300 microwave digestion apparatus.

Table 5.1: The operating conditions used for the microwave digestion of the synthesized REE complexes and yttrium metal.

Parameter	Condition
Power	600 Watts
Ramp	15 min
Hold	45 min
Pressure rate	0.5 bar/sec
Temperature	240 °C
Pressure	60 bar
Weight	0.5 g
Volume of the acid	8.00 mL
Reagents	98 % H_2SO_4, 65 % HNO_3, 32 % HCl, 80 % H_3PO_4 and *aqua regia* ($1HNO_3$:3HCl)

5.2.3 Bench-top digestion hotplate

A Heidolph MR Hei-Tec hotplate/stirrer was used for open beaker digestion. Most of the REE complexes were digested at 90 ˚C for 30 minutes.

5.2.4 Inductively Coupled Plasma-Optical Emission Spectrometry (ICP-OES)

A Shimadzu ICP-7510 sequential plasma spectroscopy unit (**Figure 5.2**) was used for the quantitative analysis of four REEs namely europium, terbium, dysprosium and yttrium. The internal settings of the technique are reported in **Table 5.2**.

Figure 5.2: Shimadzu ICPS-7510 sequential plasma spectroscopy unit.

Table 5.2: The operating conditions of the Shimadzu ICPS-7510 for analysis of europium, terbium, dysprosium and yttrium.

Parameter	Condition
RF power	1.2 W
Observation height	Low
Coolant Gas	14.0 L/min
Plasma Gas	1.20 L/min
Carrier Gas	0.70 L/min
Volume	5 mL
Reagents	98 % H_2SO_4, 65 % HNO_3, 32 % HCl and *aqua regia* ($1HNO_3$:3HCl)

5.2.5 CHNS-micro analyser

The LECO TruSpec CHNS Micro analyser (**Figure 5.3**) was used for the quantification of the % C, H and N in the TPPO complexes.

Figure 5.3: LECO TruSpec Micro analyser.

5.2.6 Infrared spectroscopy (IR)

The IR spectra of all the synthesized TPPO complexes were recorded with a Scimitar Series FTS 2000 Digilab IR spectrometer (**Figure 5.4**) at the wavenumber range of 600 - 4000 cm^{-1}. The instrument is equipped with a pressure tip that contain the sample on the sampling area of the crystal plate for analysis.

Figure 5.4: Scimitar Series Digilab IR.

5.2.7 Melting point apparatus

The Gallenkamp melting point apparatus (**Figure 5.5**) was used to determine the melting points of the synthesized TPPO complexes of europium, terbium, dysprosium and yttrium. Its booster heater allows for the rapid heating of samples with high melting points (above 230 ˚C).

Figure 5.5: Gallenkamp melting point apparatus.

5.2.8 Thermogravimetric analysis (TGA)

A Mettler Toledo TS0801120 TGA model was used to study the mass loss with heating $Dy(NO_3)_3 \cdot xH_2O$. The compound was heated using conditions illustrated in **Table 5.3**.

Table 5.3: The operating conditions of the TGA for $Dy(NO_3)_3 \cdot xH_2O$ analysis.

Parameter	Condition
Onset temperature (T_{onset})	30.0 ˚C
Maximum temperature (T_o)	600.0 ˚C
Rate of heating	10 ˚C.min^{-1}
Gas	Argon
Stabilization time	25 min
Gas flow rate	80 mL.min^{-1}

5.3 Chemicals and reagents

The different metal samples as well as the metal nitrates, namely europium (ingot under oil, 99 % trace metals basis), terbium (chips, 99.9 % trace metals basis), dysprosium (chips, 99.9 % trace metals basis) and yttrium (chips, 99.9 % trace metals basis), $Eu(NO_3)_3{\cdot}5H_2O$ (99.9 %), $Tb(NO_3)_3{\cdot}5H_2O$ (99.9 %), $Dy(NO_3)_3{\cdot}xH_2O$ (99.9 %) and $Y(NO_3)_3{\cdot}6H_2O$ (99.8 %) were purchased from Sigma Aldrich. Sulphuric acid (98 % H_2SO_4), hydrochloric acid (32 % HCl), nitric acid (65 % HNO_3), ethanol (99.5 %) and sulfur ICP standard (1000 mg/L) were bought from Merck. Phosphoric acid (80 % H_3PO_4) was sourced from Associated Chemicals Enterprices while triphenylphosphine oxide (98 % TPPO) was bought from Sigma Aldrich. The REE ICP multi-element standard for Dy, Eu, Tb and Y (1000.00 mg/L, 7.0 % HNO_3 (v/v)) and iron ICP standard (1002 ± 5 mg/L, 2 % HNO_3 (v/v)) were purchased from Inorganic Ventures.

5.4 Glassware

Glassco Din (A) volumetric flasks (100.0 mL) and Schott Duran type beakers (25.0, 50.0 mL) were used during this study. All glassware were soaked in diluted HNO_3 and allowed to stand at room temperature for 24 hours before they were used.

5.5 Pipettes

Transferpette-S (1mL and 10 mL) type pipettes were used to measure and accurately transfer the required volumes of the solutions. These pipettes are accurate in measurements and easy to adjust and calibrate.

5.6 Preparation of deionised water

Deionised water was prepared in the lab using the equipment illustrated in **Figure 5.6**. Using this system, the water is purified via a reverse osmosis process. Deionised water was used for all experimental solutions. The system of preparing deionised water was bought from AJD traders. The conductivity of this deionised water was measured as 168 µs at 19.8 ˚C using a Hanna HI 98311 DIST conductometer.

Figure 5.6: The process of reverse osmosis (a) and water storage facility (b).

5.7 General experimental procedure

Deionised water was used to fill the volumetric flasks to the 100.0 mL mark prior to analysis by ICP-OES. In this study europium, terbium, dysprosium and yttrium were analyzed at their most sensitive wavelengths (381.966, 384.873, 353.171 and 324.228 nm respectively) in different acids (65 % HNO_3, 98 % H_2SO_4, 32 % HCl or *aqua regia* (3 HCl:1 HNO_3)). Analysis of all samples was performed in triplicate. The results are reported as the average of the concentrations together with the standard deviation to indicate the uncertainty in the last digit of the average value.[110]

5.8 Preparation of ICP-OES standards

The ICP standards were prepared from multi-element standards of Dy, Eu, Tb and Y (1000.00 mg/L, 7.0 % HNO_3 (v/v)). Different volumes were obtained and transferred to volumetric flasks (100.0 mL) using Transferpette-S pipettes to prepare calibration standards of 0.0 (blank), 1.0, 2.0, 3.0, 5.0 and 10 ppm. 5 mL of different acids (65 % HNO_3, 98 % H_2SO_4, 32 % HCl and *aqua regia*) were added separately depending on the sample solution (to ensure matrix matching), and deionised water was used to fill all solutions to the mark.

[110] DA Skoog, FJ Holler and TA Nieman. *Principles of Instrumental Analysis 5th Ed*. University of Kentucky, USA, 1997. pp.307-310.

5.8.1 Determination of LOD and LOQ's

The LODs and LOQs of the REEs were determined using the ICP-OES by recording the intensities of the blank (10 replicates) at the wavelengths reported in **Table 5.4**. The LODs and LOQs were calculated using **Equations 5.1** and **5.2** respectively.

$$LOD = \frac{3 \times SD}{m} \qquad \textbf{5.1}$$

$$LOQ = 10 \times LOD \qquad \textbf{5.2}$$

Where SD is the standard deviation of the blank (0.0 ppm) and m is the slope of the calibration curve.

Table 5.4: The LODs and LOQs of Eu, Tb, Dy and Y dissolved in different acids at the selected wavelengths.

Measurements	In HNO_3			
	Eu (381.966 nm)	**Tb (384.873 nm)**	**Dy (353.171 nm)**	**Y (324.228 nm)**
Mean(SD)	0.343(9)	0.1083(8)	0.519(2)	0.138(1)
Slope	7.5856	0.1764	4.8344	5.2089
LOD	0.0037	0.0139	0.0012	0.0006
LOQ	0.0366	0.1385	0.0119	0.0064
	In HCl			
	Eu (381.966 nm)	**Tb (384.873 nm)**	**Dy (353.171 nm)**	**Y (324.228 nm)**
Mean(SD)	0.528(9)	0.227(2)	0.443(5)	0.572(6)
Slope	6.1107	0.2141	3.3322	6.1020
LOD	0.0047	0.0216	0.0043	0.0029
LOQ	0.0470	0.2157	0.0434	0.0292
	In H_2SO_4			
	Eu (381.966 nm)	**Tb (384.873 nm)**	**Dy (353.171 nm)**	**Y (324.228 nm)**
Mean(SD)	0.351(6)	0.253(1)	0.519(3)	0.85(2)
Slope	5.7632	0.2256	3.3612	5.8774
LOD	0.0030	0.0174	0.0030	0.0089
LOQ	0.0300	0.1738	0.0300	0.0894
	In *aqua regia* (HNO_3:3HCl)			
	Eu (381.966 nm)	**Tb (384.873 nm)**	**Dy (353.171 nm)**	**Y (324.228 nm)**
Mean(SD)	-	-	-	0.55(2)
Slope	-	-	-	8.2855
LOD	-	-	-	0.0060
LOQ	-	-	-	0.0600

5.8.2 Quantification of europium, terbium, dysprosium and yttrium in the metal sample using ICP-OES

5.8.2.1 Acid digestion method

The europium metal which was covered in oil was taken out and cut into smaller pieces in a glove box to prevent its oxidation (not as reactive as Y) while yttrium

metal was also cut into pieces at room temperature. The dysprosium and terbium metals were both received as small pieces.

Small pieces (0.0421 g to 0.0558 g) of all these metals (Eu, Tb, Dy and Y) were accurately weighed and transferred into 100.0 mL volumetric flasks containing 10 mL deionised water, followed by addition of 5 mL of concentrated HNO_3 (65 %) to dissolve the metal pieces. After 30 minutes the europium, terbium and dysprosium were completely dissolved in the diluted HNO_3 while visual inspection still indicated the presence of a substantial amount of yttrium not dissolved. The undissolved Y species were removed by filtration and the solutions were filled to the 100.0 mL mark of the volumetric flasks with deionised water. Solutions were allowed to stand at room temperature for 2 hours prior to ICP-OES analysis. Europium (381.966 nm), terbium (384.873 nm), dysprosium (353.171 nm) and yttrium (324.228 nm) were analyzed and the results of this analysis in HNO_3 are presented in **Table 5.5**.

The analysis confirmed the total dissolution of Eu, Tb and Dy and the partial dissolution of the yttrium metal (**Table 5.5**). The same dissolution procedure was repeated using HCl and H_2SO_4. ICP-OES was used for quantitative analysis and the obtained results are presented in **Tables 5.6** and **5.7**.

Table 5.5: The % recoveries of europium, terbium, dysprosium and yttrium metals in HNO_3.

	Calculated concentration (ppm)	Experimental concentration (ppm)	%Recovery
Eu	5.8200	5.8222	100.04
	4.9200	4.9192	99.98
	5.2200	5.2200	100.00
Mean(SD)			100.01(3)
%RSD			0.03
Tb	5.6300	5.6131	99.70
	4.2100	4.1942	99.62
	4.5500	4.5299	99.56
Mean(SD)			99.63(7)
%RSD			0.58
Dy	5.4400	5.3937	99.15
	5.0800	5.0377	99.17
	5.3900	5.3858	99.92
Mean(SD)			99.4(4)
%RSD			0.44
Y	5.3200	4.9310	92.69
	4.3800	4.0564	92.61
	4.6000	4.2441	92.26
Mean(SD)			92.5(2)
%RSD			0.84

Table 5.6: The % recoveries of europium, terbium, dysprosium and yttrium metals in HCl.

	Calculated concentration (ppm)	Experimental concentration (ppm)	%Recovery
Eu	3.9400	3.8879	98.68
	4.9300	4.8556	98.49
	4.4300	4.3576	98.37
Mean(SD)			98.5(2)
%RSD			0.16
Tb	5.6900	3.7429	65.78
	4.8100	3.1056	64.57
	5.7700	3.8054	65.95
Mean(SD)			65.4(8)
%RSD			1.15
Dy	5.3400	2.0278	37.97
	6.2100	2.3068	37.15
	4.9200	1.8855	38.32
Mean(SD)			37.8(6)
%RSD			1.60
Y	5.7900	2.1970	37.95
	7.0400	2.6145	37.14
	5.4300	2.0747	38.21
Mean(SD)			37.8(6)
%RSD			1.48

Interestingly, HCl only succeeded in the total dissolution of Eu with extremely poor recoveries for Dy and Y of ~40 %.

Table 5.7: The % recoveries of europium, terbium, dysprosium and yttrium metals in H_2SO_4.

	Calculated concentration (ppm)	Experimental concentration (ppm)	%Recovery
Eu	5.7500	3.9008	67.84
	5.7600	3.9613	68.77
	5.9100	4.0001	67.68
Mean(SD)			68.1(6)
%RSD			0.87
Tb	4.6700	4.6913	100.46
	5.3900	5.3901	100.00
	5.9900	6.0042	100.24
Mean(SD)			100.2(2)
%RSD			0.23
Dy	4.9600	4.8495	97.77
	4.4800	4.4094	98.42
	5.4400	5.3241	97.87
Mean(SD)			98.0(4)
%RSD			0.36
Y	4.5600	4.1436	90.87
	6.4900	5.9014	90.93
	5.5900	5.1067	91.36
Mean(SD)			91.1(3)
%RSD			0.29

Yttrium gave low recoveries in all the diluted acids (HNO_3, HCl, H_2SO_4) which were investigated including the diluted *aqua regia* (**Table 5.8**). The use of H_2SO_4 as dissolution medium resulted in good recoveries of Tb and Dy, but lower Y recoveries and finally poor Eu recoveries. The dissolution of Y was expanded to the use of *aqua regia* and the results are reported in **Table 5.8**.

Table 5.8: The % recovery of yttrium in *aqua regia*.

	Calculated concentration (ppm)	Experimental concentration (ppm)	%Recovery
Y	3.5800	3.37053	94.15
	2.4000	2.24993	93.75
	2.8900	2.70401	93.56
Mean(SD)			93.8(3)
%RSD			0.32

The recovery of Y using *aqua regia* also indicated only a 93 % dissolution and it was decided to use *aqua regia* as dissolution medium but introduced the microwave to try and improve the dissolution process.

5.8.2.2 Microwave digestion of yttrium metal

In microwave digestion, 8 mL of 98 % H_2SO_4, 32 % HCl, 80 % H_3PO_4 and *aqua regia* were separately used to dissolve yttrium metal. After digestion, the metal was insoluble by visual inspection in all acids and soluble in *aqua regia.* The *aqua regia* solutions were transferred into the 100.0 mL volumetric flasks and allowed to stand at room temperature for 2 hours. Visual inspection indicated complete sample dissolution of the Y metal and ICP-OES was used to analyse the yttrium and the results are reported in **Table 5.9**.

Table 5.9: The % recovery of yttrium metal in *aqua regia*.

	Calculated concentration (ppm)	Experimental concentration (ppm)	%Recovery
Y	3.9500	3.8524	97.53
	3.9200	3.8200	97.45
	5.1400	5.0249	97.76
Mean(SD)			97.6(2)
%RSD			0.17

The recovery of only 97.6 % of the Y metal, inspite of the complete dissolution prompted the investigation to try and find the presence of significant amount of impurities which may be the reason for the less than satisfactory results. The latter

solution of yttrium was qualitatively analyzed to trace the possibility of other elements associated with the metal. Sulfur (S) and iron (Fe) were found to be present in the solution, their standards were prepared and the obtained calibration curves are illustrated in **Figures 5.7** and **5.8**.

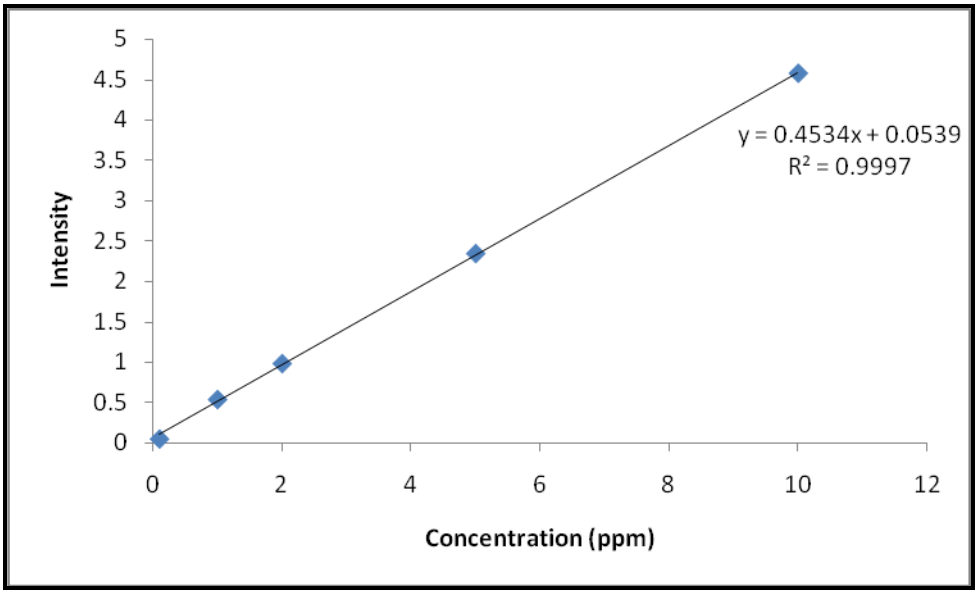

Figure 5.7: Calibration curve of iron at 238.204 nm.

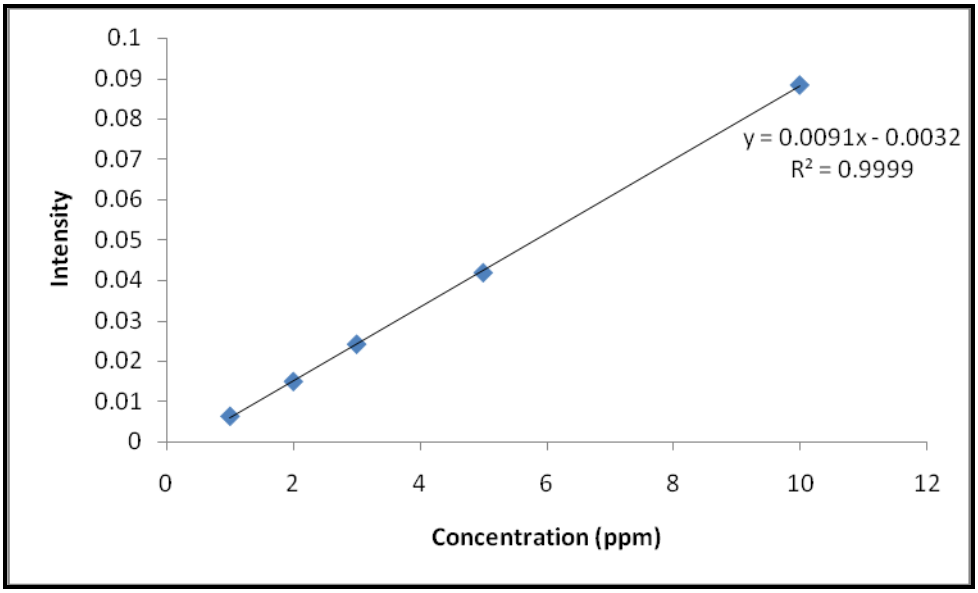

Figure 5.8: Calibration curve of sulphur at 180.731 nm.

The LODs and LOQs for both sulphur and iron were also determined in an *aqua regia* medium. The wavelengths of 180.731 nm and 238.204 nm were selected for S and Fe respectively. The LOD and LOQ of 0.0629 and 0.6291 for S and 0.0033 and

0.0330 for Fe were obtained. The quantitative analysis of these elements are presented in **Table 5.10**.

Table 5.10: The quantitative analysis of Y, S and Fe in yttrium metal dissolved in *aqua regia*.

	Calculated concentration (ppm)	Experimental concentration (ppm)	%Recovery
Y	3.9500	3.8524	97.53
	3.9200	3.8200	97.45
	5.1400	5.0249	97.76
Mean(SD)			97.6(2)
%RSD			0.17
S		4.9584	1.26
		4.8584	1.23
		9.6308	1.87
Mean(SD)			1.5(4)
Fe		0.8976	0.23
		0.8875	0.23
		0.9315	0.18
Mean(SD)			0.21(3)
Y, S and Fe			99.01
			98.92
			99.82
Mean(SD)			99.3(5)
%RSD			0.50

5.8.3 Quantitative determination of europium, terbium, dysprosium and yttrium in inorganic compounds using ICP-OES

Triplicate samples of $Eu(NO_3)_3{\cdot}5H_2O$, $Tb(NO_3)_3{\cdot}5H_2O$, $Dy(NO_3)_3{\cdot}xH_2O$ and $Y(NO_3)_3{\cdot}6H_2O$ were separately weighed (0.0269 g to 0.0355 g) and transferred into 100.0 mL volumetric flasks each containing 10 mL of deionised water. HNO_3 (65 %, 5 mL) was added to the solutions and filled to the mark with deionised water and allowed to stand for 2 hours at room temperature. ICP-OES was used for the analysis

of the samples with the operation conditions mentioned in **Paragraph 5.2.4**, **Table 5.2**. The analytical results are presented in **Table 5.11**.

Table 5.11: The % recoveries of europium, terbium, dysprosium and yttrium in inorganic compounds.

	Calculated concentration (ppm)	Experimental concentration (ppm)	%Recovery
$Eu(NO_3)_3 \cdot 5H_2O$	12.4604	12.4571	99.97
	11.5374	11.5648	100.24
	12.5669	12.5551	99.91
Mean(SD)			100.0(2)
%RSD			0.18
$Tb(NO_3)_3 \cdot 5H_2O$	10.5218	10.5272	100.05
	10.7045	10.8103	100.99
	10.2660	10.2322	99.67
Mean(SD)			100.2(7)
%RSD			0.68
$Dy(NO_3)_3 \cdot xH_2O$	12.6359	9.5197	75.34
	13.3820	10.0774	75.31
	13.0556	9.9316	76.07
Mean(SD)			75.6(4)
%RSD			0.57
$Y(NO_3)_3 \cdot 6H_2O$	6.7087	6.6760	99.51
	6.4534	6.4098	99.32
	6.5462	6.5066	99.39
Mean(SD)			99.4(1)
%RSD			0.10

Uncertainty with respect to the number of water molecules (crystal waters) associated with $Dy(NO_3)_3$, prompted a TGA study in anticipation that a more accurate molecular formula of the compound will improve the % recovery of the dysprosium.

5.8.4 Thermogravimetric analysis (TGA) of $Dy(NO_3)_3 \cdot xH_2O$

A 13.81 mg $Dy(NO_3)_3 \cdot xH_2O$ sample was weighed in an alumina cup and introduced to the TGA to determine the amount of water molecules present. The sample was heated at the rate of 10 ˚C/min to obtain the mass loss. The TGA graph (**Figure 5.9**) showed several stages of potential mass loss of the compound. The calculations indicate that the mass of the compound contains about 20 % water which was lost during the heating process.

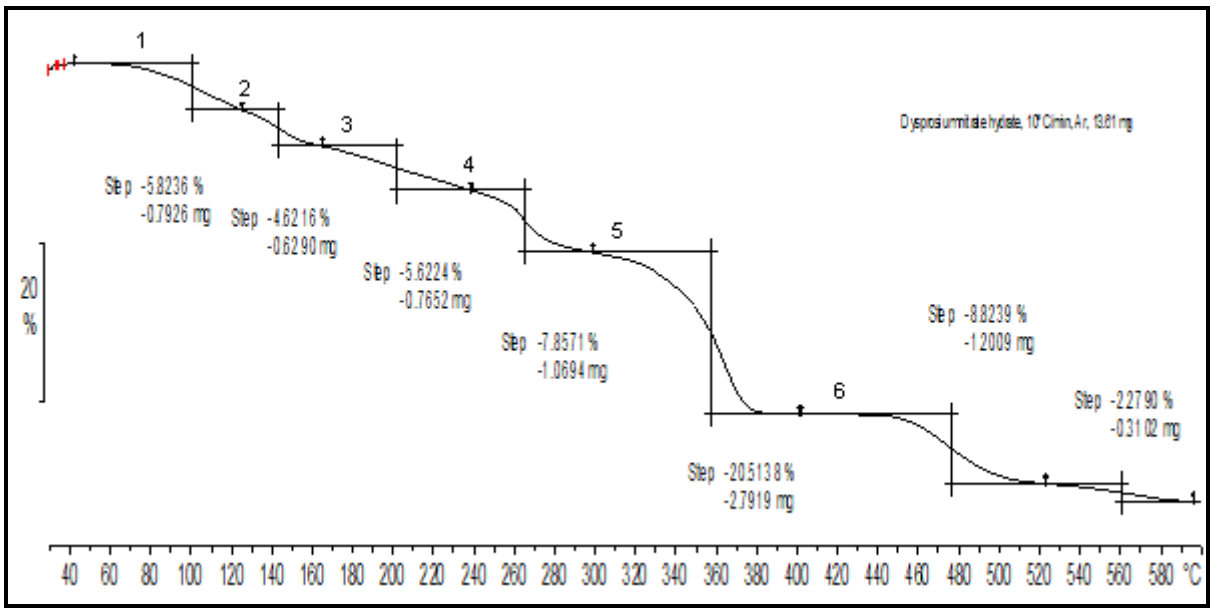

Figure 5.9: TGA of $Dy(NO_3)_3 \cdot xH_2O$.

The results of the TGA further indicate that the value for x in $Dy(NO_3)_3 \cdot xH_2O$ is either 5 or 6 and thereby suggesting the $Dy(NO_3)_3 \cdot 5H_2O$ and $Dy(NO_3)_3 \cdot 6H_2O$ formulas. The results were found to be in good agreement with the calculated values which are tabulated in **Table 5.12**. It became clear that the formula of the Dy compound used in this study is $Dy(NO_3)_3 \cdot 6H_2O$ instead of $Dy(NO_3)_3 \cdot 5H_2O$.

Table 5.12: The % recovery of water molecules present in $Dy(NO_3)_3 \cdot xH_2O$ after TGA.

Step	% Weight loss due to different number of water molecules			
	$4H_2O$	**$5H_2O$**	**$6H_2O$**	**$7H_2O$**
1	4.3	4.1	3.9	3.8
2	8.6	8.2	7.9	7.6
3	12.9	12.3	11.8	11.4
4	17.1	16.4	15.8	15.2
5		**20.5**	**19.7**	**19.0**
6			23.7	22.8

Bolded: Possible water molecules.

The molecular compounds of $Dy(NO_3)_3 \cdot 6H_2O$ was further investigated by ICP-OES analysis to confirm the presence of the 6 crystal waters. The sample was accurately weighed (0.0283 g) and quantitatively transferred into a 100.0 mL volumetric flask containing 10 mL deionised water followed by addition of HNO_3 (65 %, 5 mL). The solution was filled to the mark with deionised water and allowed to stand at room temperature for 2 hours and analyzed using ICP-OES (**Table 5.13**). The ICP-OES analysis of this solution gave low recoveries of 97(1) % despite the complete dissolution which was visually observed. The poor results led to the investigation of the time dependence of the analysis and the same solution was analyzed over a period of 5 days (**Table 5.13**).

Table 5.13: The recovery of $Dy(NO_3)_3 \cdot 6H_2O$ over a five day period.

	Sample	Day 1	Day 2	Day 3	Day 4	Day 5
% recovery	1	97.74	96.51	99.51	99.50	100.84
	2	97.44	97.21	99.32	96.73	100.17
	3	95.96	98.54	99.39	95.66	100.79
Mean(SD)		97(1)	97(1)	99.4(1)	97(2)	100.6(4)
%RSD		0.98	1.06	0.10	2.04	0.37

5.8.5 Synthesis of triphenylphosphine oxide (TPPO) complexes of europium, terbium, dysprosium and yttrium[111]

The different REE nitrate salts $Ln(NO_3)_3 \cdot xH_2O$ ($Eu(NO_3)_3 \cdot 5H_2O$, $Tb(NO_3)_3 \cdot 5H_2O$, $Dy(NO_3)_3 \cdot 6H_2O$ and $Y(NO_3)_3 \cdot 6H_2O$) were accurately weighed (0.3016 g to 0.3056 g) and dissolved in 10 mL ethanol while TPPO (0.5917 - 0.6574 g, 3 mmol) was also dissolved in 10 mL ethanol and allowed to stand at room temperature for 5 minutes to dissolve completely. The ethanolic solutions of the inorganic compounds were then added to the ethanolic TPPO solutions (REE's:TPPO = 1:3) and allowed to react at room temperature for 24 hours (**Figure 5.10**). White precipitates of the complexes (**Figure 5.11**) were isolated from all solutions with filtration while the ethanol filtrates were discarded. The complexes were dried at room temperature for 48 hours.

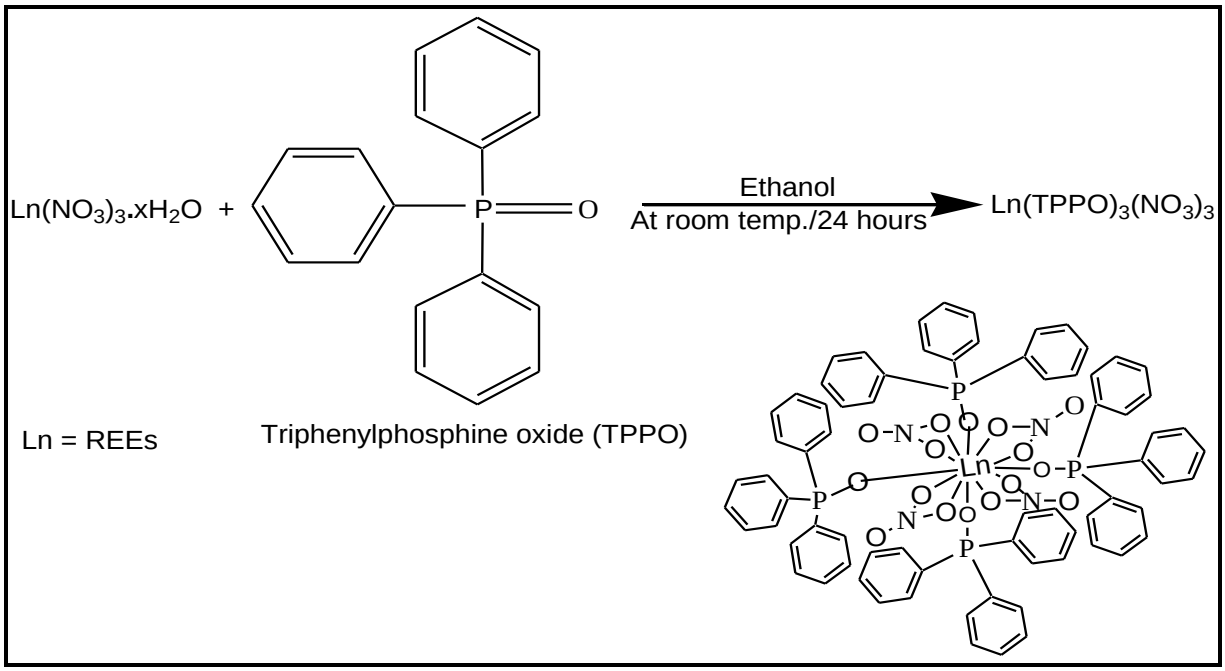

Figure 5.10: Synthesis of the different REE TPPO complexes.[111]

[111] K Kuhn. Submitted in partial fulfilment of the requirements for the degree*, Magister Scientiae at the Nelson Mandela Metropolitan University library*, 2012, pp.19-20.

Figure 5.11: The white precipitates of the formed TPPO complexes ($[Ln(TPPO)_3(NO_3)_3]$) synthesized in ethanol.

5.8.6 Bench-top digestion of the synthesized TPPO complexes ($[Ln(TPPO)_3(NO_3)_3]$)

The isolated TPPO complexes of Dy, Tb, Eu and Y ($[Ln(TPPO)_3(NO_3)_3]$) were accurately weighed (0.0449 g to 0.0491 g) separately and transferred to 25 mL glass beakers. Deionised water (10 mL) was added to each complex followed by HNO_3 (65 %, 5 mL). Two colourless layers, even upon heating, were observed in all cases (for 98 % H_2SO_4, 32 % HCl, 80 % H_3PO_4 and *aqua regia*). The resultant two layers of the solutions were not analyzed by ICP-OES as the one layer was oil and the other layer the acid.

5.8.7 Microwave digestion method

In the next step, TPPO complexes ($[Ln(TPPO)_3(NO_3)_3]$) were accurately weighed (0.0480 g to 0.0509 g) and transferred into the PTFE vessels and 8 mL 65 % HNO_3 was added to each of the complexes, sealed and introduced to the microwave digestion. On completion of the microwave cycle the solutions were allowed to cool. Visual inspection indicated incomplete or poor dissolution (**Table 5.14**, column 3). The digestion method was repeated with 98 % H_2SO_4, 32 % HCl, 80 % H_3PO_4 and *aqua regia* and only 98 % H_2SO_4 appeared to dissolve all the REE complexes completely (**Table 5.14**, column 3). The H_2SO_4 solutions were subsequently transferred to the 100.0 mL volumetric flasks, filled to the mark with deionised water

and allowed to stand at room temperature for 24 hours. The solutions were then refilled to the mark with deionised water and analyzed using ICP-OES (**Table 5.15**).

Table 5.14: Dissolution of TPPO complexes $[Ln(TPPO)_3(NO_3)_3]$ in different acids.

Acid	Bench-Top digestion	Microwave digestion
HNO_3	Insoluble	Insoluble
HCl	Insoluble	Insoluble
Aqua regia	Insoluble	Insoluble
H_3PO_4	Insoluble	Insoluble
H_2SO_4	Insoluble	Complete dissolution

Table 5.15: The % recoveries of Eu, Tb, Dy and Y in TPPO complexes ($[Ln(TPPO)_3(NO_3)_3]$) dissolved in H_2SO_4.

	Calculated concentration (ppm)	Experimental concentration (ppm)	%Recovery
$[Eu(TPPO)_3(NO_3)_3]$	6.7117	6.6477	99.05
	6.7247	6.6690	99.17
	6.6858	6.6249	99.09
Mean (SD)			99.10(6)
%RSD			0.06
$[Tb(TPPO)_3(NO_3)_3]$	6.4662	6.4222	99.32
	6.8838	6.8171	99.03
	6.9242	6.9098	99.79
Mean(SD)			99.4(4)
%RSD			0.39
$[Dy(TPPO)_3(NO_3)_3]$	7.0309	7.0077	99.67
	7.0721	7.0757	100.05
	7.3331	7.3438	100.146
Mean(SD)			99.9(3)
%RSD			0.25
$[Y(TPPO)_3(NO_3)_3]$	4.0779	3.9341	96.47
	4.0859	3.9277	96.13
	4.0939	3.9125	95.57
Mean(SD)			96.1(5)
%RSD			0.48

5.8.8 Melting point determination

The synthesized TPPO complexes ($[Ln(TPPO)_3(NO_3)_3]$) were ground to a fine powder and transferred to melting point glass tubes which was subsequently introduced to the melting point determination. Melting point values are presented in **Table 5.16**.

Table 5.16: Melting point determination of the TPPO complexes ([$Ln(TPPO)_3(NO_3)_3$]).

Complex	Melting point(˚C)
[$Eu(TPPO)_3(NO_3)_3$]	224-226
[$Tb(TPPO)_3(NO_3)_3$]	220-222
[$Dy(TPPO)_3(NO_3)_3$]	218-219
[$Y(TPPO)_3(NO_3)_3$]	220-222

5.8.9 CHNS micro analysis (Combustion Analysis)

Different standards of approximately 2 mg were accurately weighed in tin capsules, transferred and introduced into the carousel head of the Leco for analysis. The analysis were performed in triplicate. After running of the standards, the TPPO complexes [$Ln(TPPO)_3(NO_3)_3$] of similar mass (~ 2 mg) were introduced into the CHNS micro analyser for the determination of C, H and N. The results obtained, together with the calculated values for the different complexes are presented in **Table 5.17**.

Table 5.17: Determined concentrations of C, H and N.

Complex	Molecular formulae	%Found*			%Expected**		
		C	H	N	C	H	N
[$Eu(TPPO)_3(NO_3)_3$]	$EuC_{45}H_{27}N_3O_{12}$	56.3(1)	3.90(4)	4(1)	55.25	3.84	3.58
[$Tb(TPPO)_3(NO_3)_3$]	$TbC_{45}H_{27}N_3O_{12}$	55.5(1)	3.90(1)	3.2(3)	54.93	3.81	3.56
[$Dy(TPPO)_3(NO_3)_3$]	$DyC_{45}H_{27}N_3O_{12}$	55.6(2)	3.8(1)	5(1)	54.76	3.80	3.55
[$Y(TPPO)_3(NO_3)_3$]	$YC_{45}H_{27}N_3O_{12}$	59.0(6)	4.07(2)	6(2)	58.39	4.06	3.79

*****Standard deviations are based on triplicate analysis

******Theoretical values

5.8.10 Analysis of TPPO complexes ([$Ln(TPPO)_3(NO_3)_3$]) by Infrared (IR) spectroscopy

The free TPPO ligand and its complexes ([$Ln(TPPO)_3(NO_3)_3$]) were characterized using IR spectroscopy. The obtained IR spectra are presented in Figures **5.12** - **5.16**.

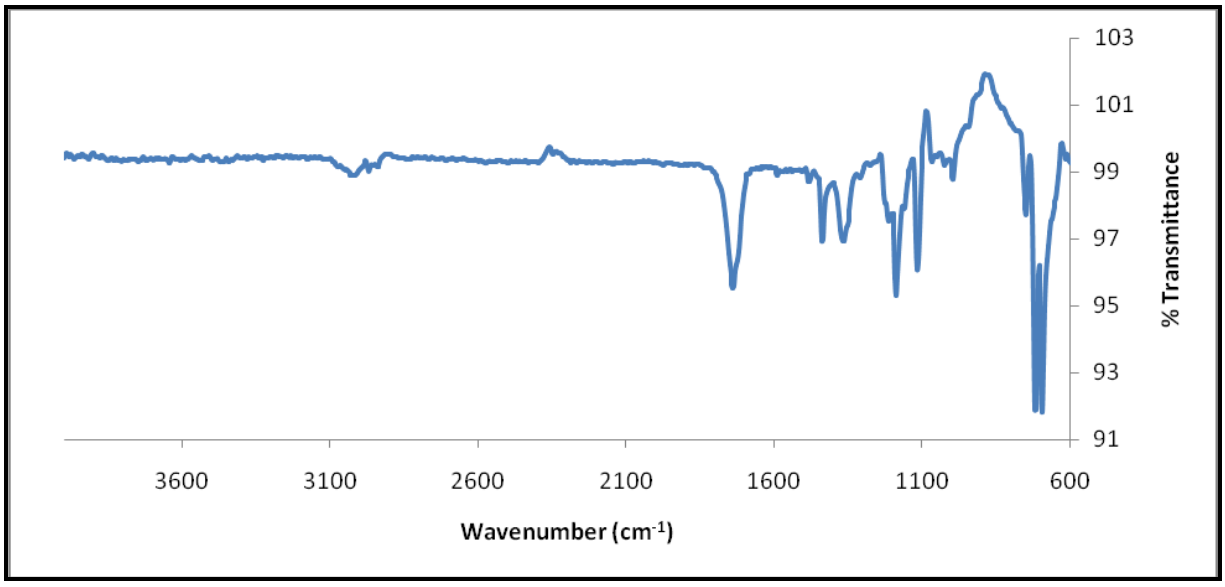

Figure 5.12: The IR spectrum of TPPO.

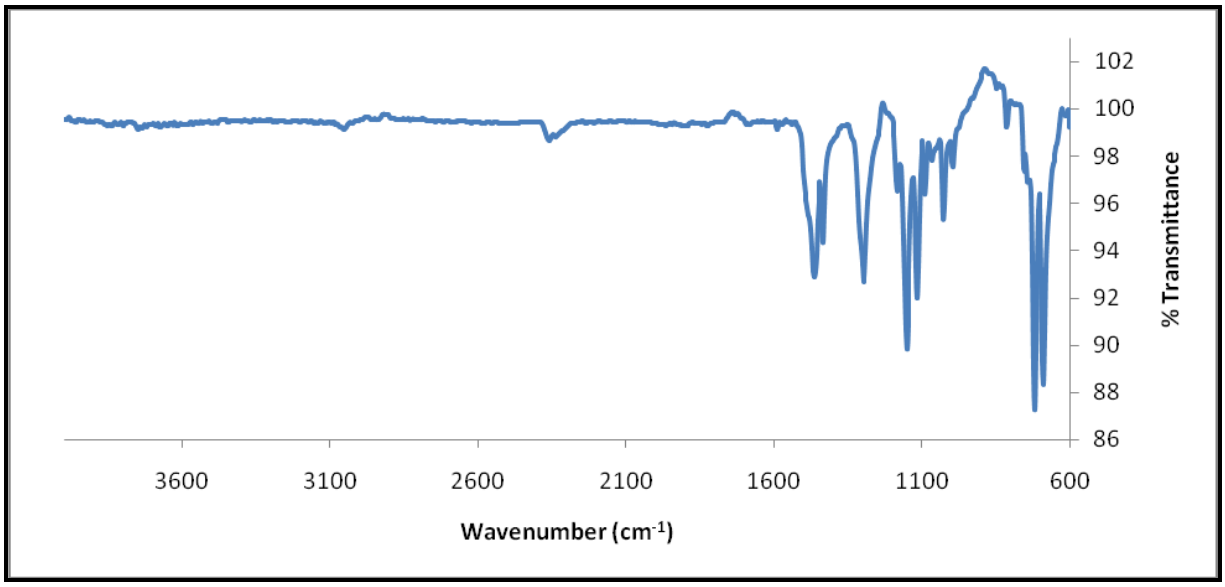

Figure 5.13: The IR spectrum of $[Eu(TPPO)_3(NO_3)_3]$.

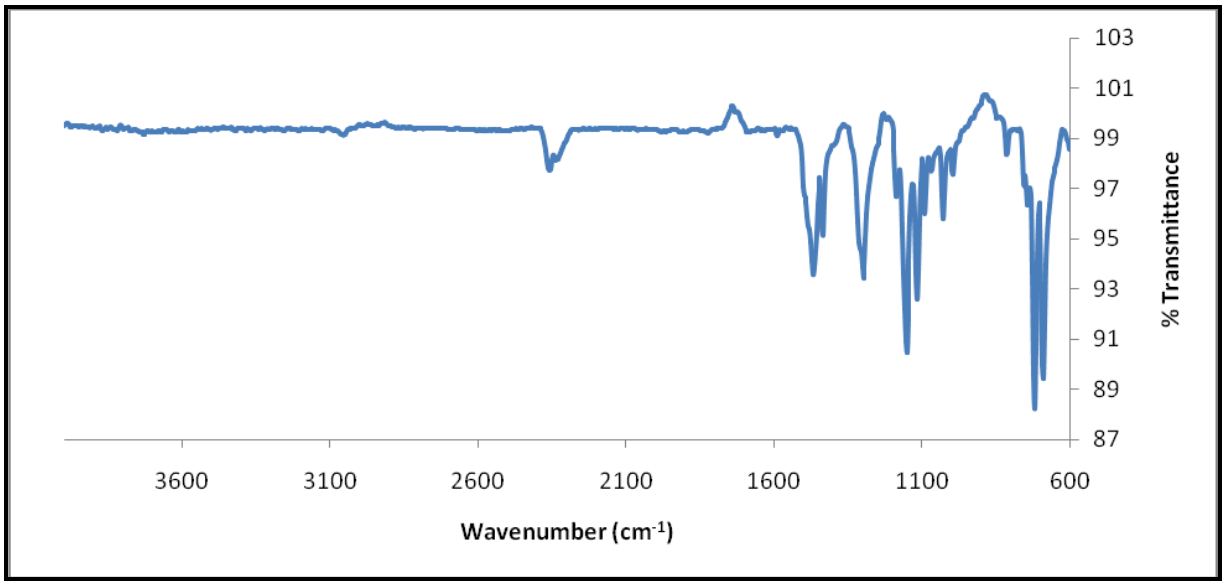

Figure 5.14: The IR spectrum of $[Tb(TPPO)_3(NO_3)_3]$.

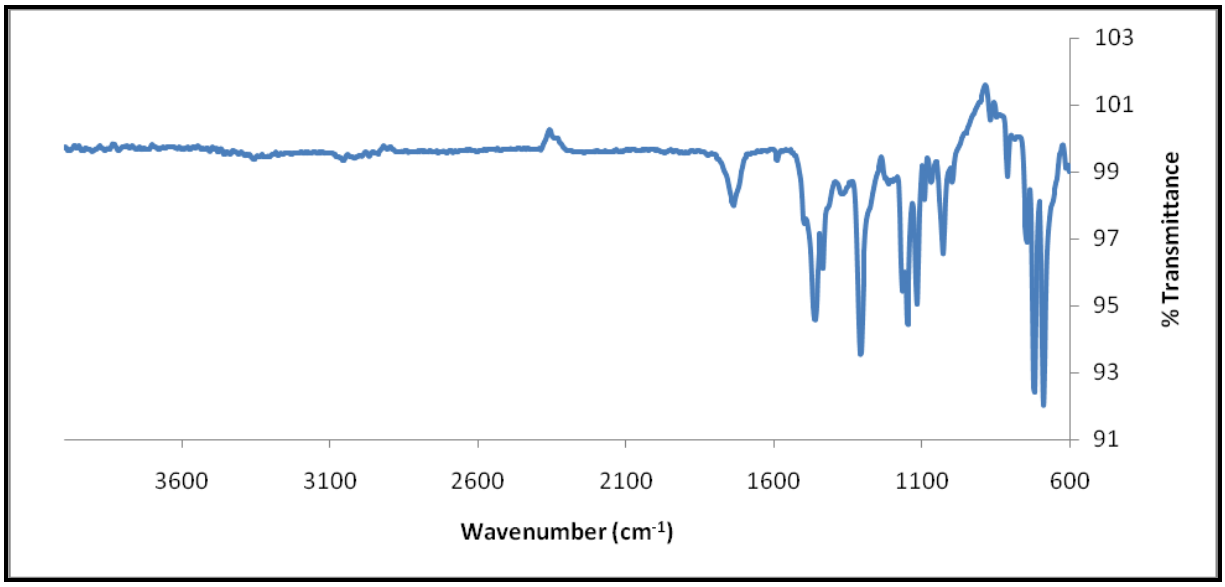

Figure 5.15: The IR spectrum of $[Dy(TPPO)_3(NO_3)_3]$.

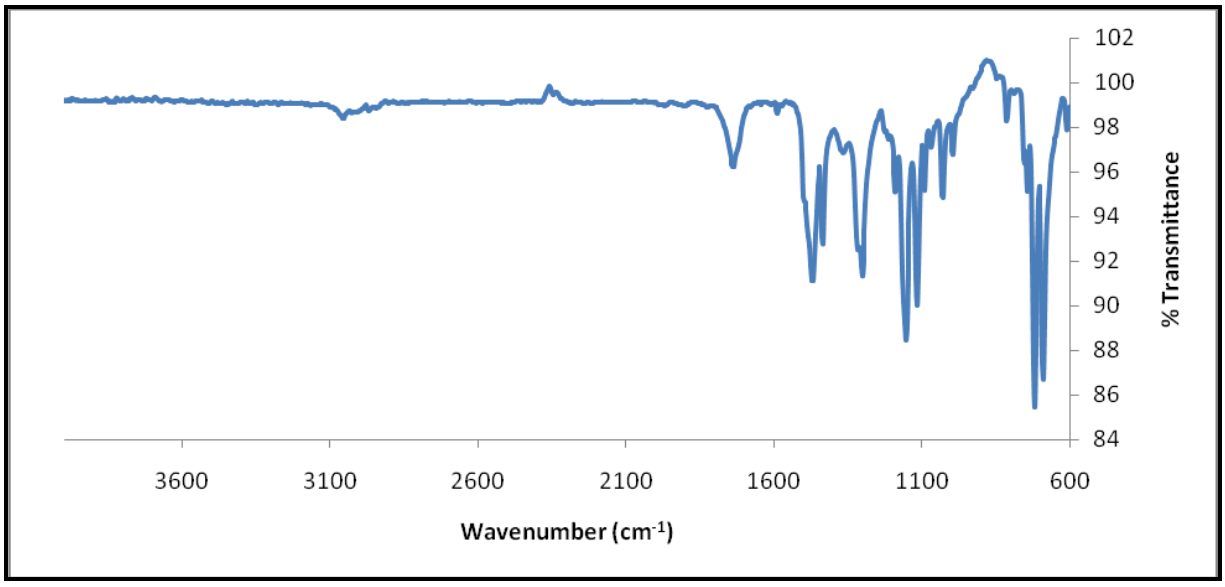

Figure 5.16: The IR spectrum of $[Y(TPPO)_3(NO_3)_3]$.

The IR spectrum of the TPPO ligand (**Figure 5.12**) was compared with the spectra of the $[Ln(TPPO)_3(NO_3)_3]$ complexes (**Figures 5.13** - **5.16**). The IR data of the TPPO free ligand and the complexes is presented in **Table 5.18**.

Table 5.18: The IR data of the TPPO complexes ($[Ln(TPPO)_3(NO_3)_3]$).

Complex	ν (PO)	ν (NO_3)	ν (NO_3)	ν (NO_3)
TPPO	1188.2	-	-	-
$[Eu(TPPO)_3(NO_3)_3]$	1153.7	1466.9	1298.9	1030.4
$[Tb(TPPO)_3(NO_3)_3]$	1154.5	1469.1	1300.1	1030.0
$[Dy(TPPO)_3(NO_3)_3]$	1151.3	1453.9	1309.9	1030.3
$[Y(TPPO)_3(NO_3)_3]$	1157.2	1471.8	1304.4	1031.7

A successful synthesis of REE complexes of the TPPO ligand was accomplished in ethanol. Dissolution of the resultant complexes was only successful in H_2SO_4 by microwave digestion. The ICP-OES analysis of europium, terbium and dysprosium indicated good average recoveries. Microwave digestion of the complexes in HNO_3, HCl, H_3PO_4, and *aqua regia* was not successful for dissolution. Bench-top digestion and diluted acid dissolution were also unsuccessful.

5.9 Discussion of the results

5.9.1 Limit of detection and quantification (LOD and LOQ)

Before analysis of europium, terbium, dysprosium and yttrium the limit of detection (LODs) and quantification (LOQs) were determined for analysis by ICP-OES. The LODs and LOQs (**Table 5.4**) of Eu, Tb, Dy and Y were determined at the wavelengths of 381.966, 384.873, 353.171 and 324.228 nm respectively in HNO_3, HCl, H_2SO_4 and *aqua regia.* The LODs of Eu, Tb, Dy and Y ranged between 0.0030 - 0.0047, 0.0139 - 0.0216, 0.0012 - 0030, 0.0006 - 0.0089 ppm with the LOQs of 0.0300 - 0.0470, 0.1385 - 0.2157, 0.0119 - 0.0434 and 0.0064 - 0.0894 ppm respectively. Yttrium showed the lowest LODs followed by europium, dysprosium and lastly terbium. Bangai *et al.*[58] reported the LODs and LOQs of 0.0100 and 0.1000 µg/mL for europium and 0.2000 and 2.0000 µg/mL for dysprosium respectively (at least a factor 2 to 5 higher as in the current study) using ICP-OES while Bentlin *et al*.[60] obtained LODs of 0.034 for Eu, 0.349 for Tb and 0.165 mg/L for Dy with LOQs of 0.3400 (~3 order is of magnitude higher), 3.4900 and 1.6500 mg/L respectively (see **Chapter 3**, **Section 3.4**). These literature LODs and LOQs are much higher when compared to those obtained in this study.

5.9.2 Quantification of metals in acid

The acid digestion method was performed at room temperature using different acids as dissolution medium. Good recoveries of 100.01(3), 99.63(7) and 99.4(4) % for europium, terbium and dysprosium respectively were obtained with HNO_3 as acid while unsatisfactory recovery of 92.5(2) % was obtained for yttrium (**Table 5.5**). In the next step HCl was used as acid and good results were obtained for europium with an average recovery of 98.5(2) % Eu, (**Table 5.6**) while poor recoveries of approximately ~40 % were obtained for dysprosium and yttrium and 65.4(8) % recovery for terbium. H_2SO_4 was then used and successfully dissolved terbium and dysprosium with average recoveries of 100.2(2) and 98.0(4) % (**Table 5.7**) respectively but only partially dissolved europium and yttrium with recoveries of 68(1) % and 91(1) % respectively. In *aqua regia* yttrium gave a lower recovery of 93.8(3) %. In the next step microwave assisted acid digestion was used due to the unsatisfactory results of yttrium. A summary of these results are presented in **Table 5.19**.

Table 5.19: Acid dissolution selectivity of Eu, Tb, Dy and Y.

Acid	%Metal			
	Eu	Tb	Y	Dy
HNO_3	100.01(3)	99.63(7)	92.5(2)	99.4(4)
HCl	98.5(2)	65.4(8)	37.8(6)	37.8(6)
H_2SO_4	68.1(6)	100.2(2)	91.1(3)	98.0(4)
Aqua regia	-	-	93.8(3)	-
Microwave (aqua regia)	-	-	97.6(2)	-

-: not used for dissolution

The interesting part about this dissolution results is that not one acid (HNO_3 , HCl, H_2SO_4 or *aqua regia*) was found to be capable of digesting all the metals (europium, terbium, dysprosium and yttrium) in this study completely. HNO_3 was the most successful in dissolving most of these metals at levels greater than 90% although unsatisfactory Y recoveries were obtained. The HCl on the other hand, selectively dissolved more than 98% Eu with only 65 % Tb and up to 38 % each of Dy and Y. These results have shown the potential for selective metal dissolution of europium from a mixture of terbium with yttrium and dysprosium. It should in principle be possible by adjustment of experimental conditions to enrich these elements in different matrices using HCl dissolution. The H_2SO_4 dissolution also showed some selectivity towards the dissolution of Tb and Dy while ~32 % of Eu remains undissolved.

The named bench-top acid dissolution of the pure metal clearly indicated that yttrium metal is not completely dissolved by any of the acids investigated. It was then decided to use more robust dissolution conditions to try and recover all of the weighed yttrium. The metal was then digested in the microwave using HNO_3, HCl and H_2SO_4 in separate attempts under 60 bar and 240 ˚C for 45 minutes. Again the yttrium metal recovery indicated incomplete dissolution under the applied experimental conditions. A recovery of 97.6(2) % Y was however obtained using *aqua regia* as dissolution medium in the microwave digestion under similar pressure, temperature and time conditions. In this instance visual inspection indicated the complete dissolution of the metal and the analytical results also indicated improved recoveries as compared to the acid dissolution and bench-top digestion method

(open beaker digestion) for the REEs and yttrium metal. In another study Ivanova *et al.*[53] also successfully digested samples containing REEs by microwave digestion and obtained an yttrium recovery of 97.8(6) %. This low recovery prompted an investigation into the possible presence of impurities that might be associated with yttrium metal, as visual inspection indicated the complete dissolution of the metal. The same solution was qualitatively analyzed for other elements and the presence of sulfur and iron were detected as impurities. Sulfur and iron were subsequently quantified by ICP-OES and recoveries of 1.5(4) % and 0.21(3) % were obtained respectively. A total recovery of 99.3(5) % was obtained for the mass of the metal if all these impurities are added, yielding satisfactory Y recovery in light of the presence of the associated impurities.

5.9.3 Quantification of $Ln(NO_3)_3 \cdot xH_2O$

Europium, terbium, dysprosium and yttrium were quantitatively determined in the inorganic nitrate salts, namely $Ln(NO_3)_3 \cdot xH_2O$ in HNO_3 solution. Satisfactory results were obtained for Eu, Tb and Y of 100.0(2) %, 100.2(7) % and 99.4(1) % respectively. A poor recovery of 75.6(4) % for Dy (**Table 5.11**) was obtained under this experimental conditions (HNO_3 dissolution). One of the problems with the dysprosium nitrate was the lack of certainty regarding the number of crystal waters associated with it ($Dy(NO_3)_3 \cdot xH_2O$). However, the poor Dy recovery could therefore be a result of the incorrect prediction of the molecular formula and this suspicion led to $Dy(NO_3)_3 \cdot xH_2O$ being also analyzed using TGA to quantify the amount of crystal waters associated with the salt. The TGA analysis indicated five steps with a total mass loss of 20 % which was assumed to be the mass of crystal waters in the compound. Calculations were done based on this mass loss to assign the compound the correct molecular formula and 4, 5, 6 and 7 crystal waters were considered. Six crystal waters were found to account for 20 % mass loss and it was found to be a better indication of the salt's correct molecular formula, namely $Dy(NO_3)_3 \cdot 6H_2O$ (see **Table 5.13**).

5.9.4 Quantification of TPPO complexes

The TPPO complexes of europium, terbium, dysprosium ($[Ln(TPPO)_3(NO_3)_3]$) and yttrium were synthesized. The assessment of the success of the synthesis entailed re-dissolution as well as the analysis of the synthesized REE complexes. Different

mineral acids, namely 65 % HNO_3, 98 % H_2SO_4, 32 % HCl, 80 % H_3PO_4 and *aqua regia* were investigated in the acid digestion technique (open beaker dissolution). The complexes formed two colourless layers (organic and aqueous) that were observed by visual inspection. These results clearly indicate that a bench-top digestion method was not a good choice for the dissolution of synthesized complexes and secondly that carbon built-up in the ICP torch can be expected if these solutions were analyzed. In the next step a microwave acid assisted digestion method was investigated.

The $[Ln(TPPO)_3(NO_3)_3]$ complexes were digested in the microwave system using H_2SO_4 under 60 bar and 240 ˚C for 45 minutes. Good metal recoveries of 99.10(6) % for europium, 99.4(4) % for terbium and 99.9(3) % for dysprosium (see **Table 5.15**) were obtained from the microwave acid assisted dissolution of synthesized complexes with a lower than expected recovery of 96.1(5) % for yttrium.

5.9.5 Characterization of TPPO complexes ($[Ln(TPPO)_3(NO_3)_3]$)

The melting points of the synthesized TPPO complexes ($[Ln(TPPO)_3(NO_3)_3]$) were also determined (**Table 5.16**) in this study. The obtained melting points of $[Eu(TPPO)_3(NO_3)_3]$, $[Tb(TPPO)_3(NO_3)_3]$, $[Dy(TPPO)_3(NO_3)_3]$, and $[Y(TPPO)_3(NO_3)_3]$ were 224 - 226, 220 - 222, 218 - 219 and 220 - 222 ˚C respectively. In literature Kuhn[111] obtained the melting points of 205, 222 and 237 ˚C for $[Eu(TPPO)_3(NO_3)_3]$, $[Tb(TPPO)_3(NO_3)_3]$ and $[Dy(TPPO)_3(NO_3)_3]$ respectively. The melting point differences of the $[Eu(TPPO)_3(NO_3)_3]$ and $[Dy(TPPO)_3(NO_3)_3]$ reported by Kuhn and those obtained in the current study can be due to the differences in product purity.

The CHNS micro analyser was used in this study to confirm the identity of the synthesized TPPO complexes ($[Ln(TPPO)_3(NO_3)_3]$). An agreement between the calculated and experimental C and H concentrations was excellent for $[Eu(TPPO)_3(NO_3)_3]$, $[Tb(TPPO)_3(NO_3)_3]$, $[Dy(TPPO)_3(NO_3)_3]$ and $[Y(TPPO)_3(NO_3)_3]$. In $[Eu(TPPO)_3(NO_3)_3]$ and $[Tb(TPPO)_3(NO_3)_3]$ recoveries of 101.9(1) % and 101.0(1) % for C, 102.6(4) % and 102.4(1) % for H were obtained. The other two complexes $[Dy(TPPO)_3(NO_3)_3]$ and $[Y(TPPO)_3(NO_3)_3]$ gave recoveries for C of 101.5(2) % and 101.0(6) % respectively with the satisfactory H recoveries of 100.0(0) % and 100.2(2) % respectively. Discrepancies between the expected values

and experimental results were observed for the % N content. N recoveries of 112(1) %, 89.9(3) %, 141(1) % and 158.3(2) % for [Eu(TPPO)$_3$(NO$_3$)$_3$], [Tb(TPPO)$_3$(NO$_3$)$_3$], [Dy(TPPO)$_3$(NO$_3$)$_3$] and [Y(TPPO)$_3$(NO$_3$)$_3$] respectively were obtained (**Table 5.17**) in all the studied complexes. Disregarding the N results, the obtained C and H results could still confirm the successful preparation of the desired [Ln(TPPO)$_3$(NO$_3$)$_3$] complexes.

A possible explanation for these poor % N recoveries can be the poor decomposition of the inorganic type of NO$_3$ ligands in these complexes to N$_2$, which is analyzed by the Leco micro analyser. More research with regard to the nitrogen conversion of different nitrogen containing ligands need to be carried out to get better insight into these discrepancies.

The final part in the characterization of the TPPO complexes concerned the IR spectra of the synthesized complexes. The ν(PO) vibration at 1188.2 cm^{-1} which was found in the IR spectrum (**Figure 5.18**) for the TPPO ligand can be seen as different from those of the synthesized complexes, of which the vibrations ranged between 1151.8 - 1157.2 cm^{-1}. The nitrate vibrations were obtained at 1453.9 - 1471.8, 1298.9 - 1309.9 and 1030.0 - 1031.7 cm^{-1} in TPPO complexes ([Ln(TPPO)$_3$(NO$_3$)$_3$]). The absence of the 1188.2 cm^{-1} streching frequency for the complexes ([Ln(TPPO)$_3$(NO$_3$)$_3$]) indicated that the TPPO coordinated to the europium, terbium, dysprosium and yttrium. Spectra of the [Ln(TPPO)$_3$(NO$_3$)$_3$] complexes showed that the central atom (Eu, Tb, Dy and Y) was bonded to three nitrate groups. Levason *et al*.[112] found the ν(PO) vibrations at 1195 cm^{-1} and 1155 - 1160 cm^{-1} for TPPO and REEs complexes respectively with the bidentate nitrate vibrations at 1475, 1310, 1030, and 815 cm^{-1}. Alencar *et al*.[113] reported the ν(PO) vibrations at 1195 cm^{-1} for TPPO, a shift of approximately 56 cm^{-1} compared to the REE complexes. In this study the ν(PO) vibration shifted by 6.8 cm^{-1} compared to the reported results of Levason *et al*. and Alencar *et al*. Only three nitrate vibrations were determined that were in agreement with those reported by Levason *et al*. (except 815 cm^{-1}). The shift between the TPPO and TPPO complexes obtained in this study is 31 cm^{-1} compared to 56 cm^{-1} reported by Alencar *et al*.

[112] W Levason, EH Newman, M Webster. *Polyhedron*, 2000, **19**, pp.2697-2705.

5.10 Conclusion

In this study, different types of compounds of the four middle REEs namely europium, terbium, dysprosium and yttrium were studied for dissolution and recovery. These results indicated the metals, metal nitrates and the organometallic TPPO complexes can successfully be dissolved and recovered using a suite of different dissolution methods and ICP-OES quantification. The synthesized TPPO complexes were characterized with different physical techniques which included IR and CHNS micro analysis. The obtained complexes were analyzed to determine the metal concentrations in the compounds using ICP-OES. Since the ICP-OES analysis requires a prior dissolution of the sample, three different digestion methods (open acid digestion, microwave acid assisted and acid dissolution) were investigated. The best results, with recoveries of 99.10(6) % for Eu, 99.4(4) % for Tb and 99.9(3) % for Dy, except for 96.1(5) % for Y, were obtained using microwave digestion. The microwave digestion and acid dissolution methods for Eu, Tb, Dy and Y showed recoveries of 100.01(3) %, 99.63(7) %, 99.4(4) % and 97.6(2) % respectively.

The concentrations of the non-metal elements namely C, H and N were determined using CHNS micro analysis. The obtained results confirmed the predicted chemical formulae. The complexes were also characterized using infrared (IR). Europium, terbium, dysprosium and yttrium gave excellent results in inorganic compounds after the TGA determination suggested the 6 crystal waters for $Dy(NO_3)_3 \cdot xH_2O$.

5.11 Method validation

Method validation is important as analytical results will be assessed for reliability, reproducibility and quality. Validation parameters such as linearity, sensitivity, accuracy, precision, specificity, LOD, LOQ and robustness are included / calculated as part of the validation process. The student *t*-test is used to determine accuracy of the experimentally obtained values compared to that of the expected or theoretical value. In this study, the statistical test (**Equation 5.4**) was calculated at the 95 %

[113] FL Alencar, LB Zinner, K Zinner and JEX Matos. *J. Coord. Chem*., 1999, **46**, pp. 471-478.

confidence interval. Rejection is considered when the *t* value lies outside the specified boundaries which was ±4.30 for 2 degrees of freedom.[114]

$$t = \frac{\bar{x} - \mu_0}{SD / \sqrt{N}} \qquad \textbf{5.4}$$

In **Equation 5.4**, $\bar{x}$ is the mean of the concentration, μ_0 represents the accepted concentration, SD is the standard deviation and N is number of replicates. The standard deviation about regression (S_r), slope (S_m) and intercept (S_b) are calculated using **Equation 5.5** - **5.7**.

$$S_r = \sqrt{\frac{S_{yy} - m^2 S_{xx}}{N - 2}} \qquad \textbf{5.5}$$

S_{yy} is sum of the square of the diviation from the mean for individual values of y and and S_{xx} is sum of the square of the diviation from the mean for individual values of x.

$$S_m = \sqrt{\frac{S_r^2}{S_{xx}}} \qquad \textbf{5.6}$$

$$S_b = S_r \sqrt{\frac{1}{N - \left(\Sigma x_i\right)^2 / \Sigma x_i^2}} \qquad \textbf{5.7}$$

5.11.1 Validation of the metals (europium, terbium, dysprosium and yttrium)

The *t* values of Eu (in HNO_3), Dy (in HNO_3) and terbium (in H_2SO_4) were within the 95 % confidence interval and results were accepted. The results are presented in **Tables 5.20** - **5.32** and the validation parameters were evaluated as described in **Section 5.10**.

[114] DA Skoog, DM West, FJ Holler, SR Crouch. *Fundamentals of Analytical Chemistry 8th Ed*. Belmont, USA. Brooks/Cole, 2004. p.147.

Table 5.20: Validation of europium in HNO_3 using ICP-OES.

Validation criteria	Parameter	HNO_3
Recovery	Mean(SD)	100.01(3)
Precision	%RSD	0.16
Robustness	-	-
Working range	Calibration curve	1-10 ppm
Linearity	r^2	0.9990
Sensitivity	Slope (m)	7.5856
Selectivity	S_m	0.1361
Error of the slope	Intercept	2.1043
Specificity	S_b	1.0645
t-value		0.46
Decision		Accepted

Table 5.21: Validation of terbium in HNO_3 using ICP-OES.

Validation criteria	Parameter	HNO_3
Recovery	Mean(SD)	9.63(7)
Precision	%RSD	1.15
Robustness	-	-
Working range	Calibration curve	1-10 ppm
Linearity	r^2	0.9999
Sensitivity	Slope (m)	0.1764
Selectivity	S_m	0.0012
Error of the slope	Intercept	0.0283
Specificity	S_b	0.0039
t-value		-9.19
Decision		Rejected

Table 5.22: Validation of dysprosium in HNO_3 using ICP-OES.

Validation criteria	Parameter	HNO_3
Recovery	Mean(SD)	99.4(4)
Precision	%RSD	1.60
Robustness	-	-
Working range	Calibration curve	1-10 ppm
Linearity	r^2	0.9997
Sensitivity	Slope (m)	4.8344
Selectivity	S_m	0.0510
Error of the slope	Intercept	0.3884
Specificity	S_b	0.1649
t-value		-2.30
Decision		Accepted

Table 5.23: Validation of yttrium in diluted HNO_3 using ICP-OES.

Validation criteria	Parameter	HNO_3
Recovery	Mean(SD)	92.5(2)
Precision	%RSD	1.48
Robustness	-	-
Working range	Calibration curve	1-10 ppm
Linearity	r^2	1.0000
Sensitivity	Slope (m)	5.2089
Selectivity	S_m	0.0222
Error of the slope	Intercept	0.7707
Specificity	S_b	0.0718
t-value		-57.06
Decision		Rejected

Table 5.24: Validation of europium in HCl using ICP-OES.

Validation criteria	Parameter	HCl
Recovery	Mean(SD)	98.5(2)
Precision	%RSD	0.16
Robustness	-	-
Working range	Calibration curve	1-10 ppm
Linearity	r^2	0.9999
Sensitivity	Slope (m)	6.102
Selectivity	S_m	4.9940
Error of the slope	Intercept	0.8181
Specificity	S_b	16.1644
t-value		-16.41
Decision		Rejected

Table 5.25: Validation of terbium in HCl using ICP-OES.

Validation criteria	Parameter	HCl
Recovery	Mean(SD)	65.4(8)
Precision	%RSD	1.15
Robustness	-	-
Working range	Calibration curve	1-10 ppm
Linearity	r^2	1.0000
Sensitivity	Slope (m)	0.2141
Selectivity	S_m	0.1748
Error of the slope	Intercept	0.0187
Specificity	S_b	0.5658
t-value		-79.29
Decision		Rejected

Table 5.26: Validation of dysprosium in HCl using ICP-OES.

Validation criteria	Parameter	HCl
Recovery	Mean(SD)	37.8(6)
Precision	%RSD	1.60
Robustness	-	-
Working range	Calibration curve	1-10 ppm
Linearity	r^2	0.9996
Sensitivity	Slope (m)	3.3322
Selectivity	S_m	2.7216
Error of the slope	Intercept	0.6775
Specificity	S_b	8.8090
t-value		-178.23
Decision		Rejected

Table 5.27: Validation of yttrium in HCl using ICP-OES.

Validation criteria	Parameter	HCl
Recovery	Mean(SD)	37.8(6)
Precision	%RSD	1.48
Robustness	-	-
Working range	Calibration curve	1-10 ppm
Linearity	r^2	0.9997
Sensitivity	Slope (m)	6.1107
Selectivity	S_m	4.9791
Error of the slope	Intercept	1.0013
Specificity	S_b	16.1163
t-value		-193.41
Decision		Rejected

Table 5.28: Validation of europium in H_2SO_4 using ICP-OES.

Validation criteria	Parameter	H_2SO_4
Recovery	Mean(SD)	68.1(6)
Precision	%RSD	0.87
Robustness	-	-
Working range	Calibration curve	1-10 ppm
Linearity	r^2	0.9999
Sensitivity	Slope (m)	5.7632
Selectivity	S_m	4.7059
Error of the slope	Intercept	0.9730
Specificity	S_b	15.2318
t-value		-93.84
Decision		Rejected

Table 5.29: Validation of terbium in H_2SO_4 using ICP-OES.

Validation criteria	Parameter	H_2SO_4
Recovery	Mean(SD)	100.2(2)
Precision	%RSD	0.23
Robustness	-	-
Working range	Calibration curve	1-10 ppm
Linearity	r^2	0.9996
Sensitivity	Slope (m)	0.2256
Selectivity	S_m	0.1842
Error of the slope	Intercept	0.0278
Specificity	S_b	0.5963
t-value		1.77
Decision		Accepted

Table 5.30: Validation of dysprosium in H_2SO_4 using ICP-OES.

Validation criteria	Parameter	H_2SO_4
Recovery	Mean(SD)	98.0(4)
Precision	%RSD	0.36
Robustness	-	-
Working range	Calibration curve	1-10 ppm
Linearity	r^2	0.9995
Sensitivity	Slope (m)	3.3612
Selectivity	S_m	2.7453
Error of the slope	Intercept	0.2896
Specificity	S_b	8.8859
t-value		-9.75
Decision		Rejected

Table 5.31: Validation of yttrium in H_2SO_4 using ICP-OES.

Validation criteria	Parameter	H_2SO_4
Recovery	Mean(SD)	91.1(3)
Precision	%RSD	0.29
Robustness	-	-
Working range	Calibration curve	1-10 ppm
Linearity	r^2	0.9999
Sensitivity	Slope (m)	5.8774
Selectivity	S_m	4.7992
Error of the slope	Intercept	0.8313
Specificity	S_b	15.5339
t-value		-58.60
Decision		Rejected

Table 5.32: Validation of yttrium in *aqua regia* using ICP-OES.

Validation criteria	Parameter	Microwave digestion *(aqua regia)*
Recovery	Mean(SD)	97.6(2)
Precision	%RSD	0.17
Robustness	-	-
Working range	Calibration curve	1-10 ppm
Linearity	r^2	0.9999
Sensitivity	Slope (m)	8.2855
Selectivity	S_m	4.6489
Error of the slope	Intercept	0.3912
Specificity	S_b	15.0472
t-value		-25.93
Decision		Rejected

The rejection of results for the metals were much higher compared with the accepted results. The incomplete dissolution of the metals is one of the reasons for rejection of the results. Another reason is the extremely small standard deviations obtained for these results. Small SD's lead to very narrow acceptance levels or easly rejected results, even at +99 % recovery. Therefore the obtained average recoveries were lower than that of the accepted values. The results of Eu and Dy metals were accepted and regarded as accurate by the validation method.

5.11.2 Inorganic compounds

Europium, terbium, dysprosium and yttrium were well recovered from inorganic compounds. The results were validated and only europium and terbium were accepted at the 95 % confidence interval. The same conditions used for metals were used for validation in inorganic compounds (**Tables 5.33** - **5.36**).

Table 5.33: Validation of europium in HNO_3 using ICP-OES.

Validation criteria	Parameter	HNO_3
Recovery	Mean(SD)	100.0(2)
Precision	%RSD	0.18
Robustness	-	-
Working range	Calibration curve	1-10 ppm
Linearity	r^2	0.9998
Sensitivity	Slope (m)	5.0584
Selectivity	S_m	0.3731
Error of the slope	Intercept	0.2600
Specificity	S_b	14.0212
t-value		0.40
Decision		Accepted

Table 5.34: Validation of terbium in HNO_3 using ICP-OES.

Validation criteria	Parameter	HNO_3
Recovery	Mean(SD)	100.2(7)
Precision	%RSD	0.68
Robustness	-	-
Working range	Calibration curve	1-10 ppm
Linearity	r^2	0.9999
Sensitivity	Slope (m)	0.1764
Selectivity	S_m	0.1429
Error of the slope	Intercept	0.0309
Specificity	S_b	0.4627
t-value		0.61
Decision		Accepted

Table 5.35: Validation of dysprosium in HNO_3 using ICP-OES.

Validation criteria	Parameter	HNO_3
Recovery	Mean(SD)	99.6(1)
Precision	%RSD	0.14
Robustness	-	-
Working range	Calibration curve	1-10 ppm
Linearity	r^2	1.0000
Sensitivity	Slope (m)	2.6067
Selectivity	S_m	2.1284
Error of the slope	Intercept	0.3138
Specificity	S_b	6.8892
t-value		-5.07
Decision		Rejected

Table 5.36: Validation of yttrium in HNO_3 using ICP-OES.

Validation criteria	Parameter	HNO_3
Recovery	Mean(SD)	99.4(1)
Precision	%RSD	0.10
Robustness	-	-
Working range	Calibration curve	1-10 ppm
Linearity	r^2	1.0000
Sensitivity	Slope (m)	4.8352
Selectivity	S_m	3.9481
Error of the slope	Intercept	0.6614
Specificity	S_b	12.7789
t-value		-10.78
Decision		Rejected

The experimental results of dysprosium and yttrium were rejected at the 95 % confidence interval. The reason for rejection being the extremely small standard deviations obtained for these results. That resulted in the rejection of Dy and Y even

though a recovery of greater than 99 % was obtained. This implies that the obtained recoveries were not in agreement with the expected results.

5.11.3 Synthesized TPPO complexes of europium, terbium, dysprosium and yttrium

The TPPO complexes were dissolved by H_2SO_4 using microwave digestion. The obtained results were validated for europium, terbium, dysprosium and yttrium. Only terbium and dysprosium were accepted at the 95 % confidence interval while other results were rejected. The validated parameters used were the same as for metals and inorganic compounds. The results are presented in **Tables 5.37** - **5.40**.

Table 5.37: Validation of europium in H_2SO_4 using ICP-OES.

Validation criteria	Parameter	Microwave digestion (H_2SO_4)
Recovery	Mean(SD)	99.10(6)
Precision	%RSD	0.06
Robustness	-	-
Working range	Calibration curve	1-10 ppm
Linearity	r^2	1.0000
Sensitivity	Slope (m)	7.2495
Selectivity	S_m	5.9192
Error of the slope	Intercept	1.0046
Specificity	S_b	19.1590
t-value		-24.52
Decision		Rejected

Table 5.38: Validation of terbium in H_2SO_4 using ICP-OES.

Validation criteria	Parameter	Microwave digestion (H_2SO_4)
Recovery	Mean(SD)	99.4(4)
Precision	%RSD	0.39
Robustness	-	-
Working range	Calibration curve	1-10 ppm
Linearity	r^2	0.9995
Sensitivity	Slope (m)	0.1908
Selectivity	S_m	0.1558
Error of the slope	Intercept	0.0320
Specificity	S_b	0.5044
t-value		-2.80
Decision		Accepted

Table 5.39: Validation of dysprosium in H_2SO_4 using ICP-OES.

Validation criteria	Parameter	Microwave digestion (H_2SO_4)
Recovery	Mean(SD)	99.9(3)
Precision	%RSD	0.25
Robustness	-	-
Working range	Calibration curve	1-10 ppm
Linearity	r^2	0.9998
Sensitivity	Slope (m)	3.0069
Selectivity	S_m	2.4555
Error of the slope	Intercept	0.6265
Specificity	S_b	7.9479
t-value		-0.31
Decision		Accepted

Table 5.40: Validation of yttrium in H_2SO_4 using ICP-OES.

Validation criteria	Parameter	Microwave digestion (H_2SO_4)
Recovery	Mean(SD)	96.1(5)
Precision	%RSD	0.48
Robustness	-	-
Working range	Calibration curve	1-10 ppm
Linearity	r^2	1.0000
Sensitivity	Slope (m)	6.3326
Selectivity	S_m	5.1706
Error of the slope	Intercept	1.0241
Specificity	S_b	16.7360
t-value		-14.97
Decision		Rejected

Europium and yttrium resulted in rejection while on the other side terbium and dysprosium were considered accepted. The results were affected by low standard deviations (extremely low) for rejection of Eu, despite its recovery of more than 99 %. The rejection might be due to disagreement between the obtained recoveries of europium and yttrium with the expected results.

5.12 Conclusion

Validation parameters were obtained for all the experimental results. All experimental results were obtained at the working range of 1-10 ppm of the ICP-OES standard concentrations with excellent linearity (r^2) ranging between 0.9990 - 1.000 compared to the minimum acceptable value of 0.997[115]. The summary of the different dissolution methods and their level of success is illustrated in **Table 5.41**.

[115] ME Swartz and IS Krull. *Analytical Method Development and Validation.* New York, USA. Marcel Dekker Inc, 1997, p. 54

Table 5.41: A summary of the accepted / rejected results at 95 % confidence interval.

Metal	Dissolution method	*Level of success
Eu	Acid dissolution (HNO_3)	√
Tb		X
Dy		√
Y		X
Eu	Acid dissolution (HCl)	X
Tb		X
Dy		X
Y		X
Eu	Acid dissolution (H_2SO_4)	X
Tb		√
Dy		X
Y		X
Y	Acid dissolution (*aqua regia*)	X
Inorganic compound		
$Eu(NO_3)_3{\cdot}5H_2O$	Open digestion (HNO_3)	√
$Tb(NO_3)_3{\cdot}5H_2O$		√
$Dy(NO_3)_3{\cdot}6H_2O$		X
$Y(NO_3)_3{\cdot}6H_2O$		X
REE complex		
$[Eu(TPPO)_3(NO_3)_3]$	Microwave digestion (H_2SO_4)	X
$[Tb(TPPO)_3(NO_3)_3]$		√
$[Dy(TPPO)_3(NO_3)_3]$		√
$[Y(TPPO)_3(NO_3)_3]$		X

*√: Successful

X: Unsuccessful

6 Evaluation and future work of this study

6.1 Introduction

This chapter will evaluate the success of the study as measured against the overall and specific goals set out in **Chapter 1, Section 1.2** as well as identify possible research projects that were identified in the course of this investigation.

6.2 Evaluation of the study

The main focus of the study was to successfully dissolve and quantify four of the central group of rare earth elements that may be present in minerals such as xenotime and gadolinite. The specific aims of this study as identified in **Chapter 1** were to develop and validate analytical methods for the accurate quantification of Eu, Dy, Tb and Y according to the following strategy:

- Perform a detailed literature study on the analytical techniques for the analysis of REEs.
- Determine the ability of different acids with or without microwave digestion method for dissolving the complexes.
- Quantify REEs (Eu, Tb, Y and Dy) accurately and determine their recoveries in pure REE metal, inorganic compounds and organometallic complexes.
- Compare results obtained using different techniques such as ICP-OES, IR and CHNS-micro analyis (LECO).
- Statistically validate these methods.

The results obtained in this study indicates a large degree of success with regard to the set objectives (**Chapter 1**) in relation to the results obtained in **Chapter 5**. Different acids (65 % HNO_3, 32 % HCI, 98 % H_2SO_4, 80 % H_3PO_4 and *aqua regia*) were used to dissolve the different metals, inorganic compounds ($Ln(NO_3)_3{\cdot}xH_2O$)

and organometallic TPPO complexes. Europium, terbium, dysprosium and yttrium were successfully dissolved in different acid mediums. HNO_3 completely dissolved Eu, Tb and Dy as indicated by the metal recoveries using ICP-OES. HCl succeeded in dissolving only europium, while the metals (Tb, Dy and Y) were recovered below the expected values. H_2SO_4 on the other hand, successfully dissolved terbium but poor dissolution of the other metals (Dy, Eu and Y) were obtained. *Aqua regia* used in microwave assisted digestion improved the recovery of the Y metal, compared to open beaker digestion. Sulfur and iron were found as impurities associated with the yttrium metal. In summary all metals were successfully dissolved to the level of satisfaction and accurately quantified.

All the metal nitrate salts ($Ln(NO_3)_3{\cdot}xH_2O$) were successfully dissolved in HNO_3 and quantitatively analyzed by ICP-OES. Total recovery of europium, terbium and yttrium were obtained. Satisfactory dysprosium recovery was obtained only after the correct number of crystal waters ($6H_2O$) were determined by TGA.

Characterization of the different TPPO complexes ($[Ln(TPPO)_3(NO_3)_3]$) using infrared (IR) characterization confirmed the identity of these compounds as coordinated with the triphenylphosphine oxide (TPPO) ligand. The composition of the complexes was confirmed using CHNS micro analyses. The agreement between the theoretical and calculated values of the % C and H was excellent while the % N content turned out to be disappointing.

The synthesized organometallic TPPO complexes were successfully dissolved in H_2SO_4 using microwave digestion since normal acid dissolution and bench-top digestion were unsuccessful. The quantitative analysis of europium, terbium and dysprosium indicated that H_2SO_4 dissolution was extremely successful with total recoveries recorded, but a lower yttrium recovery (96.1(5) %) were obtained.

All the results were statistically validated and the parameters which were investigated included linearity, sensitivity, accuracy, precision, specificity, LOD, LOQ and robustness at a confidence limit of 95 %. Unsuccessful dissolution, low recovery and small standard deviation are the reasons why some of the results for europium, terbium, dysprosium and yttrium (even at +99 % recovery) were rejected (using the

Student t-test). In summary all the set objectives in **Chapter 1** were successfully accomplished in this study.

6.3 Future work

The current study can be expanded to the separation of the different rare earth TPPO complexes using sublimation (see differences in melting point), selective crystallization and solvent extraction (formation of immiscible liquid layers during the dissolution process). Other possibilities include the use of other types of ligands which may induce differences in the type of complexes as well as differences in the physical and chemical properties which will allow for the development of new separation and isolation techniques for these REEs. Possible ligands which can be used include sasac (thioacetyl acetone) and hpt^-(2-pyridinethiolato-*N*-oxide).

The problems associated with the poor nitrogen recoveries during the analysis of the TPPO complexes also call for some investigation. Standards (EDTA and sulfamethazine) used as control samples and to calibrate the LECO (micro-analysis) gave satisfactory nitrogen recoveries (99.0 to 100.8 %) which confirmed the proper functioning of the equipment as well as the calibration curves. A possible study may include the nitrogen analysis of a large number of nitrogen-containing organometallic and inorganic compounds to try and identify the type of nitrogens which analyse incorrectly.

Other types of dissolution agents such as alkalis (NaOH, Na_2CO_3 *etc*.) and different types of fluxes (acid, base or redox fluxes) can also be investigated as possible dissolution mediums.

An analytical study on mineral ores such as xenotime and gadolinite will also add valuable information to the possible development of new or alternative beneficiation processes for this group of rare earth elements.

Summary

The middle group of rare earth elements containing Eu, Tb, Y and Dy are mostly associated with two minerals, namely xenotime and gadolinite. This group of elements play a vital role in the manufacturing of modern technological products such as phosphors, electronic products and super magnets.

The main objectives of this study were to perform i) a detailed literature study to get abreast of the analytical techniques used for the analysis of these REEs, ii) to establish the ability of different acids (with or without microwave assisted digestion) to dissolve the different types of chemical compounds containing these four rare earth elements, iii) accurately quantify (recover) the REEs in the pure metals, in the metal nitrate compounds as well as in organometallic complexes, iv) characterization of newly synthesized organometallic complexes using IR spectrometry, TGA and CHNS-micro element analysis and v) to statistically validated the quality of the analytical results.

Six different acids, namely 98 % H_2SO_4, 65 % HNO_3, 32 % HCI, 80 % H_3PO_4 and *aqua regia*, were evaluated as dissolution agents for the pure metals (Eu, Tb, Dy and Y) as well as the newly synthesized organometallic TPPO complexes. Bench-top dissolution at room-temperature was initially evaluated as dissolution technique. Nitric acid dissolution yielded excellent results for three of the elements and 100.01(3) % of the europium was recovered, 99.63(7) % of the terbium and 99.4(4) % of the metallic dysprosium. Yttrium recovered the lowest of the four elements with only 92.5(2) %. Hydrochloric acid turned out to be a poor dissolution reagent and dissolved only 98.5(2 %) europium, 65.4(8) % terbium and even lower dysprosium and yttrium recoveries of 37.8(6) %. Open beaker dissolution using H_2SO_4 recovered 68.1(6) % Eu, 100.2(2) % Tb, 98.0(4) % Dy and 91.1(3) % Y. Finally *aqua regia* was evaluated under the same conditions and dissolved only 93.8(3) % yttrium. Microwave digestion, using *aqua regia* improved the yttrium recovery to 97.6(2) %. Further analysis of the metal for possible impurities indicated the presence of Fe and S impurities and the quantitative analysis confirmed the presence of 1.5(4) % Fe and 0.21(3) % S.

Summary

The metal nitrate salts ($Ln(NO_3)_3 \cdot xH_2O$) of the four REEs were successfully dissolved (visual inspection) in HNO_3 and recoveries of 100.0(2) % for europium, 100.(7) % for terbium, 99.4(1) % for yttrium and 75.6(4) % for dysprosium were obtained. The unsatisfactory recovery results (in spite of the absence of any remaining material after dissolution) of dysprosium prompted a further investigation to determine the appropriate molecular formula of the $Dy(NO_3)_3 \cdot xH_2O$ salt. Thermogravimetric analysis (TGA) was used to determine the number of crystal waters and results indicated the most appropriate molecular formula should be $Dy(NO_3)_3 \cdot 6H_2O$. This improved the dysprosium recoveries to 99.6(1) %.

The same five acids (HNO_3, HCI, H_2SO_4, H_3PO_4 and *aqua regia*) were used in an attempt to dissolve the newly synthesized organometallic TPPO complexes. The formation of two immiscible liquids after digestion rendered these methods unsuccessful. Microwave digestion with 98 % H_2SO_4 managed to completely dissolve all of these organometallic complexes without the formation of the two colourless (oil and water) layers. The recoveries of 99.10(6) %, 99.4(4) %, 99.9(3) % and 96.1(5) % for europium, terbium, dysprosium and yttrium respectively were obtained.

Infrared (IR) and CHNS micro analysis were used to characterize the different TPPO complexes. The IR spectra of the different complexes compared favourably with the previously prepared and reported compounds while excellent % C and H values were obtained. Interestingly and against expectations, poor % N values were obtained for all the complexes.

The experimental results for the quantitative analysis of europium, terbium, dysprosium and yttrium obtained from the metals, inorganic compounds and synthesized organometallic TPPO complexes were validated using ICP-OES results. The statistical validation of all the analytical results was performed at a 95 % confidence interval. Validation of the obtained results also included the evaluation of parameters such as linearity, sensitivity, accuracy, precision, specificity, LOD, LOQ and robustness. Unsuccessful dissolution, low recoveries and small standard deviations are the reasons why some of the results (even at +99 % recovery) were rejected.

Opsomming

Die middelste groep skaars-aard elemente (SAE) bevattende Eu, Tb, Y en Dy word meestal met twee minerale, naamlik xenotiem en gadoliniet, geassosieer. Hierdie groep elemente speel `n belangrike rol in die vervaardiging van moderne tegnologiese produkte soos ligfosfors, elektroniese produkte en supermagnete.

Die hoofdoelwitte van hierdie studie was om i) `n volledige literatuurstudie uit te voer om op hoogte te kom van die analitiese tegnieke wat gebruik word vir die analise van hierdie SAE's, ii) die effektiwiteit van verskillende sure te bepaal (met of sonder behulp van mikrogolfvertering) om verskillende tipes chemiese verbindings wat hierdie vier skaars aardelemente bevat op te los, iii) die hoeveelheid SAE's in die suiwer metale, asook in die verskillende metaalnitraatverbindings en organometaalkomplekse akkuraat te bepaal (herwinning), iv) karakterisering van nuut-bereide organometaalkomplekse deur middel van IR spektrometrie, TGA en CHNS mikro-element analise, en v) om stastisties die kwaliteit van die analitiese resultate te bevestig.

Ses verskillende sure, naamlik 98 % H_2SO_4, 65 % HNO_3, 32 % HCl, 80 % H_3PO_4 en koningswater (*aqua regia)*, is as oplosreagense vir die suiwer metale (Eu, Tb, Dy en Y) asook die nuut-vervaardigde organometaal TPPO-komplekse geëvalueer. Oplosreaksies by kamertemperatuur is aanvanklik as oplossingstegniek geevalueer. Salpetersuur het herwinning van 100.01(3) % vir europium gelewer, 99.63(7) % vir terbium en 99.4(4) % van die metalliese disprosium. Slegs 92.5(2) % yttrium herwinning is met salpetersuur verkry. Soutsuur blyk `n swakker oplossingsreagens vir al die metale te wees en het slegs 98.5(2) % europium, 65.4(8) % terbium en selfs laer herwinnings vir disprosium en yttrium van 37.8(6) % gelewer. Oop-beker suurvertering met H_2SO_4 het 68.1(6) % Eu, 100.2(2) % Tb, 98.0(4) % Dy en 91.1(3) % Y herwin. Laastens is koningswater onder dieselfde toestande geëvalueer en slegs 93.8(3) % yttrium is herwin. Mikrogolfvertering met behulp van koningswater het die yttrium herwinning na 97.6(2) % verhoog. Verdere analise van die metaal het die teenwoordigheid van Fe en S as onsuiwerhede aangetoon en die kwantitatiewe analise het die teenwoordigheid van 1.5(4) % Fe en 0.21(3) % S in die metaal bevestig.

Die metaalnitrate ($Ln(NO_3)_3 \cdot xH_2O$) van die vier SAE's is suksesvol in HNO_3 opgelos (visuele inspeksie) en europium, terbium, yttrium en disprosium herwinnings van 100.0(2), 100.(7), 99.4(1) en 75.6(4) % onderskeidelik vir die vier elemente verkry. Die onbevredigende herwinningsresultate vir disprosium (ten spyte van die afwesigheid van enige oorblywende materiaal na oplossing) het gelei tot `n verdere ondersoek om die korrekte molekulêre formule van die $Dy(NO_3)_3 \cdot xH_2O$ sout vas te stel. Termogravimetriese analise (TGA) is gebruik om die aantal kristalwaters te bepaal en die resultate het aangedui dat die mees korrekte molekulêre formule $Dy(NO_3)_3 \cdot 6H_2O$ moet wees. Dit het die disprosium herwinning na 99.6(1) % verbeter.

Dieselfde vyf sure (HNO_3, HCI, H_2SO_4, H_3PO_4 en koningswater) is gebruik om die nuut vervaardigde organometaal TPPO-komplekse te probeer oplos. Met die vorming van twee nie-mengbare vloeistowwe (kleurlose olie en water lae) na vertering is hierdie metode as onsuksesvol beskou. Mikrogolfvertering met 98 % H_2SO_4 het daarin geslaag om hierdie organometaal komplekse volledig op te los met die vorming van een homogene oplossing. Herwinnings van 99.10(6) %, 99.4(4) %, 99.9(3) % en 96.1(5) % is onderskeidelik vir europium, terbium, disprosium en yttrium verkry.

Infrarooi (IR) en CHNS mikro-analise is vervolgens gebruik om die verskillende TPPO komplekse te karakteriseer. Die IR spektra van die verskillende komplekse het goed ooreengestem met dié wat vir voorheen-bereide en gerapporteerde komplekse verkry is, terwyl uitstekende % C en H waardes verkry is. Interessant genoeg, en teen die verwagting in, is `n swak % N verkry vir al die komplekse.

Laastens is die kwaliteit van die eksperimentele resultate wat vir die kwantitatiewe analises van die verskillende chemiese verbindings verkry is, met behulp van metode-validasie teen `n 95 % betroubaarheidsinterval ge-evalueer. Validering van parameters soos linieâriteit, sensitiwiteit, akkuraatheid, presisie, spesifisiteit, waarnemingsvlakke, kwantifiseringsvlakke en metode-robuustheid is ook ingesluit. Onsuksesvolle of gedeelte oplosbaarheid, lae herwinnings asook klein standaardafwykings is redes waarom sommige van die resultate (selfs teen +99 % herwinningsvlakke) verwerp is.